REPORT DOCUMENTATION PAGE

Form Approved
OMB No 0704-0188

1a REPORT SECURITY CLASSIFICATION: UNCLASSIFIED	1b RESTRICTIVE MARKINGS
2a SECURITY CLASSIFICATION AUTHORITY	3 DISTRIBUTION / AVAILABILITY OF REPORT: DISTRIBUTION UNLIMITED; APPROVED FOR PUBLIC RELEASE
2b DECLASSIFICATION / DOWNGRADING SCHEDULE	
4 PERFORMING ORGANIZATION REPORT NUMBER(S)	5 MONITORING ORGANIZATION REPORT NUMBER(S)
6a NAME OF PERFORMING ORGANIZATION: NAVAL POSTGRADUATE SCHOOL; 6b OFFICE SYMBOL (If applicable): EC	7a NAME OF MONITORING ORGANIZATION
6c ADDRESS (City, State, and ZIP Code): MONTEREY, CA 93943-5000	7b ADDRESS (City, State, and ZIP Code)
8a NAME OF FUNDING / SPONSORING ORGANIZATION; 8b OFFICE SYMBOL (If applicable)	9 PROCUREMENT INSTRUMENT IDENTIFICATION NUMBER
8c ADDRESS (City, State, and ZIP Code)	10 SOURCE OF FUNDING NUMBERS: PROGRAM ELEMENT NO; PROJECT NO; TASK NO; WORK UNIT ACCESSION NO

11 TITLE (Include Security Classification)
A COMPUTER MODEL FOR THE TRANSMISSION CHARACTERISTICS OF DIELECTRIC RADOMES

12 PERSONAL AUTHOR(S)
FRANCIS, ROBERT M.

13a TYPE OF REPORT	13b TIME COVERED	14 DATE OF REPORT (Year, Month, Day)	15 PAGE COUNT
MASTER'S THESIS	FROM _____ TO _____	1992 MARCH	123

16 SUPPLEMENTARY NOTATION
The views in this thesis are those of the author and do not reflect the official policy or position of the Department of Defense or the U.S. Government.

17 COSATI CODES			18 SUBJECT TERMS (Continue on reverse if necessary and identify by block number)
FIELD	GROUP	SUB-GROUP	RADOME; DIELECTRIC; RADIATION; BACKSCATTER; ELECTROMAGNETIC FIELDS; METHOD OF MOMENTS; OGIVE

19 ABSTRACT (Continue on reverse if necessary and identify by block number)

The electric far field radiation pattern is determined for a uniformly illuminated, linearly polarized circular aperture transmitting through a dielectric radome located in the near field of the aperture. A modified electric field integral equation is solved using the method of moments procedure and the thin shell approximation for dielectrics. The resulting solution was computer coded for ogive and spherical radome shapes. The program is designed in a modular fashion to accomodate the addition of different antenna types, illumination functions or radome shapes.

20 DISTRIBUTION / AVAILABILITY OF ABSTRACT	21 ABSTRACT SECURITY CLASSIFICATION
☒ UNCLASSIFIED/UNLIMITED ☐ SAME AS RPT ☐ DTIC USERS	UNCLASSIFIED
22a NAME OF RESPONSIBLE INDIVIDUAL: D.C. JENN	22b TELEPHONE (Include Area Code): (408) 646-2254; 22c OFFICE SYMBOL: EC/JN

DD Form 1473, JUN 86 *Previous editions are obsolete*

S/N 0102-LF-014-6603

SECURITY CLASSIFICATION OF THIS PAGE

UNCLASSIFIED

Approved for public release; distribution is unlimited.

A Computer Model for the
Transmission Characteristics
of Dielectric Radomes

by

Robert M. Francis
Lieutenant, United States Navy
B.S., University of Houston

Submitted in partial fulfillment
of the requirements for the degree of

MASTER OF SCIENCE IN ELECTRICAL ENGINEERING

from the

NAVAL POSTGRADUATE SCHOOL
March, 1992

ABSTRACT

The electric far field radiation pattern is determined for a uniformly illuminated, linearly polarized circular aperture transmitting through a dielectric radome located in the near field of the aperture. A modified electric field integral equation is solved using the method of moments procedure and the thin shell approximation for dielectrics. The resulting solution was computer coded for ogive and spherical radome shapes. The program is designed in a modular fashion to accommodate the addition of different antenna types, illumination functions, or radome shapes.

TABLE OF CONTENTS

I. INTRODUCTION

The term radome was coined during World War II as a composite of two words, radar and dome. The term originally described the class of dome-shaped structures designed to house and protect radar antennas on airborne platforms. Current usage of the term has evolved to encompass any structure that protects or houses an antenna [Ref. 1].

Radomes must satisfy a diverse range of engineering requirements. These specifications can be broadly divided into two categories: electrical and aero-mechanical. Due to aero-mechanical considerations (which are not addressed in this thesis) an ogive-shaped radome is commonly found on airborne platforms. Chapter II discusses the geometry for an ogive-shaped body of revolution. Aircraft radomes, especially those used at supersonic speeds are subject to mechanical stress and aerodynamic heating so severe that the electrical characteristics of the radome may be a secondary consideration.

The goal of this thesis is to develop a computer program that provides an accurate model for the transmission characteristics of a radome, given the geometry and electrical characteristics of its material composition. This program is called LDBORMM.F, and is described in detail in subsequent chapters.

A. ELECTRICAL CHARACTERISTICS OF RADOMES

Electromagnetic transmission characteristics are a primary electrical design problem for radomes. In this thesis, the radome is modeled as a thin isotropic, homogeneous dielectric shell. The reflection coefficient (Γ) of the radome is given by

$$\Gamma = -\frac{\eta}{2 R_s + \eta} \tag{1.1}$$

where R_s is the surface resistivity of the radome and η is the impedance of free space (120π ohms). The surface resistance, which can be complex in general, is given by

$$R_s = \frac{E_t}{J_s} \tag{1.2}$$

where E_t is the tangential electric field at the surface of the radome and J_s is the surface current [Ref 2: p. 433].

From Equation (1.1), it follows that the reflectivity (Γ) of the radome increases as the surface resistance (R_s) decreases. In the limit, where R_s=0 (perfect conductor), Γ=-1 as expected. When an antenna radiates through a radome, a small portion of the main beam is reflected off of the walls and forms a lobe. This lobe is commonly called the reflection lobe or image lobe. The image lobe is usually broader than the

The primary concern regarding the image lobe is that large discrete reflectors in the detection field can become visible to the radar through this side lobe, and be interpreted as moving targets by the radar [Ref. 3: pp. 301-311]. The reason

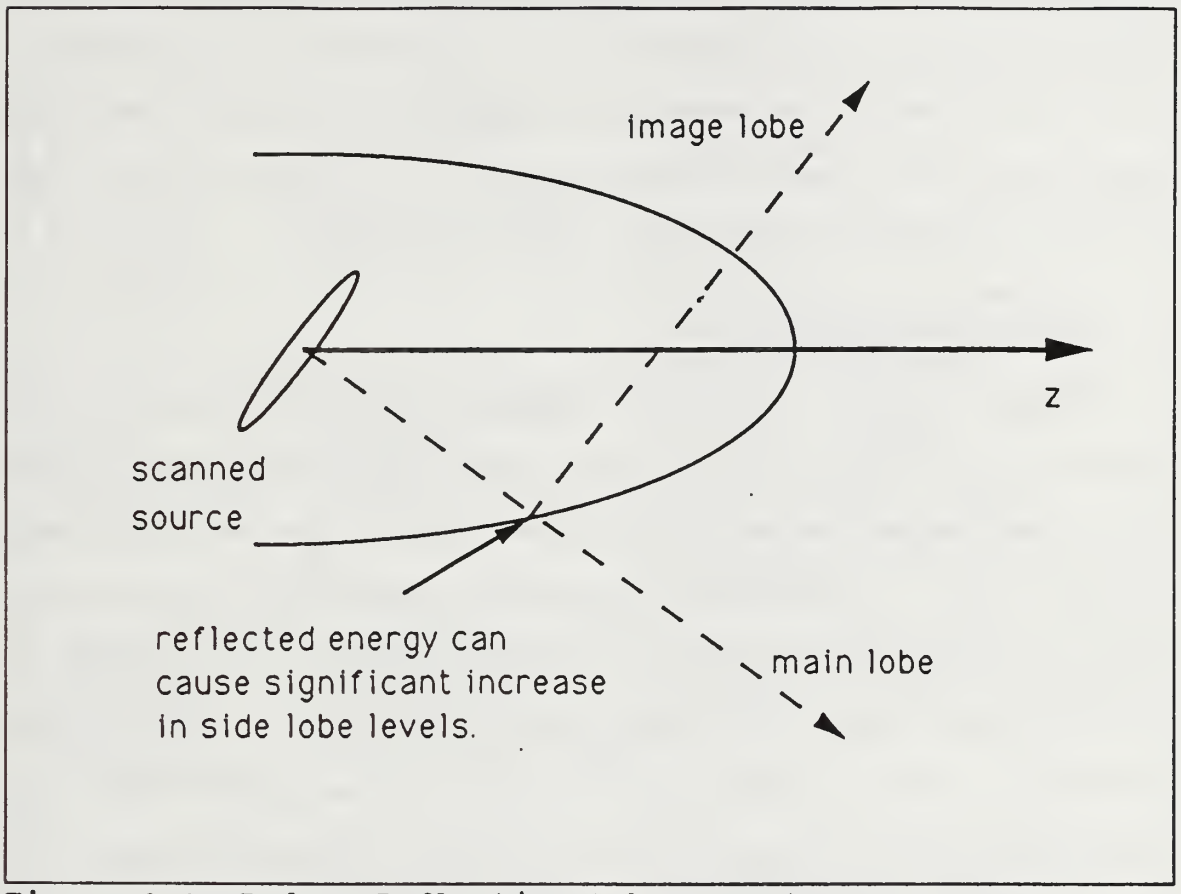

Figure 1.1. Radome Reflection Lobe Geometry.

for false detection of motion from stationary reflectors is the apparent doppler of the return of the image lobe since it is at a different angle and thus a different frequency than the main beam lobe.

The ideal radome is perfectly transparent to the electromagnetic energy that must pass through it. The

The ideal radome is perfectly transparent to the electromagnetic energy that must pass through it. The materials available and suited for radome construction in high velocity airborne systems are not transparent. Impedance mismatches (radome/air interface) and radome geometry alter the transmission characteristics of the system. The presence of a radome can affect the gain, beamwidth, sidelobe level and the direction of the boresight, as well as change the VSWR and the antenna noise temperature [Ref. 4: p. 265].

B. METHODS OF ANALYSIS

Most analytic models for radomes are based on microwave optics (ray tracing techniques). These models assume a radome curvature large enough so that the surface can be considered locally flat. In addition, multiple reflections and surface waves are usually ignored. These approximations are not valid for systems where the radome is in the near field of the antenna or the curvature of the radome causes rapid variation in the direction of the tangential vector along the surface of the radome. Consequently, ray tracing techniques are inaccurate for the analysis of high performance antenna and radome configurations. Figure 1.2 illustrates the inaccuracies inherent to ray tracing techniques. Other analytical methods are available, but have various shortcomings and limitations. Table 1.1 gives a summary of various analytic methods for the solution of electromagnetic scattering problems.

The electric field integral equation (EFIE) and the method of moments is employed in this thesis. The objective is to obtain the solution for the unknown current density which

TABLE 1.1. SUMMARY OF ANALYTIC METHODS.

METHOD	SHAPE	CHARACTERISTICS
Special Function Series Solution	spheres, infinite cylinders, spheroids	rigorous formulation;separation of variable techniques;special functions
Extended boundary condition method	homogeneous objects	rigorous integral equation formulation; harmonic expansion of Green's functions bodies
Physical optics	large planar surfaces	currents deduced from incident fields
Geometrical optics	large surfaces	discontinuous field patterns obtained at shadow and reflection boundaries
Geometrical, uniform, physical theory of diffraction	large convex surfaces with edges and discontinuities	generalization of physical and geometrical optics
Frock theory	large smooth, convex surfaces	formulation based on principle of locality
Hybrid methods	large class of scatterers	integral equation formulation; combines method of moments and optic derived methods
Method of moments, finite element and finite difference	large class of bodies, inhomogeneous objects	rigorous integral equation formulation

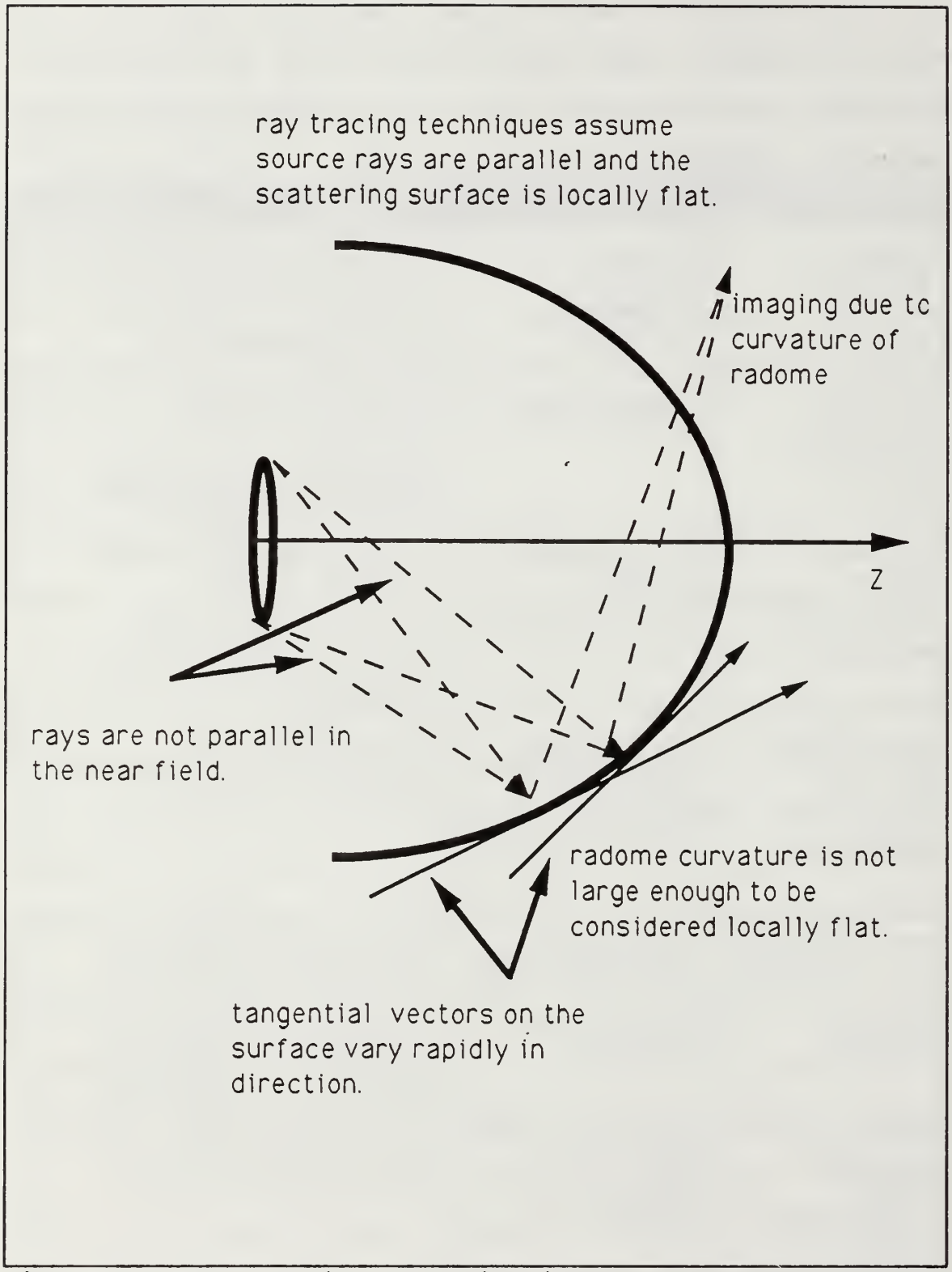

Figure 1.2. Ray Tracing Approximations.

occurs in the integral equation. The integral equation is then solved using a numerical procedure called the method of moments (MM) [Ref. 5: p. 671]. When properly implemented, a method of moments solution is considered rigorous; all of the scattering mechanisms are included. This thesis adapts a code developed by J.R. Mautz and R.F. Harrington for scattering by bodies of revolution.

The proximity of the antenna to the radome requires a near field solution of the integro-differential electric field equations. Chapter III develops the analytical solution for a radome in the near field of a circular antenna and the numerical method for its calculation.

Chapter IV provides details of the program LDBORMM.F. This program solves for the far field radiation pattern of a circular aperture transmitting through an arbitrary-shaped dielectric body of revolution. The EFIE for electromagnetic scattering is solved numerically for the system depicted in Figure 1.3.

Chapter V discusses the testing and evaluation of the main program. The effects of radome geometry and dielectric properties on the far field radiation pattern are examined.

The appendices provide copies of the source codes and a description of variables in the arguments of the subroutines and functions contained in the main program.

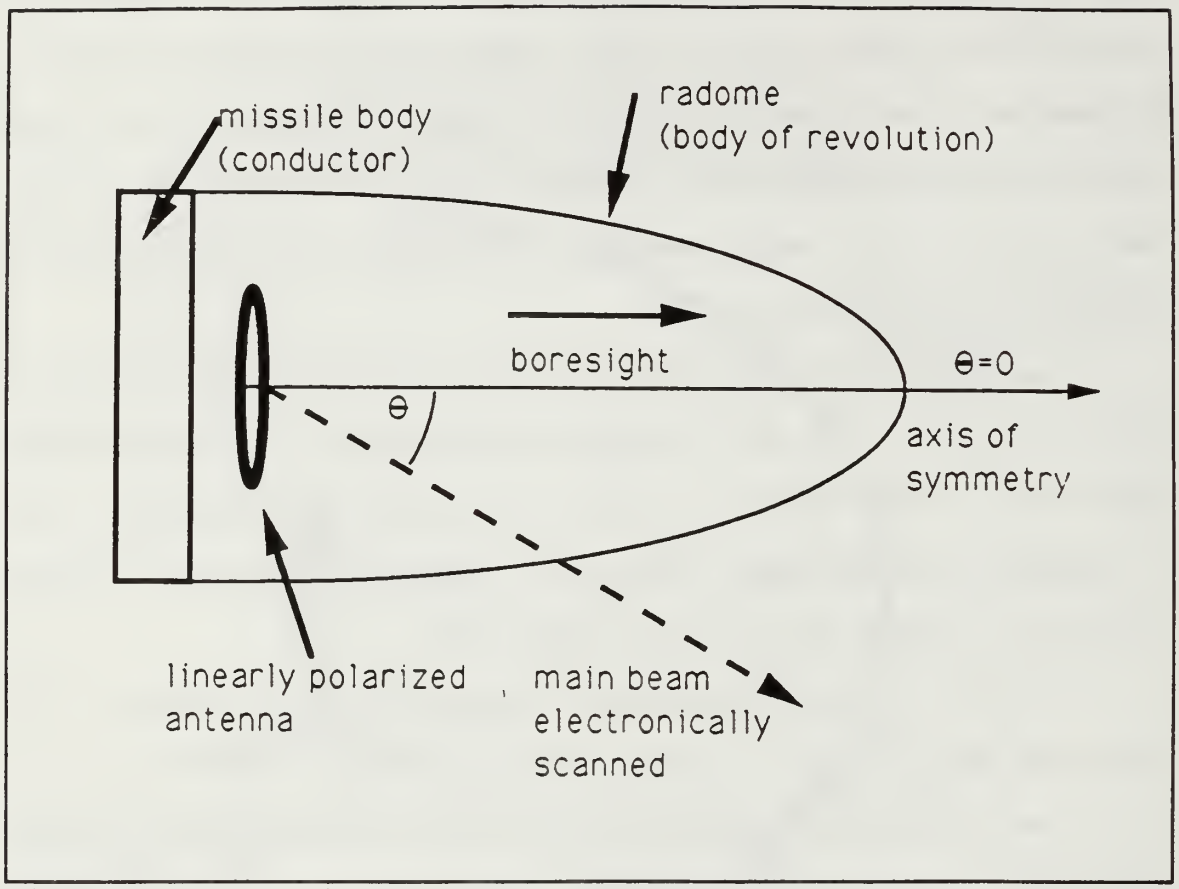

Figure 1.3 Physical Arrangement for LDBORMM.F.

II. OGIVE GEOMETRY

A. BACKGROUND

Forward-looking radar systems in missiles and aircraft are by necessity located in the nose of the platform. Aerodynamic considerations dictate an ogive-shaped radome for most applications. The basic problem is illustrated in Figure 1.3. In this thesis, the subroutine OGIVE provides the physical dimensions of the surface, where the integro-differential field equation solutions are satisfied for a loaded (i.e. dielectric) body of revolution (BOR). The subroutine TESTSPHERE generates a spherical BOR to compare numerical solutions of the main program and function subprograms with known analytical solutions. TESTSPHERE is used solely for validating the subroutines that calculate the circular aperture radiation field. It is not used in the calculation of the radome scattered fields. In all configurations the antenna is centered on the origin of the global coordinate system which is the cylindrical coordinate system of the BOR.

B. DEFINITION OF OGIVE

The ogive is a figure of revolution obtained by rotating an arc of a circle about an axis in the plane of the arc as depicted in Figure 2.1. The curve of the ogive is rotated around the z axis to produce a surface of revolution.

The profile of the surface is generated in the r-z plane by the equation

$$r(z) = \sqrt{R^2 - z^2} + b - R \qquad (2.1)$$

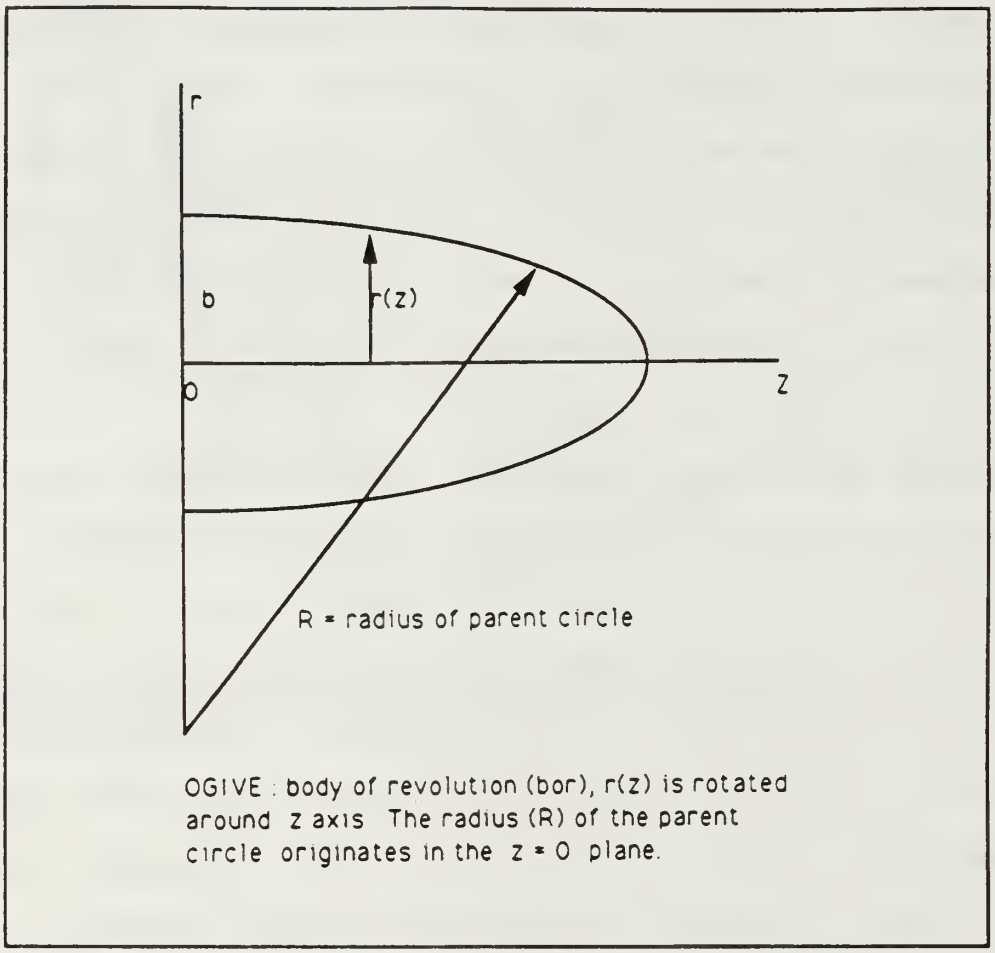

Figure 2.1 Ogive as Defined by Equation (2.1).

where R is the radius of the parent circle and b is the radius of the base.

C. MODIFIED OGIVE FOR LDBORMM.F

In the program LDBORMM.F the antenna is located at the origin of the coordinate system. In a real system, however, the antenna may be displaced on the z axis, from the origin of the defining Equation (2.1). The subroutine OGIVE prompts the user to enter the value z', which is the displacement on the z axis of the antenna location and the position on the z axis where the radius (R) of the parent circle of the ogive commences rotation. Figure 2.2 depicts the modified profile of an ogive as calculated by the subroutine OGIVE.

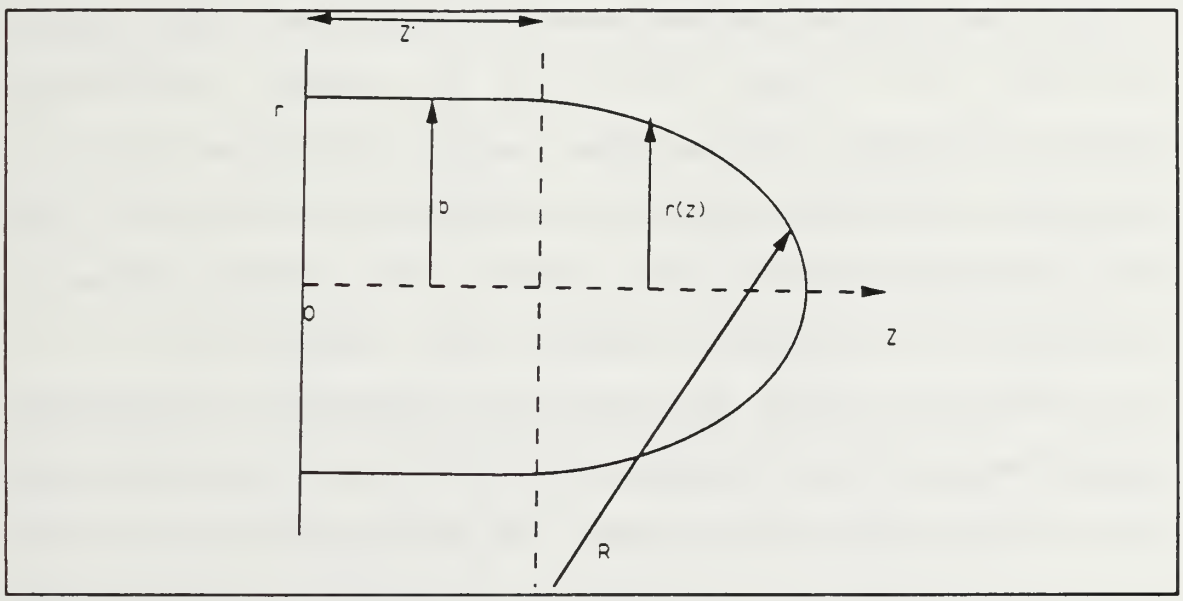

Figure 2.2 BOR Generated by Equation (2.2).

The modified definition for the radius as a function of position on the z axis is given by,

$$r(z) = \begin{cases} b & z \leq z' \\ \sqrt{R^2-(z-z')^2}+b-R & z > z' \end{cases} \qquad (2.2)$$

where z′ is the displacement on the z axis. Using this modified definition the source was located at the origin of the cylindrical coordinate system used to generate ogive(i.e., the source is located in plane z=0). To reiterate, the z′ of Equation (2.2) and Figure 2.2 denotes the distance from the origin where the radius of the parent circle is defined and is not related to the source coordinates.

D. SUBROUTINE OGIVE

The subroutine OGIVE returns values for the global variables NP, ZH and RH. NP is the number of surface generating points on the ogive in the r-z plane. In the subroutine the range of NP is limited to $3 \leq NP \leq 400$. The program prompts the user for the following inputs: radius of the parent circle (R), z′, and the base radius (b).

A standard rule of thumb for the convergence of the series approximation for the surface current is that the spacing of the surface generating points be approximately one-tenth wavelength or less. The following algorithm computes the number of points required for a segment size of approximately one-tenth of a wavelength on the BOR

$$
\begin{aligned}
Z &= \sqrt{2*R*b-b^2} \\
\theta &= ARCSIN\left(\frac{Z}{R}\right) \\
AL &= \theta*R+Z' \\
NP &= 2*INTEGER(5*AL)+1 \ .
\end{aligned}
\tag{2.3}
$$

NP is the global variable for the number of points in the r-z plane of the ogive [reference Figure 2.2]. For a circular aperture, the field incident on the radome tends to vary more rapidly as the angle off boresight increases, thus more generating points are needed. By slightly modifying the above algorithm, a surface with any arbitrary segment size can be generated.

Equation (2.3) gives the algorithm employed by the subroutine OGIVE to calculate the number of points (NP) on the ogive surface in the r-z plane. Data generated uniformly along the radome surface will be nonuniform in z, r, and θ. The subroutine TESTSPHERE generates data points with a uniform spacing in angle θ, whereas OGIVE points are uniform along S. Thus a comparison of the two outputs will not yield coincident data points. Appendix A contains the source code for subroutines OGIVE and TESTSPHERE. Appendix E provides mathematical details relevant to the distribution of data points in angle θ for the subroutines OGIVE and TESTSPHERE.

If the number of points is greater than 400, array limits are exceeded and the main program will write a warning to the screen and stop the program. For bodies of revolution where the arc length is greater than 40 λ the dimensions of the following global variables must be changed accordingly throughout the program: RH, ZH, Z, R, B, C, ZLO and ZL. ZH_n and RH_n are the product of the local coordinates z_n, r_n (computed by the BOR subroutine) and the wave number $k=2\pi/\lambda$. All spatial dimensions throughout the main program, subroutines and functions are in wavelengths (λ).

For surface shapes with definitive geometries other than an ogive or sphere the user must provide an appropriate subroutine. The subroutine must return the global variables NP, ZH, RH, b, R and Z'. These variables are required to define the generating points of the BOR profile (see Eqn.2.2). The call for the subroutine must be inserted in the logical block of code in the main program which establishes the BOR geometry. The subroutine is appended to the main program. Chapter V addresses modification of the main program for various bodies of revolution. The program LDBORMM.F saves the inputs from the BOR subroutine and writes them to the external sequential file OUTLDBOR.

III. METHOD OF MOMENTS

A. OVERVIEW

In order to calculate the scattered field pattern of a dielectric radome the electric current ($\underline{J}_s$) must be integrated over the surface of the body of revolution. The magnetic vector potential ($\underline{A}$) and scalar electric potential (Φ) are defined in terms of the surface current

$$\underline{E}^s(R,\theta,\phi) = -j\omega\underline{A}(\underline{J}_s) - \nabla\Phi(\underline{J}_s) \equiv L(\underline{J}_s) \tag{3.1}$$

where $\underline{E}^s(R,\theta,\phi)$ is the scattered electric field in spherical coordinates, and $L(\bullet)$ is an operator introduced for notational convenience. The potentials are

$$\underline{A}_s(\underline{J}_s) = \mu\int_S \underline{J}_s \frac{e^{-jkR}}{4\pi R}\, dS' \tag{3.2}$$

$$\Phi(\underline{J}_s) = \frac{1}{\varepsilon}\int_S \sigma \frac{e^{-jkR}}{4\pi R}\, dS' \tag{3.3}$$

$$\sigma = -\frac{1}{j\omega}\nabla_s \cdot \underline{J}_s \,. \tag{3.4}$$

R is the magnitude of the difference $\underline{r}$ and $\underline{r}'$, the position vectors of the field and source points respectively. The

operator $\nabla_s \bullet$ is the surface divergence on S [Ref. 6: pp. 15-16]. Figure 3.1 illustrates the quantities.

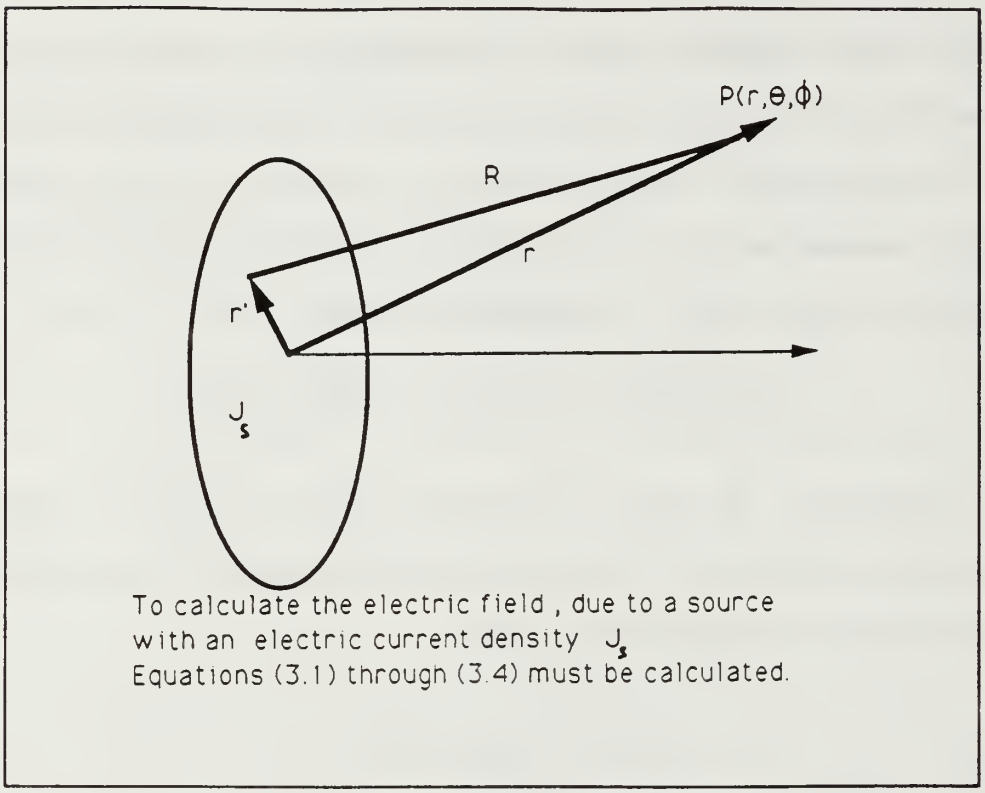

Figure 3.1. Scattering due to Surface Currents.

The objective is to solve for the current on the surface of the radome. Following the method of moments (MM), the electric current ($\underline{J}_s$) on the surface (S) is represented by

$$\underline{J}_s = \sum_{nj} \left(I^t_{nj} \, \underline{J}^t_{ni} + I^{\phi}_{nj} \, \underline{J}^{\phi}_{ni} \right) . \qquad (3.5)$$

In Equation (3.5) $\underline{J}^t$ and $\underline{J}^{\phi}$ are the tangential and azimuthal components of the current on the surface of the radome. The expansion functions for $\underline{J}_s$ are chosen to be

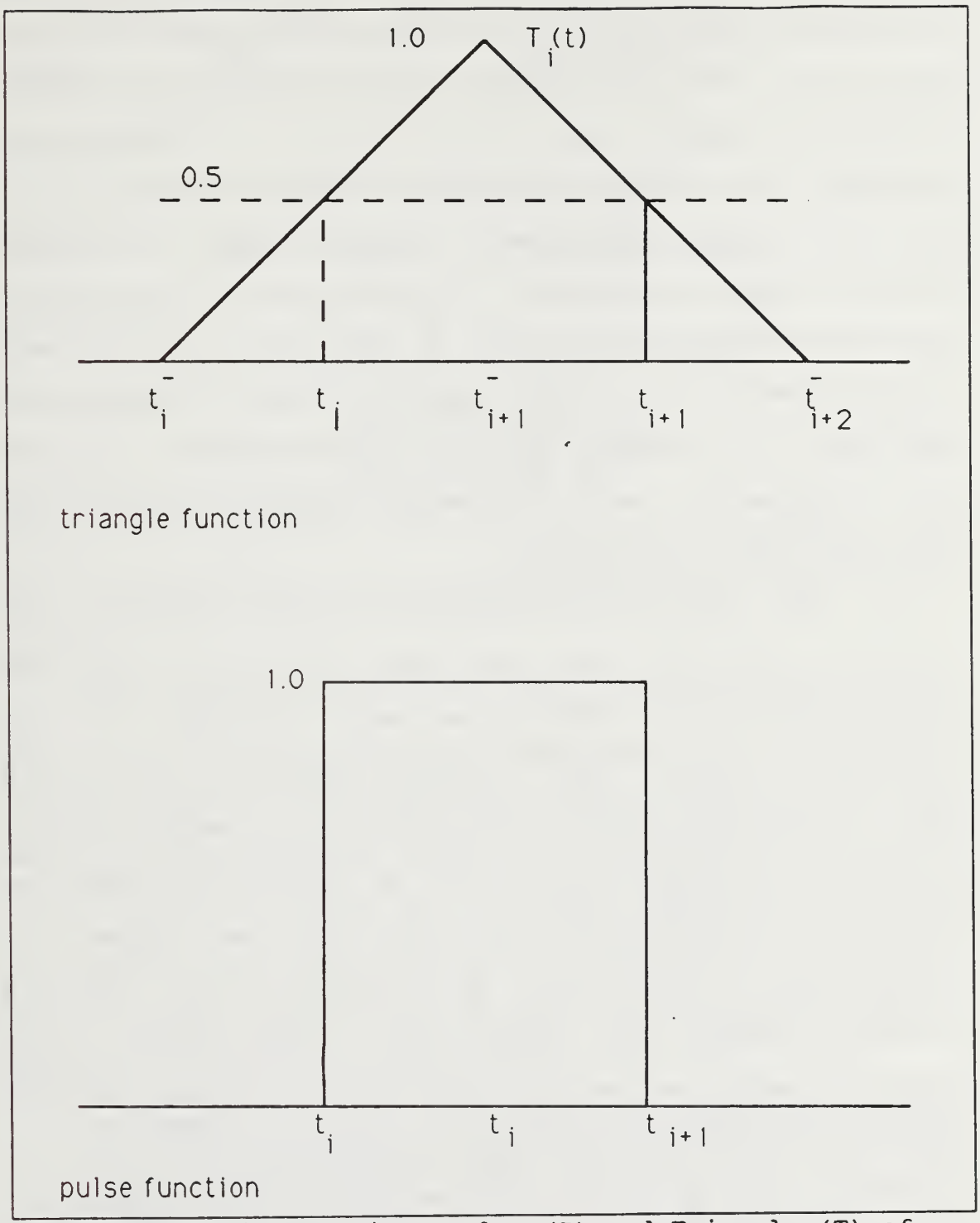

Figure 3.2 Basis Functions Pulse (P) and Triangle (T) of Equations (3.6) and (3.7)

$$\underline{J}^{t}_{nj} = \hat{t}\ \frac{T_j(t)}{r_j}\ e^{jn\phi} \qquad j=1,2,....NP-2 \qquad (3.6)$$

$$\underline{J}^{\phi}_{nj} = \hat{\phi}\ \frac{P_j(t)}{r_j}\ e^{jn\phi} \qquad j=1,2,....NP-1 \qquad (3.7)$$

where the azimuthal mode number is $n=0,\pm1,\pm2....\pm\infty$. An exact solution requires an infinite number of terms in the sum over the index n. In practice, when the source (antenna) is on the axis of symmetry, the sum converges rapidly and only a few azimuthal modes are required.

The unit vectors $\hat{t}$ and $\hat{\phi}$ are in the tangential and azimuthal directions. The functions $T_j(t)$ and $P_j(t)$ are the triangle and pulse functions as shown in Figure 3.2. The abscissa t is the arc length along the generating curve of the BOR. It is assumed that the generating curve consists of NP-1 straight line segments where NP is an integer. The expansion functions of Equations (3.6) and (3.7) are especially appropriate if the BOR is an infinitely thin perfectly conducting surface with edges. This is true because the $\hat{t}$ directed electric current approaches zero at an edge, whereas the $\hat{\phi}$ directed electric current may grow large [Ref. 7: p. 6]. The MM solution of the EFIE reduces the integral equation to a matrix equation for the unknown coefficients I^t and I^{ϕ} . This

is accomplished by the MM testing procedure. The test functions ($\underline{W}_{nj}{}^{t}$,$\underline{W}_{nj}{}^{\phi}$) are chosen to be the complex conjugates of Equations (3.6) and (3.7). Equation (3.5) is substituted into Equations (3.2) to (3.4) for the solution of Equation (3.1). The dot product of Equation (3.1) is then taken with the test functions $\underline{W}_{nj}{}^{t,\phi}$. These dot products are then integrated over the surface S. The resulting matrix equation is

$$\begin{bmatrix} I^{t} \\ I^{\phi} \end{bmatrix} = \begin{bmatrix} Z^{tt} & Z^{t\phi} \\ Z^{\phi t} & Z^{\phi\phi} \end{bmatrix}^{-1} \begin{bmatrix} V^{t} \\ V^{\phi} \end{bmatrix} \qquad (3.8)$$

where Z is a square matrix called the impedance matrix, and $\underline{V}$ is a column vector called the excitation vector [Ref. 7: pp. 6-31].

The impedance elements are identical to those described by Mautz and Harrington. Detailed equations for them appear in reference [Ref. 7] and will not be repeated here. However, the excitation elements will depend on the characteristics of the antenna and the location of the radome. The derivation of the excitation elements for a BOR in the near field of a source has not been presented elsewhere, and therefore will be derived in detail in section (3.B.).

In LDBORMM.F, the subroutine ZMAT calculates the impedance matrix and the subroutine GENEX calculates the excitation vector ($\underline{V}$). The subroutines DECOMP and SOLVE solve the system of equations resulting in the electric current coefficients

($I^{t,\phi}$). The current coefficients are substituted in Equation (3.2), which determines the surface current ($\underline{J}_s$) [Ref. 7: pp.41-64].

With the surface current ($\underline{J}_s$) calculated, the scattered electric field ($\underline{E}^s$) is determined by Equation (3.1). The total electric field, $\underline{E}(R,\theta,\phi)$, is then given by

$$\underline{E}(R,\theta,\phi) = \underline{E^s} + \underline{E^a} \qquad (3.9)$$

where $\underline{E}^a$ is the electric field of the circular aperture.

B. NEAR FIELD OF A CIRCULAR APERTURE

In order to maintain a clear picture of the analysis that follows, it is advantageous to keep in mind the following:

1. The electric current distribution over the circular aperture, which represents an antenna, is defined in Cartesian coordinates.
2. The electric field due to the aperture and the scattered electric field due to the radome are computed in spherical coordinates (R,θ,ϕ).
3. Since the ogive is a body of revolution it is generated in a cylindrical coordinate system (r,ϕ,z).
4. Primed quantities denote source coordinates, unprimed quantities denote coordinates at the point of observation (with the exception of z', which was discussed earlier).

To calculate the excitation vector ($\underline{V}$) of Equation (3.8), the electric field of the antenna must be known. Since the

antenna is typically operating in the near field of the radome, far field approximations are not valid and a more accurate method of calculation must be employed. Since many of the radar antennas used in airborne applications are circular paraboloids or slotted waveguide plates, the radiation source is modeled as a circular aperture with a uniform current distribution polarized in the x direction

$$\underline{J}(x', y', z') = J_x \hat{x} \ . \qquad (3.10)$$

For simplicity the electric current distribution over the aperture is assumed to have constant amplitude and a linear phase

$$J_x = J_0 e^{jkx' \sin\theta_s \cos\phi_s} \ . \qquad (3.11)$$

J_0 is the amplitude of the electric current, while θ_s and ϕ_s are scan angles in the spherical coordinate system. The coordinates of a point in the plane of the aperture are given by (x',y',0).

To compute the Cartesian components of the electric field, J_x is used in Equations (6-108a) to (6-108c) of Reference [Ref. 5: p. 283]. A straightforward transformation of rectangular to polar coordinates (see Appendix E) yields the following expressions for the Cartesian components of the scattered electric field

$$E_x = \frac{-j\eta J_0}{4\pi k}\iint e^{x1}\left[G_1+(r\cos\phi - r'\cos\phi')^2 G_2\right] r'\,dr'\,d\phi' \qquad (3.12)$$

$$E_y = \frac{-j\eta J_0}{4\pi k}\iint e^{x1}\,(r\cos\phi - r'\cos\phi')\,(r\sin\phi - r'\sin\phi')G_2\,r'\,dr'd\phi' \qquad (3.13)$$

$$E_z = \frac{-j\eta J_0}{4\pi k}\iint e^{x1}(r\cos\phi - r'\cos\phi')\,z\,G_2\,r'\,dr'\,d\phi' \qquad (3.14)$$

where

$$x1 = jk\left(r'\cos\phi'\sin\theta_s - R\right) \qquad (3.15)$$

$$R = \sqrt{(r-r')^2 + z^2 + 4rr'\sin^2\left(\frac{\phi-\phi'}{2}\right)} \qquad (3.16)$$

$$G1 = \frac{k^2R^2 - 1 - jkR}{R^3} \qquad (3.17)$$

$$G2 = \frac{3 + 3jkR - k^2R^2}{R^5}\ . \qquad (3.18)$$

Figure 3.3 defines the quantities used in the equations. It is assumed that the antenna is scanned such that $\phi_s = 0$.

The rectangular components of the electric field are converted to spherical components using the transformation

$$E_\theta = E_x\cos\theta\cos\phi + E_y\cos\theta\sin\phi - E_z\sin\theta \qquad (3.19)$$

$$E_R = E_x\sin\theta\cos\phi + E_y\sin\theta\sin\phi + E_z\cos\theta \qquad (3.20)$$

$$E_\phi = -E_x\sin\phi + E_y\cos\phi \ . \qquad (3.21)$$

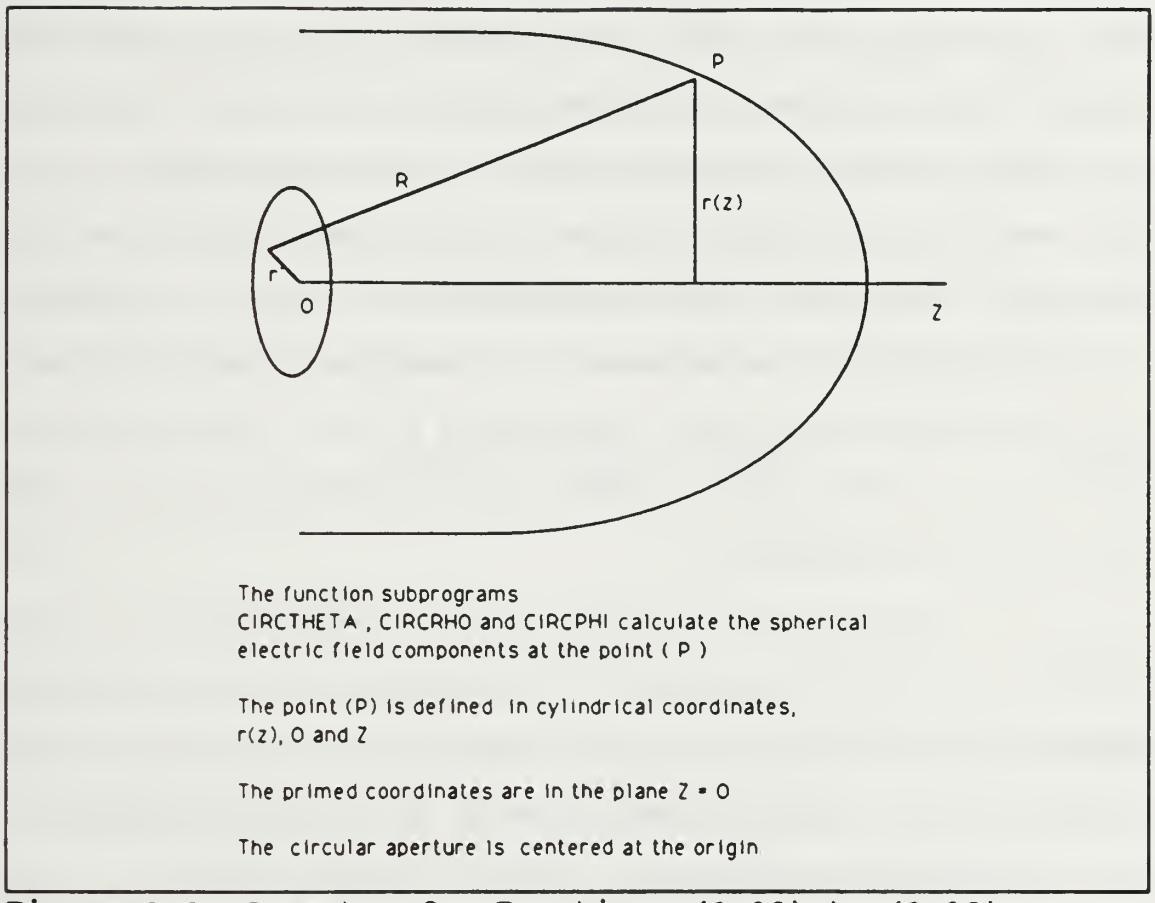

Figure 3.3 Geometry for Equations (3.12) to (3.18).

The function subprograms CIRCTHETA, CIRCRHO, and CIRCPHI calculate the spherical electric field components E_θ , E_R , and E_ϕ, respectively.

1. FUNCTION SUBPROGRAMS, CIRCTHETA, CIRCRHO, AND CIRCPHI

The function subprograms CIRCTHETA, CIRCRHO and CIRCPHI are called in the subroutine GENEX. In the main program, the vector field due to the source ($\underline{E}^a$) is added to the scattered field vector ($\underline{E}^s$) of the body of revolution to obtain the total field ($\underline{E}_{R,\theta,\phi}$), per Equation (3.9). Since the far field approximation is valid in this case, the closed form solution for a circular aperture derived in Section III.B.1.b can be used. Subroutine GENEX requires the components of $\underline{E}_a$ in the near field. The function subprograms calculate the spherical electric field components due to a uniformly illuminated circular aperture at an arbitrary point in space specified by the spherical coordinates R, θ, ϕ. The source can be scanned off boresight by entering non-zero scan angles when the program is executed.

In the subroutine GENEX, these functions are called for each point of integration in the tangential and azimuthal components of the excitation vector ($\underline{V}$) which occur in Equation (3.8), and are described in the following section.

Appendix D contains a table of the variables in the argument list of the function subprograms and the source code for CIRCSUB.F. The program CIRCSUB.F was used to validate the algorithms of CIRCTHETA, CIRCRHO and CIRCPHI. The programs TESTCIRC.M and SCANPLT.M (Appendix D) were used to

generate the analytic solution and plot the comparative results.

a. Numerical Method

To determine the electric field of the antenna and the excitation vector requires evaluating several integrals. In general these integrals can not be reduced to a closed form expression for the geometries under consideration. The integrals must therefore be integrated numerically. The chosen method for evaluating all integrals in this program is Gaussian quadrature. In Gaussian quadrature algorithms, the integral is over a normalized interval, such that $-1 \leq x \leq 1$. N-point Gaussian quadrature approximates an integral by

$$\int_x f(\chi)\, d\chi \cong \sum_{n=1}^{N} \omega_n f(\chi_n) \qquad (3.22)$$

where

$$N = 2m+2 \qquad (3.23)$$

and ω_n are the coefficients and χ_n are the zeros of the Legendre polynomial of order m ($m=0,\pm1,\pm2\ldots\infty$) [Ref. 8].

The number of terms in the sum is always an even number. The program GAUS.F (see Appendix C.) will generate an external sequential file for any range of N where $0 \leq N \leq 500$. The first record in the file is an even number (N). The remainder of the file contains N rows of χ_n and ω_n . The gaus files are stored in a subdirectory named "gaus" of the

directory containing the main program LDBORMM.F. The path to the data files is "(MAIN DIRECTORY)/gaus/gaus###, where ### is N. To create the data file (gaus###), execute GAUS.F in the subdirectory "gaus." The screen prompts the user for the data filename and an even number of points.

For integrals that are over a range other than -1 to +1, a change of variables is necessary before Gaussian quadrature is applied. Integrations over the antenna aperture (from zero radius to the antenna radius r_o) require this change of variables is given by [Ref 8: pp. 523-527]

$$r_n = \left(\frac{r_o}{2}\right)\chi_n + \frac{r_o}{2} \quad . \tag{3.24}$$

A similar technique is used to evaluate the ϕ integrals. The interval of integration for ϕ is symmetric and does not require a change of variables since, $-\pi \leq \phi \leq \pi$

$$\phi_n = \pi x_n + \pi \quad . \tag{3.25}$$

Equations (3.12) through (3.14) are integrated by this method. In the function subprograms, CIRCTHETA, CIRCRHO and CIRCPHI, the variables of integration over the aperture are PHIPRIME (ϕ') and RP (r') and the limits are from 0 to 2π and 0 to r_o, respectively.

b. Test Cases for Function Subprograms

In order to verify the algorithms and coding for CIRCTHETA, CIRCRHO and CIRCPHI the field magnitude E_θ was computed and compared with the analytical solution given by

$$E_\theta = \frac{jkr_o^2 E_0 e^{-jkR}}{R}\left[\frac{J_1(kr_o(\sin\theta-\sin\theta_s))}{kr_o(\sin\theta-\sin\theta_s)}\right]\cos(\theta) \quad (3.26)$$

where $E_0=\eta J_o$ is the electric field amplitude, J_1 is the first order Bessel function, θ_s is the scan angle and (R) is the distance from the center of the aperture to the far field point (P) of Figure 3.3. It is assumed that R is much greater than r′ in the above formula. Therefore any vector from a source point to the observation point is approximately parallel to the vector $\underline{R}$ [Ref. 9: pp. 478-487].

The far field distance for which Equation (3.26) is valid depends on radius (r_o) of the aperture. Antenna engineers commonly consider the far field to exist at distances greater than

$$R = \frac{8r_o^2}{\lambda} . \quad (3.27)$$

However in optics the far zone applies to values of R where the Fresnel number is less than one. Using the latter criterion the minimum distance for which Equation (3.26) is valid is given by [Ref. 10: pp. 95-96]

$$1 \geq \frac{k r_o^2 \lambda^2}{2\pi R}$$
$$\frac{R}{\lambda} \geq r_o^2 \,. \qquad (3.28)$$

The program TESTCIRC.M in Appendix D is used to calculate the analytical solution for E_θ in accordance with Equation (3.26). The results are compared with the calculated field computed by CIRCSUB.F. In Figures (3.4), (3.6), and (3.8) the analytical solution is plotted with a solid line while the values calculated by the test program CIRCSUB.F are plotted as points.

Figures (3.4), (3.6), and (3.8) show the convergence of the numerical solution from CIRCSUB.F as a function of the number of integration points with the analytical solution given by Equation (3.26) for one, two and five wavelength radius circular apertures. Figures (3.5), (3.7), and (3.9) show plots of the field magnitudes (E_θ, E_R, E_ϕ) versus the angle in degrees. Figures 3.10 through 3.12 show plots from CIRCTHETA and Equation (3.26) for various scan angles and aperture radii. (Note that the vertical scale in Figures 3.4 to 3.12 is in volts/meter, not dB.)

Table 3.1 summarizes parameters for Figures (3.4) through (3.12). The plotted results verify the excellent agreement between the algorithm of the function subprograms and the analytical solution. It is important to note the

number of points of integration in r′ (CNRHO) and ϕ' (CNPHI) of Equations (3.13) through Equation (3.15) required for convergence to the analytical solution of Equation (3.26). The number of points of integration in the table are the minimum number required for convergence. As the radius of the aperture increases, the number of iterations required increases as the product of CNRHO and CNPHI. For example, Test 3 requires 1200 iterations for convergence to the analytic solution. In the program LDBORMM.F the functions

TABLE 3.1. DATA SUMMARY FOR TEST CASES.

Test	Radius (r_o)	Distance (R)	CNRHO	CNPHI	Scan	Fig.
4	1 λ	400 λ	10	20	0°	3.8
1	1 λ	400 λ	10	20	0°	3.9
2	2 λ	400 λ	10	20	0°	3.6
2	2 λ	400 λ	10	20	0°	3.7
3	5 λ	2500 λ	20	60	0°	3.8
3	5 λ	2500 λ	20	60	0°	3.9
4	1 λ	100 λ	10	20	45°	3.10
5	2 λ	400 λ	10	20	60°	3.11
6	5 λ	2500 λ	20	60	60°	3.12

subprograms are called five times in the subroutine GENEX which is in turn called once for each azimuthal mode. Thus the number of calls for the function subprograms is the product of the number of integration points in t (NT), number of integration points in ϕ (NPHI), the number of azimuthal modes (MODES) and the number of generating points on the surface of

the BOR. For a large BOR, the computer run time can become significant. It is therefore prudent to test the function subprograms for the minimum number of points of integration required for convergence before executing the main program.

2. THE SUBROUTINE GENEX

The subroutine GENEX calculates the excitation vector ($\underline{V}$) for Equation (3.8). All variables in the argument list are inputs with the exception of the excitation vector. Appendix B contains a list of variables in the argument of the subroutine GENEX.

The jth element of V^t and V^ϕ are given by

$$V_n^{t,p} = \frac{1}{\eta} \iint_s \underline{W_{j,n}^t} \cdot \underline{E^a}\, ds, \qquad j=1,2,\ldots NP-2 \qquad (3.29)$$

$$V_n^{\phi,p} = \frac{1}{\eta} \iint_s \underline{W_{j,n}^\phi} \cdot \underline{E^a}\, ds, \quad j=1,2,\ldots NP-1 \qquad (3.30)$$

where the indices j and n are the same as Equations (3.6) and (3.7), and $\underline{W}^{t\phi}$ is the testing function. The test functions are chosen by Galerkin's method and therefore are the complex conjugates of the expansion functions $\underline{J}^{t\phi}$ [Equations (3.6) and (3.7)]. $\underline{E}_p^a$ is the pth component electric field of the antenna and S denotes the surface of the radome. The representation p is a generalized for the spherical components R, θ and ϕ . These components are provided by the subroutines CIRCTHETA, CIRCRHO, and CIRCPHI.

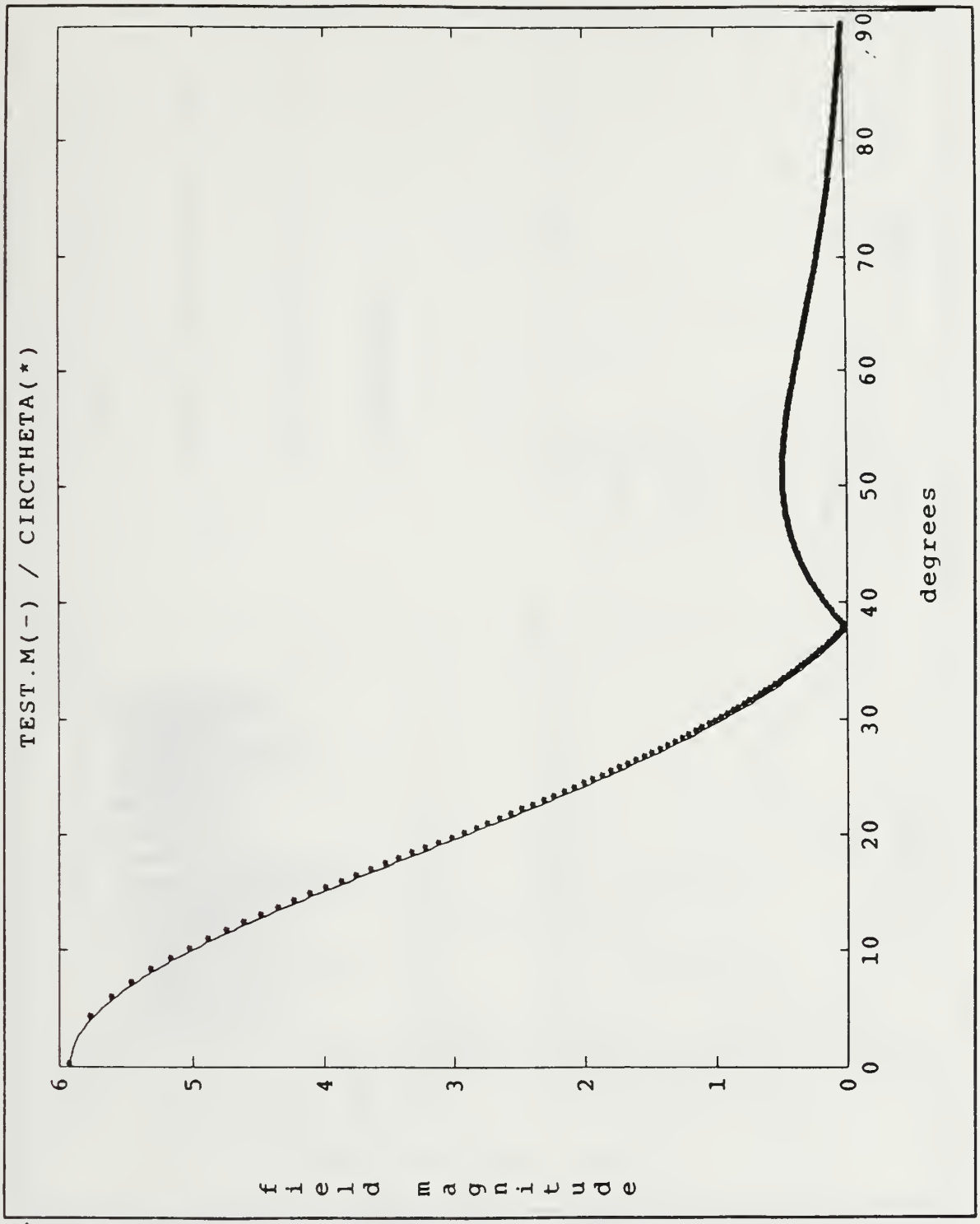

Figure 3.4 Test 1.

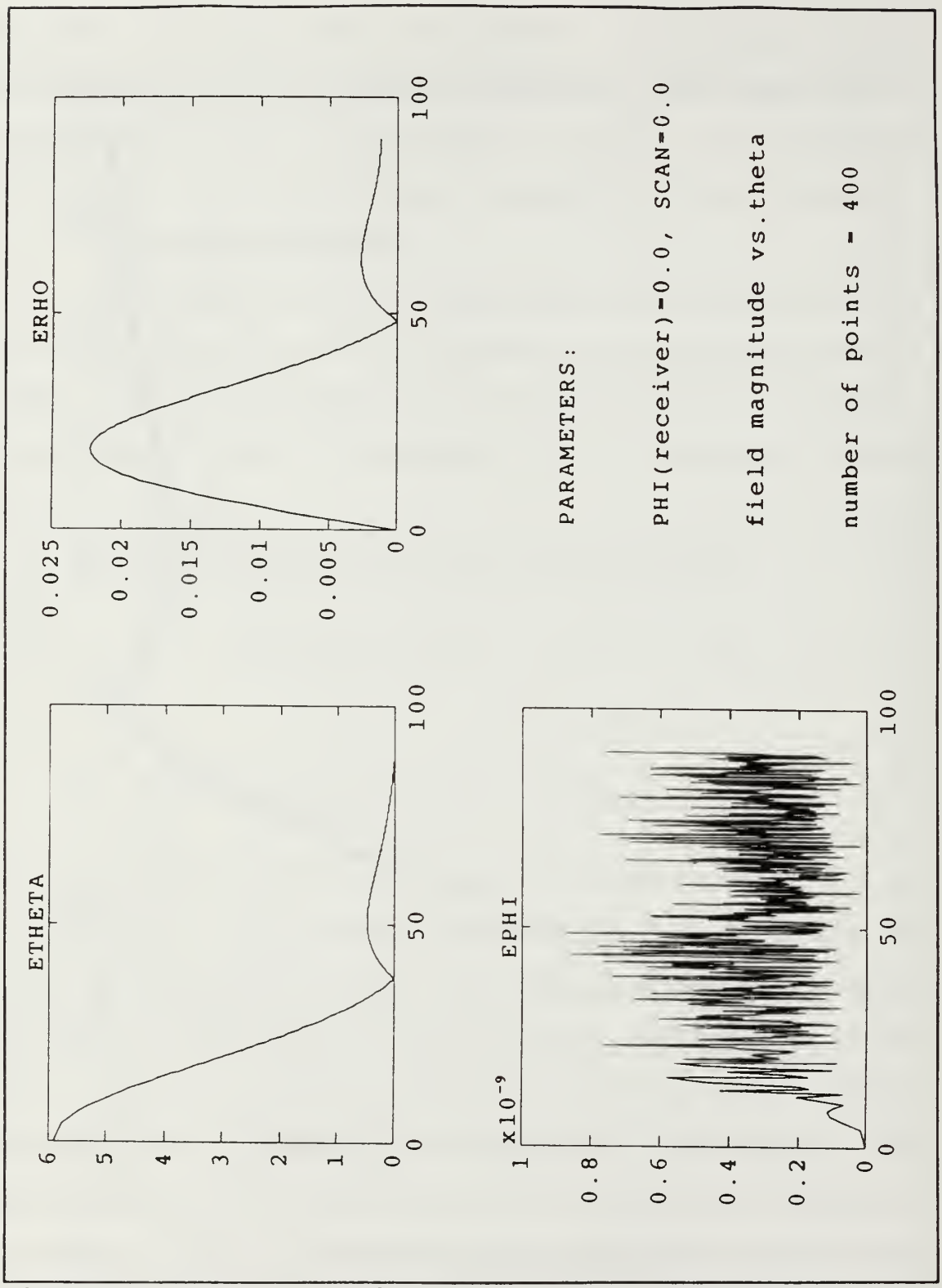

Figure 3.5 Test 1, $E(R,\theta,\phi)$ Calculated by CIRCSUB.F.

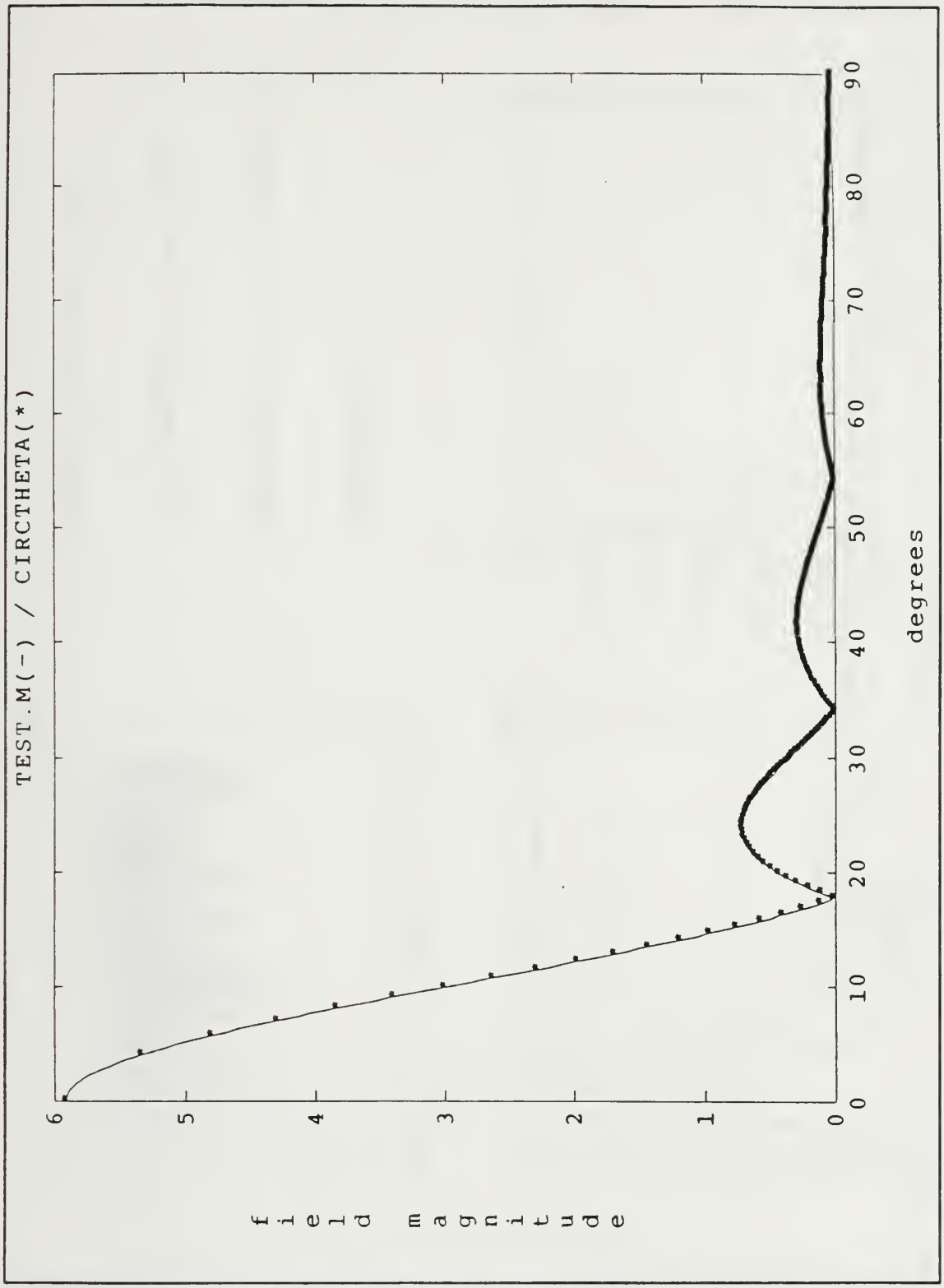

Figure 3.6 Test 2.

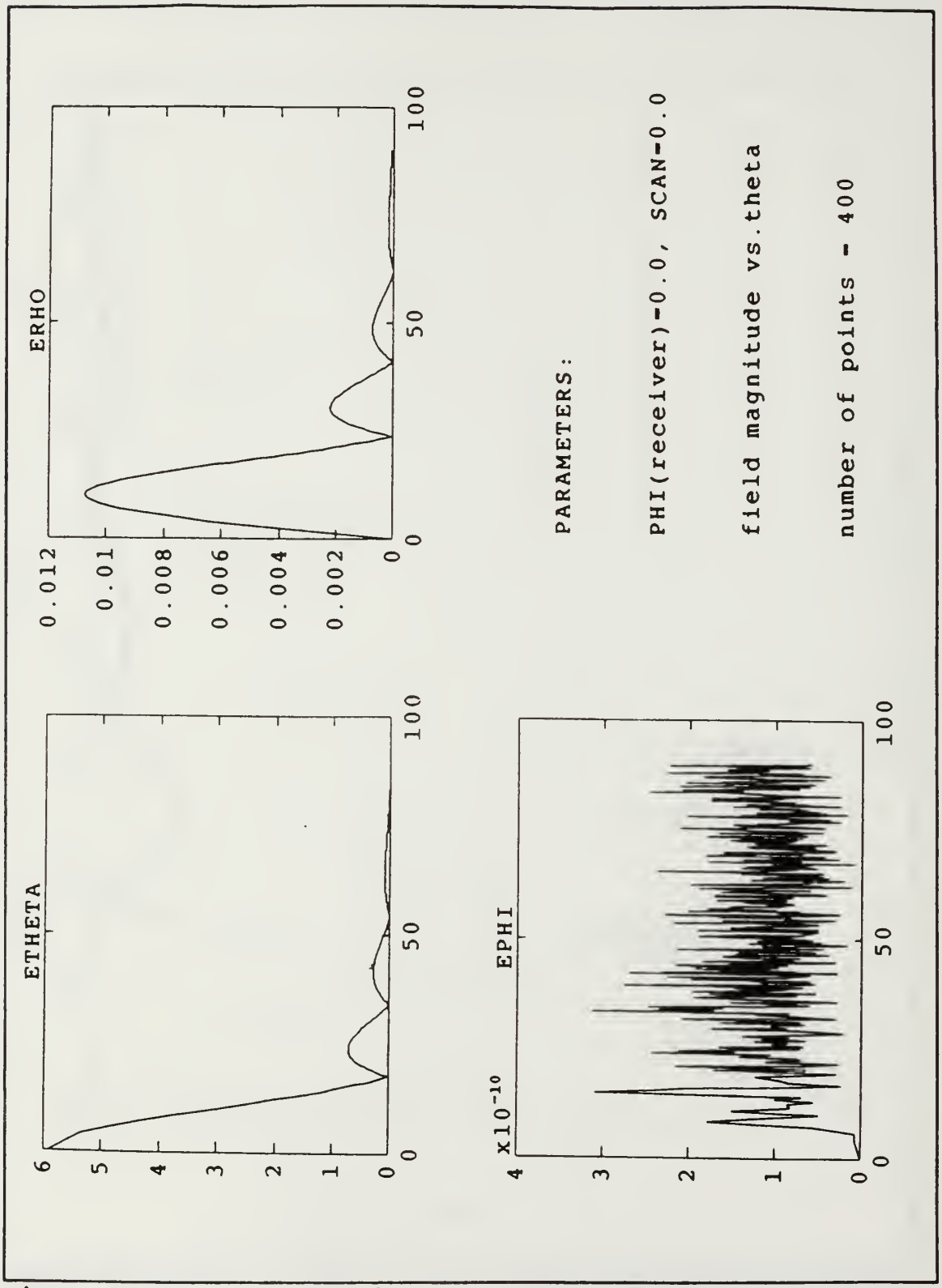

Figure 3.7 Test 2, $E(R,\theta,\phi)$ Calculated by CIRCSUB.F.

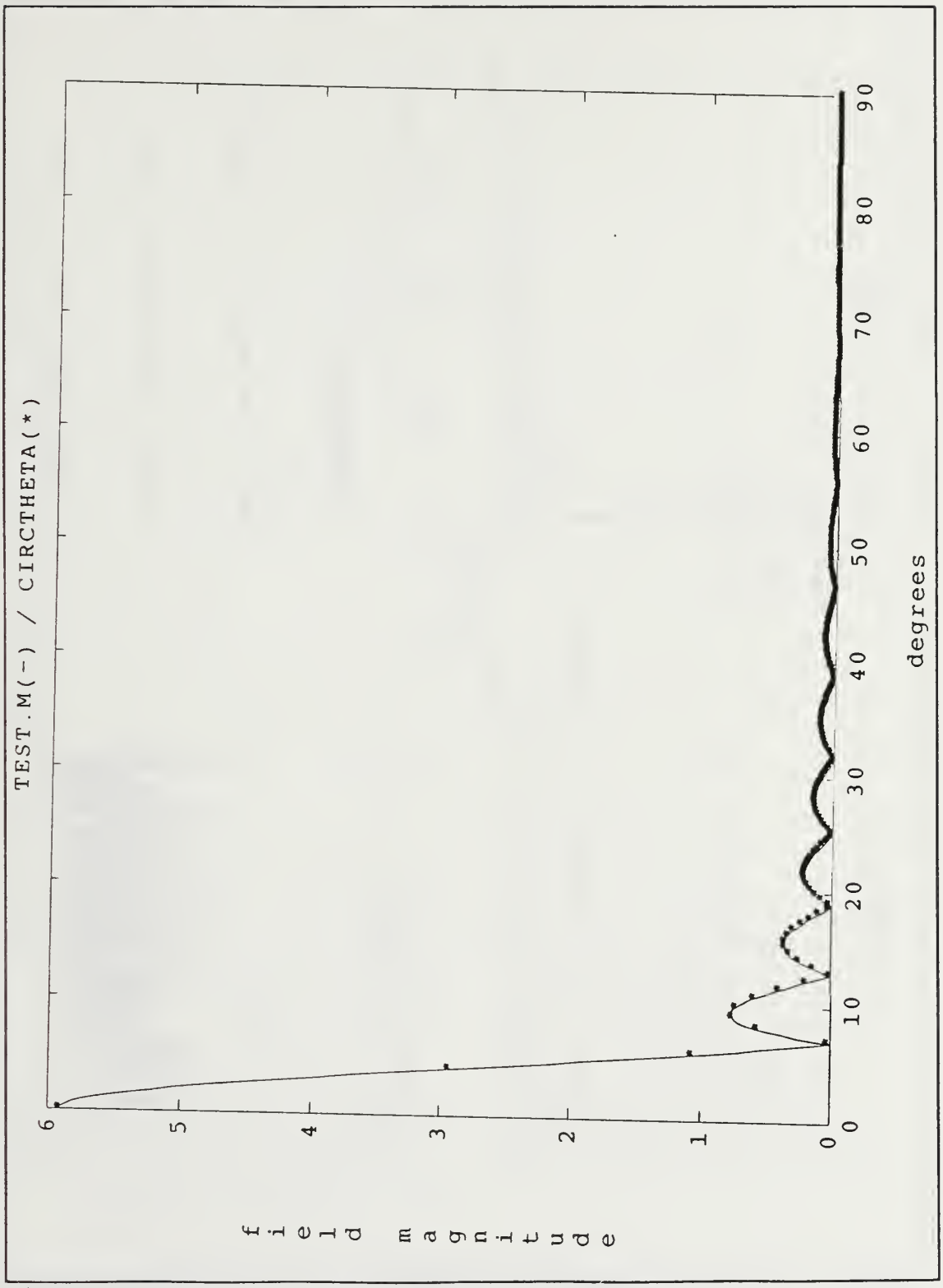

Figure 3.8 Test 3.

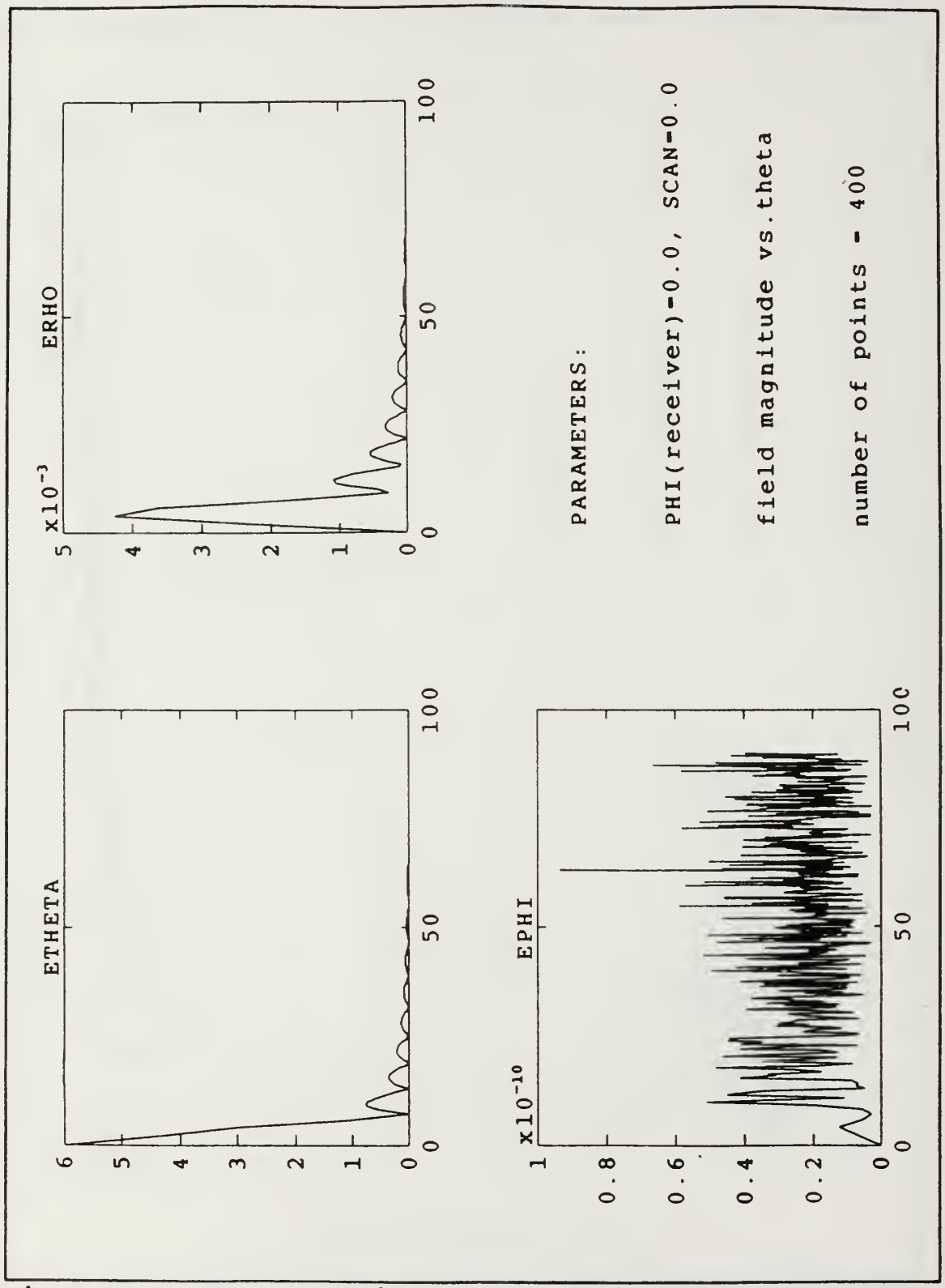

Figure 3.9 Test 3, $E(R,\theta,\phi)$ Calculated by CIRCSUB.F.

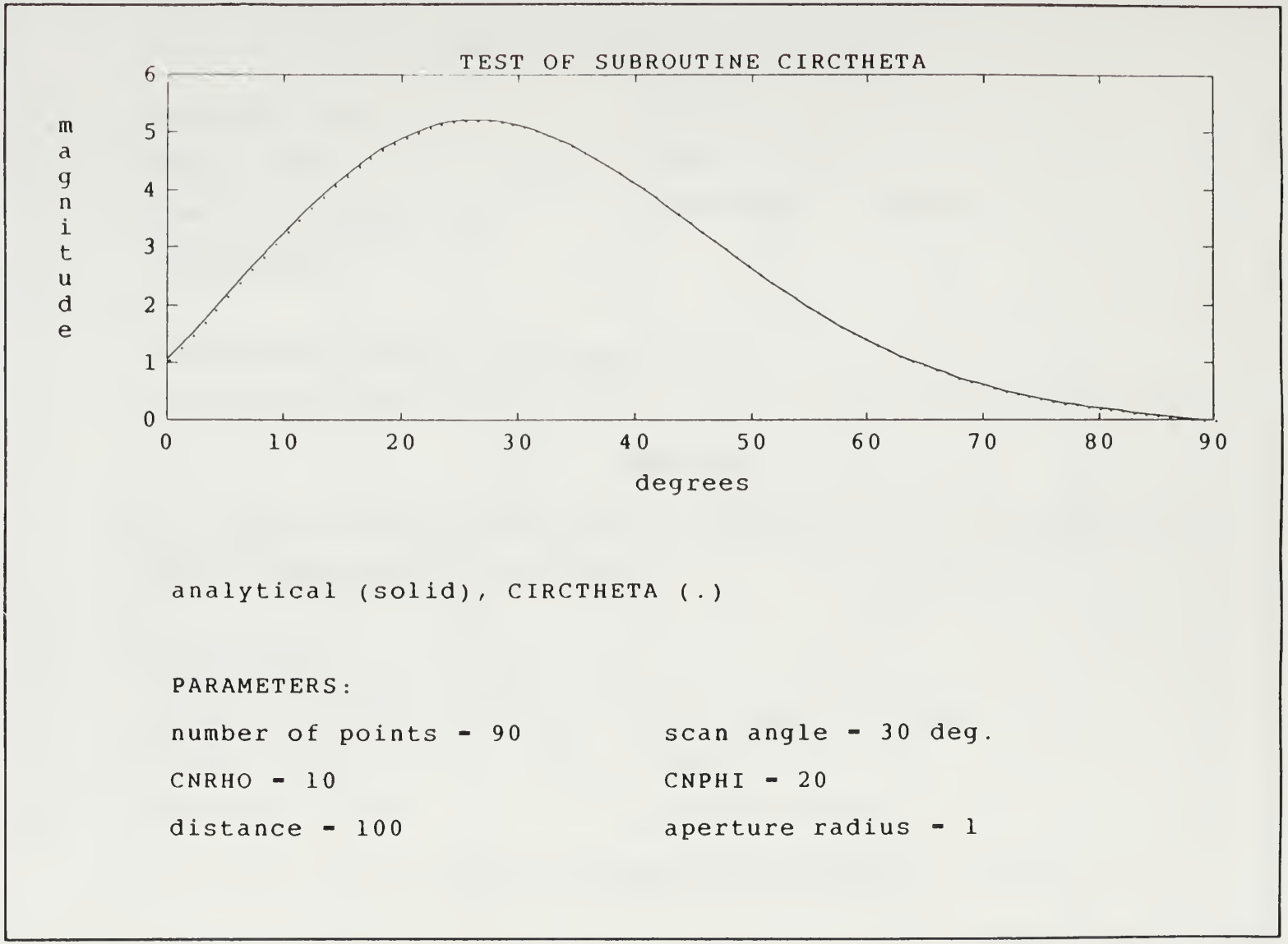

Figure 3.10 Test 4, θ Scanned to 30 Degrees.

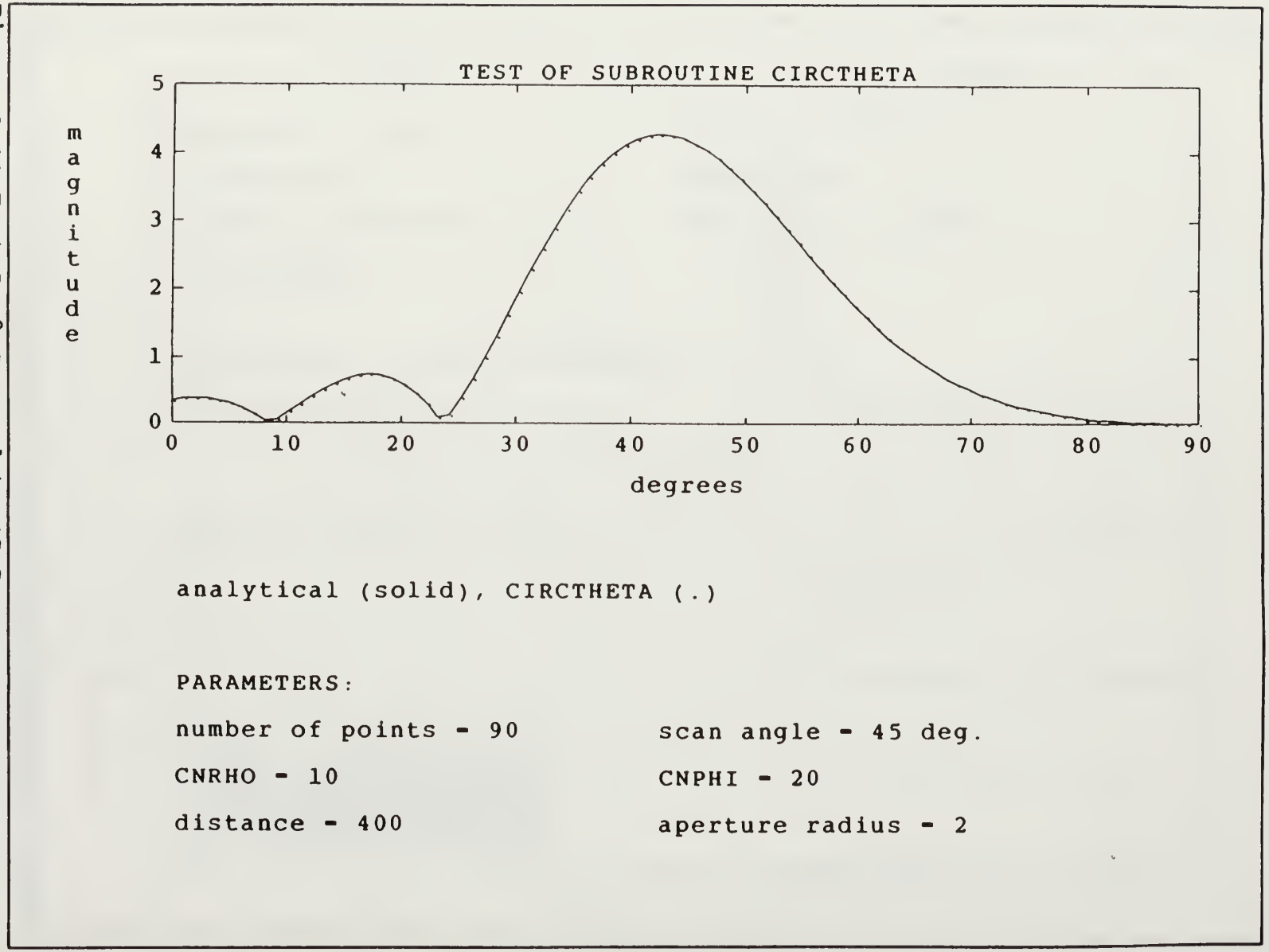

Figure 3.11 Test 5, θ Scanned to 45 Degrees.

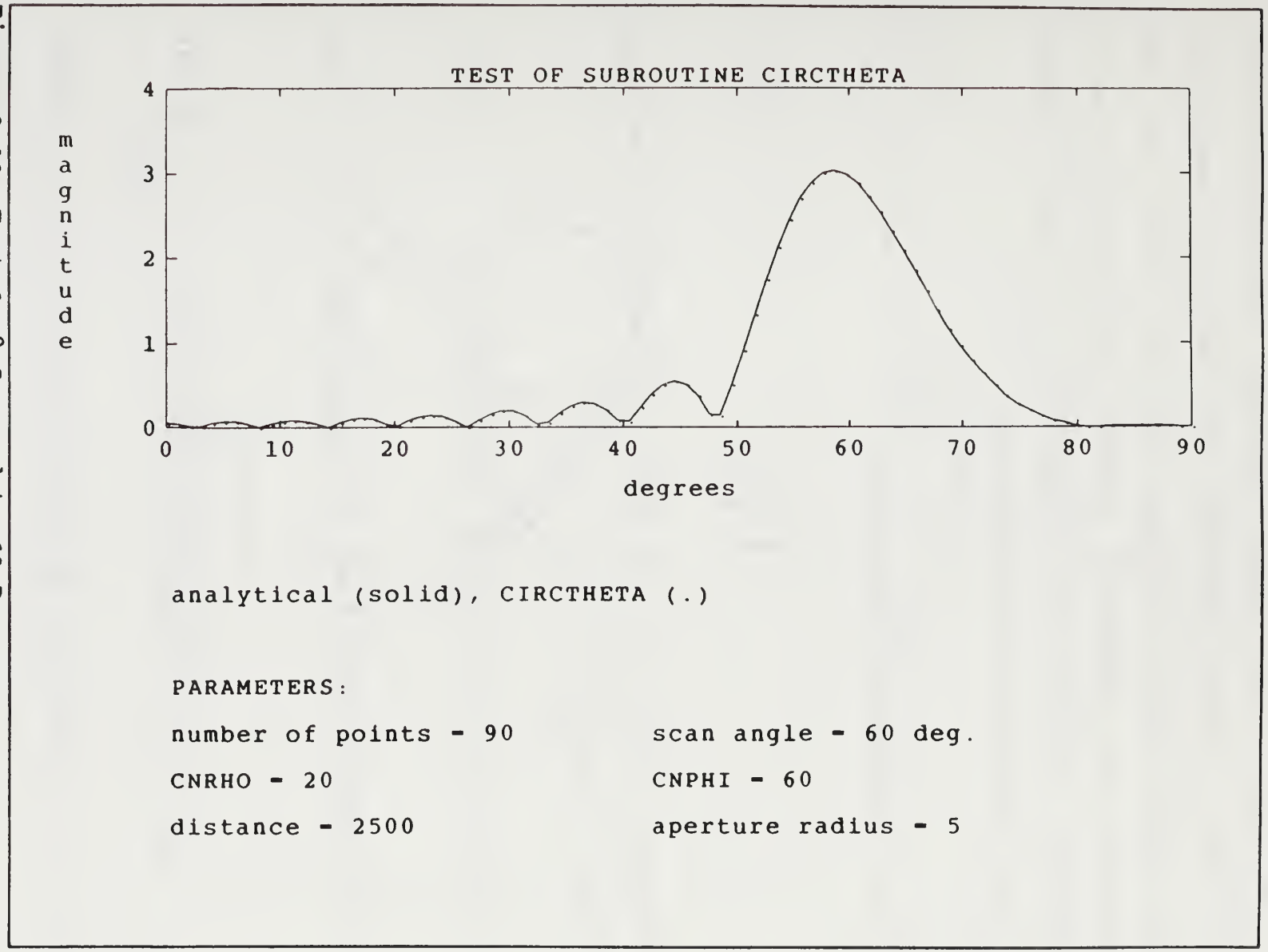

Figure 3.12 Test 6, θ Scanned to 60 Degrees.

The quantities E_R, E_θ and E_ϕ completely define $\underline{E}^a$ and are used by GENEX to evaluate Equations (3.28) and (3.29) numerically. To further reduce equations (3.28) and (3.29) to a form suitable for programming requires evaluation of the dot products. Referring to Figure 3.13, the tangent direction along the surface can be written as

$$\hat{t} = \hat{r} \sin\nu_i + \hat{z} \cos\nu_i \tag{3.31}$$

By the orthogonality properties

$$\begin{aligned} \hat{\phi} \cdot \hat{R} &= 0 \\ \hat{\phi} \cdot \hat{\theta} &= 0 \\ \hat{t} \cdot \hat{\phi} &= 0 \ . \end{aligned} \tag{3.32}$$

Therefore, from (3.28) and (3.29) $V^{t\phi}=V^{\phi R}=V^{\phi\theta}=0$. The remaining elements are

$$V_{ni}^{tR} = \int_\phi e^{-jn\phi} \left[\int_{\Delta_i} T_i^+ \, CF_i \, E_R \, dt + \int_{\Delta_{i+1}} T_i^- \, CF_{i+1} \, E_R \, dt \right] d\phi \tag{3.33}$$

$$V_{ni}^{t\theta} = \int_\phi e^{-jn\phi} \left[\int_{\Delta_i} T_i^+ \, SF_i \, E_\theta \, dt + \int_{\Delta_{i+1}} T_i^- \, SF_{i+1} \, E_\theta \, dt \right] d\phi \tag{3.34}$$

$$V_{ni}^{\phi\phi} = \int_\phi e^{-jn\phi} \int_{\Delta_i} \frac{E_\phi}{r_i} \, P_i \, dt \, d\phi \tag{3.35}$$

$$\Delta_i = t_{i+1}^- - t_i^- \tag{3.36}$$

$$\Delta_{i+1} = t_{i+2}^{-} - t_{i+1}^{-} \tag{3.37}$$

$$T_i^{\pm} = \frac{1}{2} \pm \frac{t}{\Delta_i} \tag{3.38}$$

$$SF_i = \sin(\nu_i - \theta') \tag{3.39}$$

$$CF_i = \cos(\nu_i - \theta') \ . \tag{3.40}$$

The quantities are defined in Figures 3.2 and 3.13. The

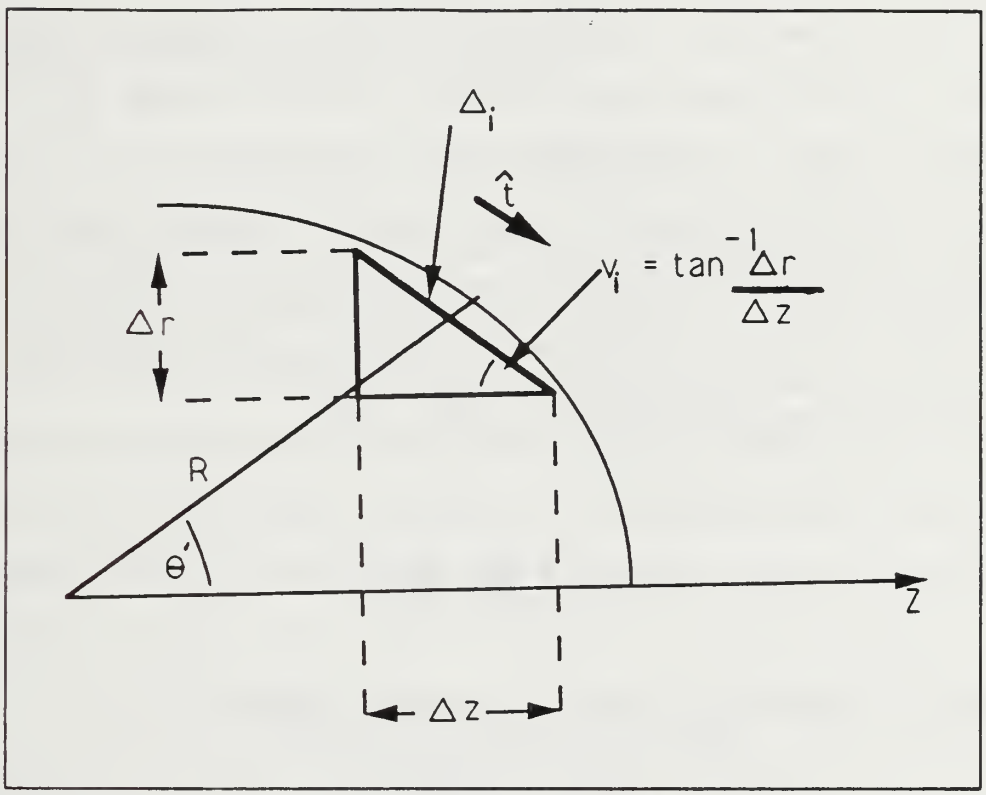

Figure 3.13 Geometry for Equations (3.30) through (3.39)

elements of the excitation vector ($\underline{V}$) are stored in the global variable R, where

$V_i^{t\theta}+V_i^{tR}$ is in R(i) i=1 to NP-2

$V_i^{\phi\phi}$ is in R(i+MT) i=1 to NP-1

and MT=NP-2 [Ref. 7: p. 57].

C. MODIFICATION OF THE IMPEDANCE MATRIX FOR DIELECTRICS

1. THIN-SHELL APPROXIMATIONS FOR DIELECTRICS

For a perfect conductor the surface resistance (R_s) is zero. To satisfy the boundary condition requires

$$\underline{E_i} = -\underline{E_s} \tag{3.41}$$

for the tangential components of the incident and scattered fields. In this case the incident field is that due to the antenna. When a dielectric body is present, the incident electric field produces a polarization current rather than a conduction current. In this case the boundary conditions state that the electric and magnetic fields must be continuous. The total electric and magnetic fields are

$$\begin{aligned} \underline{E} &= \underline{E^a} + \underline{E^s} \\ \underline{H} &= \underline{H^a} + \underline{H^s} \ . \end{aligned} \tag{3.42}$$

Maxwell's equations must be satisfied where

$$\nabla \times \underline{E} = -j\omega\mu_o \underline{H} \tag{3.43}$$

and by superposition

$$\nabla \times \underline{E^s} = -j\omega\mu_o \underline{H^s} \qquad (3.44)$$

so that

$$\nabla \times \underline{H} = j\omega\varepsilon_o \underline{E} + j\omega(\varepsilon - \varepsilon_o)\underline{E} \qquad (3.45)$$

where the second term on the right side of Equation (3.44) is nonzero for $\varepsilon \neq \varepsilon_o$.

The polarization current may be defined as

$$\underline{J_p} \equiv j\omega(\varepsilon - \varepsilon_o)\underline{E} \quad . \qquad (3.46)$$

Maxwells' second equation becomes

$$\nabla \times \underline{H_s} = j\omega\varepsilon_o \underline{E_s} + \underline{J_p} \; . \qquad (3.47)$$

Thus $\underline{E}_s$ and $\underline{H}_s$ can be determined from the polarization current ($\underline{J}_p$) radiating in free space. For dielectric bodies with $\varepsilon_r >> 1$ or very thin dielectric shells with thickness $t << \lambda$, the tangential component of the polarization current will be much greater than the normal component. In these cases the normal component can be neglected and a modified form of the EFIE results

$$L(\underline{J_p}) + \frac{1}{j\omega(\varepsilon - \varepsilon_o)t}\underline{J_p} = \underline{E^a} \qquad (3.48)$$

where the coefficient of $\underline{J}_p$ is called the surface loading or surface impedance (R_s). (Frequently it is referred to as a surface impedance because it can be complex. Here it will be called a resistance to avoid confusion with the surface

impedance approximation in which both electric and magnetic currents are allowed.) For a lossless material R_s is imaginary; for a resistive material it is real.

The new matrix equation corresponding to Equation (3.8) is

$$[I] = [Z_{MM} + Z_L]^{-1} [V] \qquad (3.49)$$

where

$$Z_{MM} = \iint_S \underline{W_m} \cdot L(\underline{J_p})\, ds \qquad (3.50)$$

$$Z_L = \iint_S \underline{W_m} \cdot R_s\, \underline{J_p}\, ds\ . \qquad (3.51)$$

2. EVALUATING THE IMPEDANCE MATRIX

The impedance matrix (Z) of Equation (3.8) is calculated by the subroutines ZMAT, ZLOAD, and ZTOT. If for some reason the impedance of the radome is zero (a perfect conductor), only the original impedance matrix from ZMAT is needed. For other materials the load impedance is calculated by ZLOAD and added to the ZMAT result by the subroutine ZTOT.

The thin shell approximation assumes the thickness(t) is much less than the wavelength (λ) and the skin depth (δ) of the shell material. This is a valid assumption for most practical radome designs and materials. The polarization current is primarily tangential to the surface of the dielectric and the normal components are negligible. This approximation is applicable to lossy as well as loss free

dielectrics. In the lossy case the load matrix (Z_L) has a real and imaginary component, while the loss free case is purely reactive.

At this point it is necessary to relate the surface impedance to the electrical properties of the material such as the dielectric constant and loss tangent. The electric field due to a thin dielectric shell is given by equation (3.48) with R_s defined by

$$R_S = \frac{1}{j\omega\Delta\varepsilon t} \tag{3.52}$$

where $\Delta\epsilon=\epsilon-\epsilon_o$ [Ref. 11: pp. 531,532]. As stated earlier, the dielectric constant of the shell may be complex. Letting $\epsilon=\epsilon'-j\epsilon''$ gives

$$R_S = \frac{1}{j\omega\,(\varepsilon'-j\varepsilon''-\varepsilon_o)\;t} \tag{3.53}$$

where $\varepsilon'=\varepsilon_o\,\varepsilon_r$. The electric loss tangent is given by

$$\tan(\delta) = \frac{\varepsilon''}{\varepsilon'} = \frac{\sigma}{\varepsilon_o\varepsilon_r} \tag{3.54}$$

where δ is the loss angle and $\sigma=\omega\varepsilon''$ is the conductivity representing all losses in the medium. Therefore the loss tangent is a measure of the power loss in the medium. A medium is a good conductor if $\sigma>>\omega\varepsilon$, and a good insulator if $\sigma<<\omega\varepsilon$ [Ref. 2: pp. 342,343]. For $\omega\varepsilon_o \cong 1/60\lambda$ and thickness $t=n\lambda$, substitution of (3.58) into (3.53) yields

$$R_S = \frac{60}{n[j(\varepsilon_r - 1) + \varepsilon_r \tan\delta]} \quad . \qquad (3.55)$$

Typical radome materials have $2 \leq \epsilon_r \leq 10$ and $0.0005 \leq \tan \delta \leq 0.005$. Inhomogeneous radomes (i.e. sandwiches) can be treated by using an equivalent dielectric constant.

IV. PROGRAM DESCRIPTION

A. DATA FLOW

The program LDBORMM.F has eight subroutines and four function subprograms. Subroutines and functions not covered here are documented in reference [Ref. 7]. Table 4.1 gives a brief description of all subroutines and function subprograms in LDBORMM.F.

TABLE 4.1 SUMMARY OF SUBPROGRAMS

NAME	TYPE	DESCRIPTION
OGIVE	subroutine	defines the radome dimensions
GENEX	subroutine	calculates the excitation vector
ZMAT	subroutine	calculates the moment matrix
ZLOAD	subroutine	calculates the submatrix for the dielectric BOR
ZTOT	subroutine	calculates the moment matrix for dielectric BOR
DECOMP	subroutine	inverts the moment matrix
SOLVE	subroutine	calculates the current coefficients
PLANE	subroutine	calculate E far field
BLOG	function	fourth order series expansion of log(x), for $x \leq 0.1$.
CIRCTHETA CIRCRHO CIRCPHI	functions	calculate the ρ, θ and ϕ components of the electric field at a point (P).

The block diagram of Figure 4.1 shows the structure of the calls for subroutines and functions in the main program.

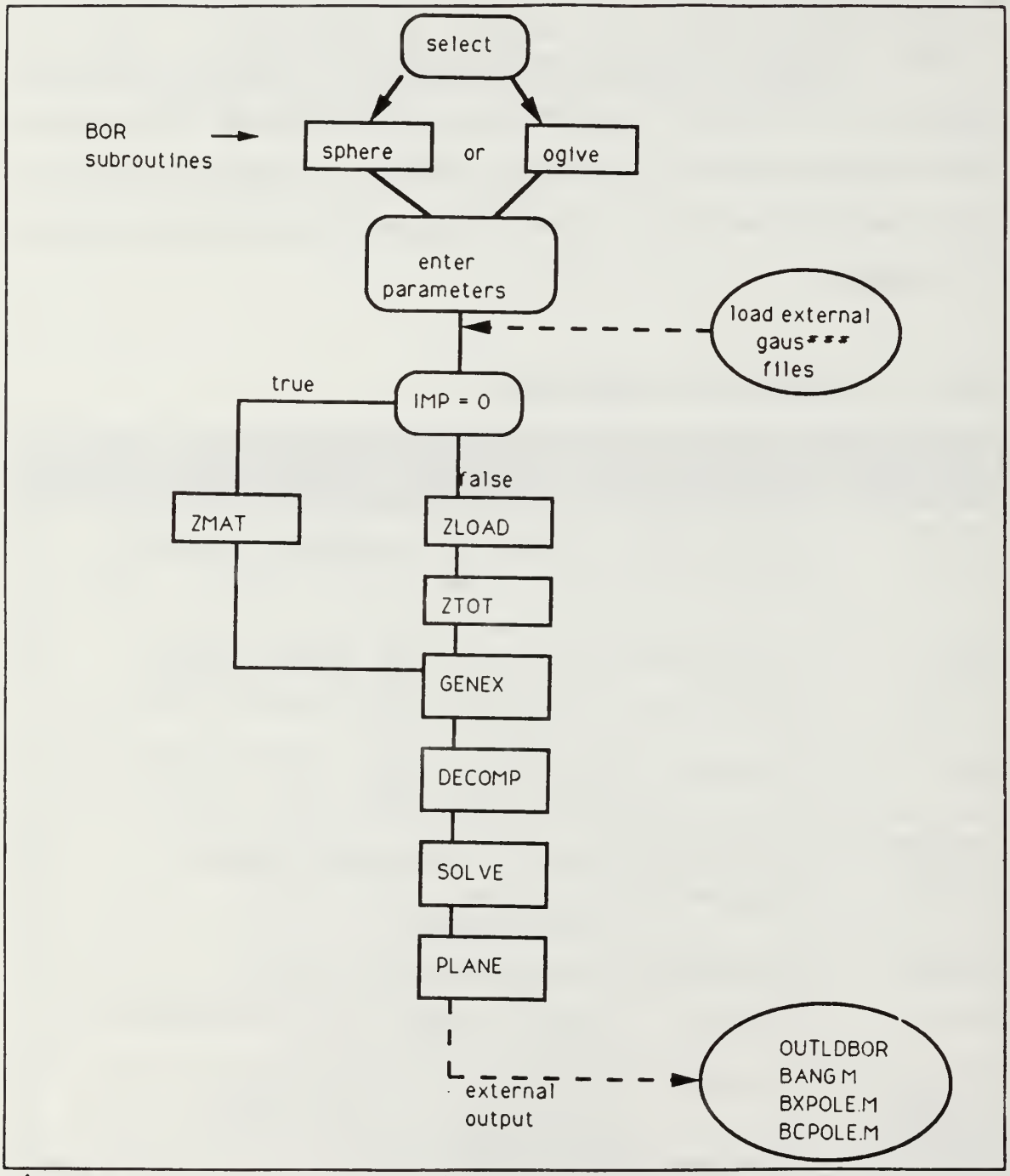

Figure 4.1 Structure of main program LDBORMM.F.

B. PROGRAM PARAMETERS

1. NUMBER OF POINTS ON BOR

The number of points (NP) must be at least 3 but less than or equal to 400. This restriction is due to the array dimensions set in the code and is not a limitation in the solution. The subroutine **OGIVE** generates segments on the surface of the BOR at approximately one tenth of one wavelength. Thus, a BOR with an arc length greater than 40 λ, matrix dimensions are exceeded for the global variables RH, ZH, Z, R, B, C, ZLO, and ZL. The subroutine **TESTSPHERE** allows the user to select the number of points on the surface of a sphere. The points generated by **TESTSPHERE** are spaced uniformly in the angle θ.

2. DIRECTORY STRUCTURE

a. Subdirectory GAUS

A subdirectory named "gaus" must contain the external sequential files with the weights and abscissas for the Gaussian quadrature algorithm. The data files are generated by the program **GAUS.F**, which is executed in the subdirectory "gaus." Appendix C contains the program **GAUS.F**. The status of the files in the main program is "OLD", thereby invoking an error condition if the file does not exist. Figure 4.2 illustrates the directory structure.

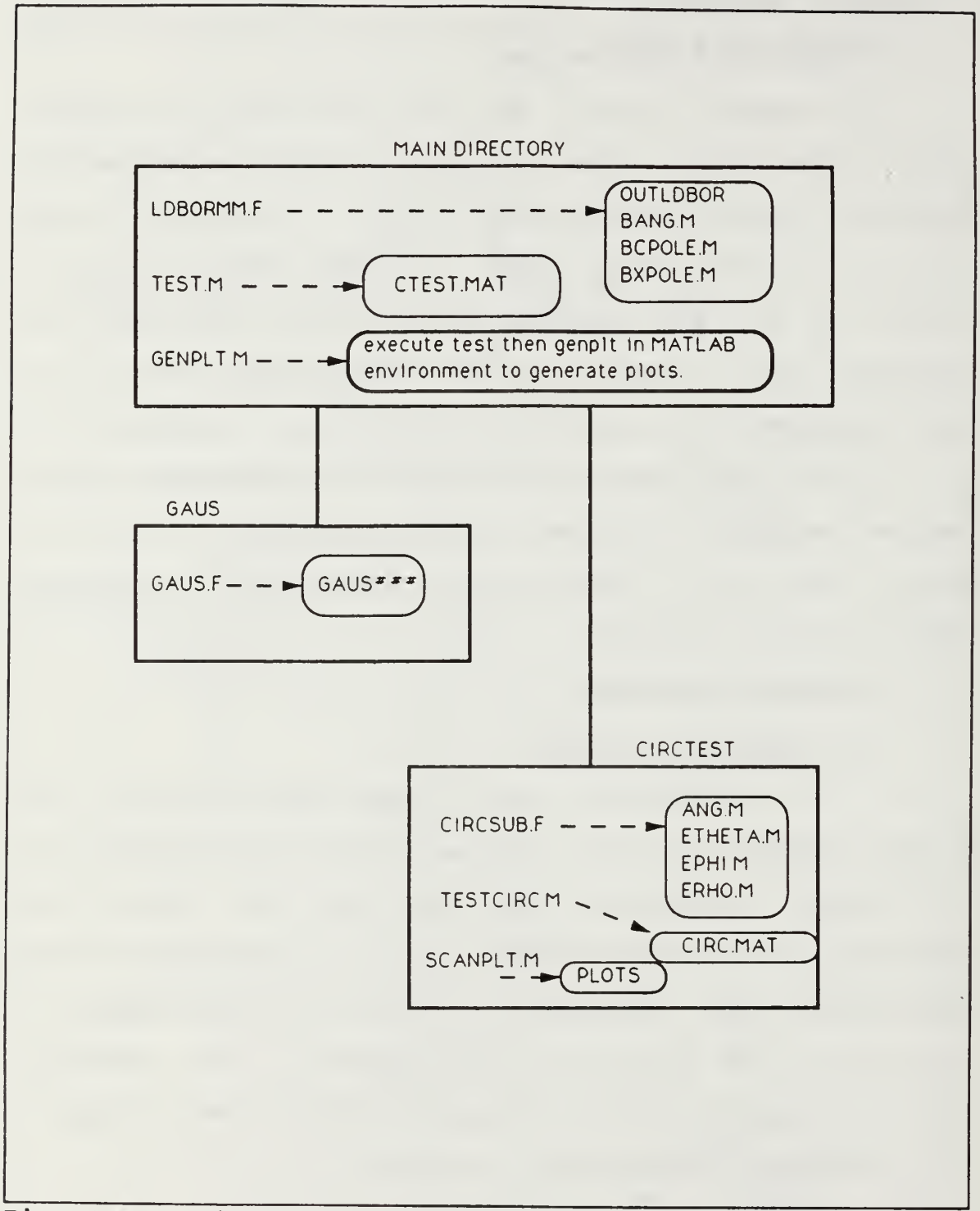

Figure 4.2 Directory Structure.

b. External Input/Output Files

The external sequential data files required for the main program are shown in Figure 4.2. The programs that generate the files are indicated by dashed lines and arrows. The dashed line originates at the generating program and the arrow terminates on the file generated.

c. The Program TEST.M

The programs TEST.M and TESTCIRC.M must be executed before the plot routines GENPLT.M and SCANPLT.M. The program TEST.M (or TESTCIRC.M) generates the analytical solution given by Equation (3.26). The parameters for BOR radius, antenna radius and scan angle are entered by the user . These parameters must be the same as the inputs to the main program. The routine GENPLT.M plots the analytical solution generated by TEST.M and the numerical solution calculated by the main program for comparison. A comparison of the two results illustrates the effect of the radome on the antenna pattern.

d. The Subdirectory CIRCTEST

The subdirectory CIRCTEST contains the programs and data files required to test for the number of terms necessary for the series approximation of the EFIE to converge to the analytic solution. The main program requires extensive execution time for large BOR or large antenna. In order to minimize run time, the minimum number of integration points over the antenna is determined by the execution of the

programs in the subdirectory CIRCTEST. The plotting routine SCANPLT.M plots the results for comparison.

Table 4.2 provides a summary of the files in this thesis.

TABLE 4.2 FILE SUMMARY

FILE NAME	PATH	DESCRIPTION
ldbormm.f	main dir./	main program, solves for the radiation pattern of radome and antenna
outldbor	main dir./	external data file for output of LDBORMM.F
bcpole.m bxpole.m bang.m	main dir./	data generated by LDBORMM.F for plotting with GENPLT.M
test.m	main dir./	program to generate solution for Eqn.(3.26)
ctest.mat	main dir./	data generated by TEST.M
genplt.m	main dir./	plotting routine
gaus.f	main dir./ gaus/	generates gaus### files
gaus###	main dir./ gaus/	data files for Gaussian quadrature integration
circsub.f	main dir./ circtest/	program to test function subprograms for minimum number of integration points
testcirc.m	main dir./ circtest	generates solution for Eqn.(3.26)
circ.mat	main dir./ circtest	data generated by TESTCIRC.M
scanplt.m	main dir./ circtest	plotting routine

C. MAIN PROGRAM MODIFICATIONS

The main program is designed in a modular fashion in order to facilitate modifications for other radome shapes, antenna types or dielectric profiles.

1. Modifications for Radome Shapes

The main program contains subprograms to generate ogive-shaped or spherical bodies of revolution. When executed the main program prompts the user for the type of BOR desired. Additional types of BORs may easily be added to the existing menu. The following modifications are required:

(a) Insert code in main program to write selection number and type of shape to screen menu.

(b) Insert code in logical block that calls subroutine generating selected shape.

(c) Append subroutine program to main program. Subroutine must return the variables NP, RH, ZH, b, R and Z'.

These variables are required for subsequent calculations and data entry to external files.

2. Modifications for Antenna Types

To modify the main program for an antenna type that is not a circular aperture:

(a) Substitute the alternate function name in the main program where ETF and EPF are assigned. These are the far field θ and ϕ components of the antenna, so a closed form approximation can be used if one exists.

(b) Substitute the alternate functions in the subroutine GENEX, to calculate the variables S1, S2, S3, S4 and S5.

(c) Append the functions to the main program.

To be consistent with the model developed earlier, the function subprograms must calculate $\underline{E}(R,\theta,\phi)$ in spherical components at points in the near field.

3. Modification of Dielectric Profile

The vector ZLO has a number of elements equal to the number of segments (NP-1) on the surface of the loaded body of revolution. The elements in the array are the complex values of the surface resistance (R_s) on each segment of the BOR. As written, the main program prompts the user to enter the complex surface impedance when the main program is executed. As presently coded, the entered value is assigned to each segment. In order to examine the effects of a nonuniform surface impedance:

(a) Modify the program to read an external sequential file of length (NP-1), with the values of the desired impedance profile.

(b) Store the values in the array ZLO in the main program before calls to ZLOAD and ZTOT. The order of storage in ZLO must correspond to the order of the coordinates stored in RH and ZH.

V. SUMMARY OF RESULTS

A. VALIDATION OF PROGRAM

In order to validate and test the main program, the surface resistance was assigned a very large value. For very large values of surface resistance, the scattered electric field ($\underline{E}^s$) approaches zero. The radiation pattern for a BOR in the far field with very large surface impedance is therefore the far field pattern of the antenna. For a circular aperture, the far field radiation pattern is given by Equation (3.26).

Figures 5.1 through 5.3 compare the values for the radiation pattern calculated by the main program and the analytic solution generated by TEST.M. The calculated values are plotted as (.) and the closed form solution to (3.26) is a solid line. The ordinate axis units are volts/meter. The abscissa is the angle from the axis of symmetry θ in degrees. The plots of Figures 5.1 to 5.3 show the magnitude of the electric field. The actual field values are complex and it is the complex values that are used to calculate the excitation elements. The figures show the parameters NP, NT, NPHI, CNRHO, CNPHI, SCAN, and ARAD as defined in Appendix B. The angle ϕ of the receiver is zero for all test cases. The number of

Figure 5.1. Convergence in Far Field, Test 1.

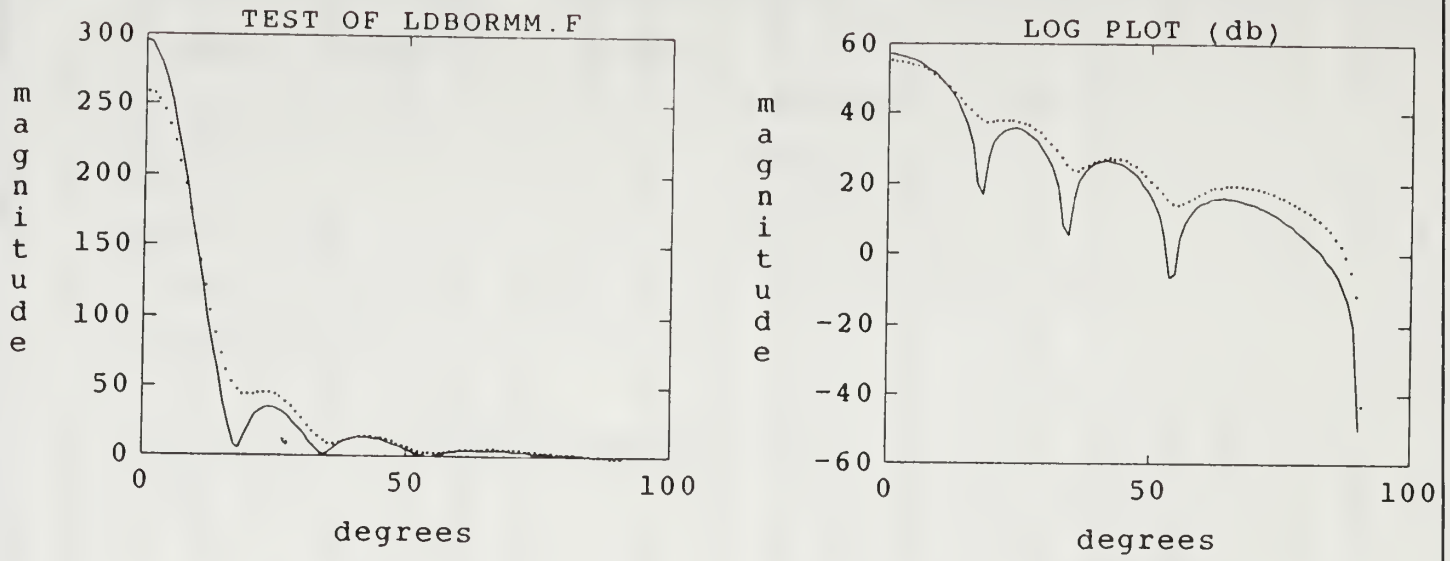

analytical (solid), LDBORMM.F(.)

PARAMETERS:

number of points = 90

NPHI = 20

NT = 2

distance = 8

complex impedance = (99999.,0.)

scan angle = 0 Deg.

CNPHI = 20

CNRHO = 10

aperture radius = 2

Figure 5.2. Convergence in Far Field, Test 2.

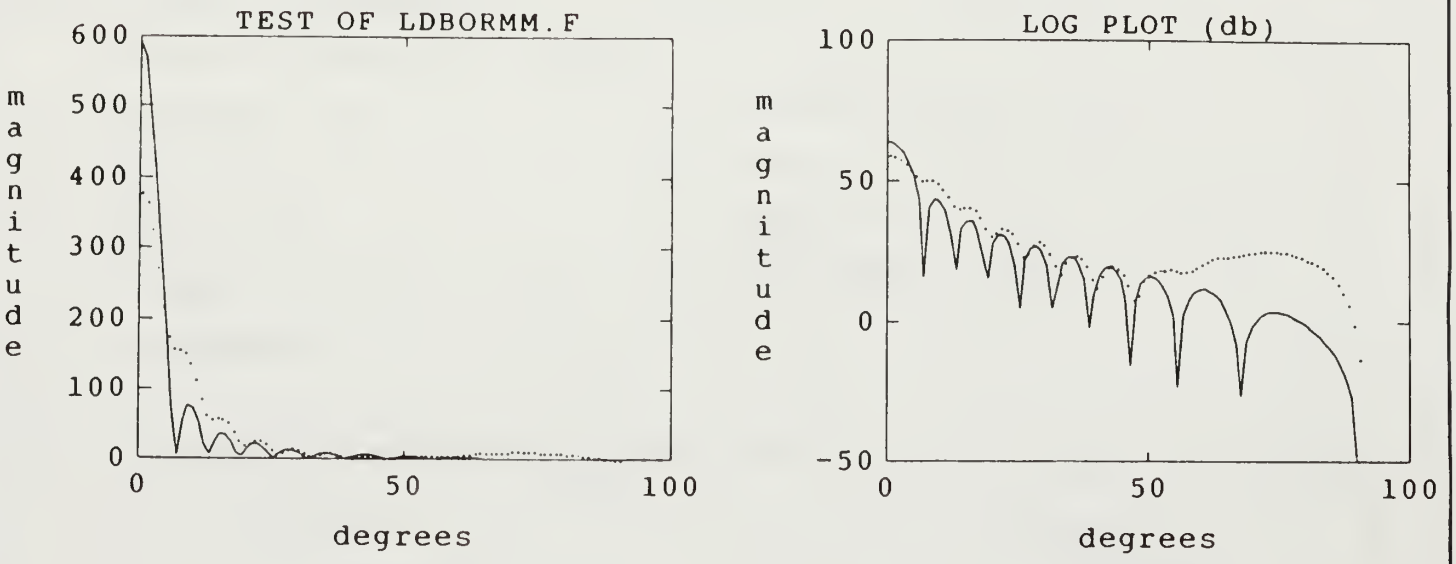

analytical (solid), LDBORMM.F(.)

PARAMETERS:

number of points - 90	scan angle - 0 Deg.
NPHI - 40	CNPHI - 40
NT - 2	CNRHO - 20
distance - 25	aperture radius - 5

complex impedance - (99999.,0.)

Figure 5.3. Convergence in Far Field, Test 3.

points of integration for the antenna were determined by the program CIRCSUB.F to insure that aperture integrations converged. Figures 3.4, 3.6, and 3.8 show the results. The number of points of integration needed over the BOR surface (NT and NPHI) becomes very large as the radial extent (hence circumference) of the radome increases. In addition to an increase in the number of integration points required, the number of azimuthal modes also increases for a large BOR. In all test cases the mode number is one ($n=\pm 1$). Test results indicate more points of integration and higher modes are required for the calculated values to converge to the analytic solution as the antenna radius or sphere radius is increased. The execution times were in the range of 2 to 4 hours on a Sun Sparcstation 2.

Figures 5.4 through 5.6 show plots of the magnitude of the spherical electric field components for the three test cases. As expected the scattered field components ETSCAT and EPSCAT are 40 db below the source field (ETF) since in all cases R_s is 10000. EPF is zero since the antenna radiation is θ polarized in this plane. Figures 5.4 through 5.6 are plots of field magnitude versus angle θ.

The plots show the convergence of the calculated values as measured against the known analytic solution of a circular aperture in the far field. These results verify the program for the case where the radome is nearly transparent for large real surface resistance in accordance with Equation (1.1).

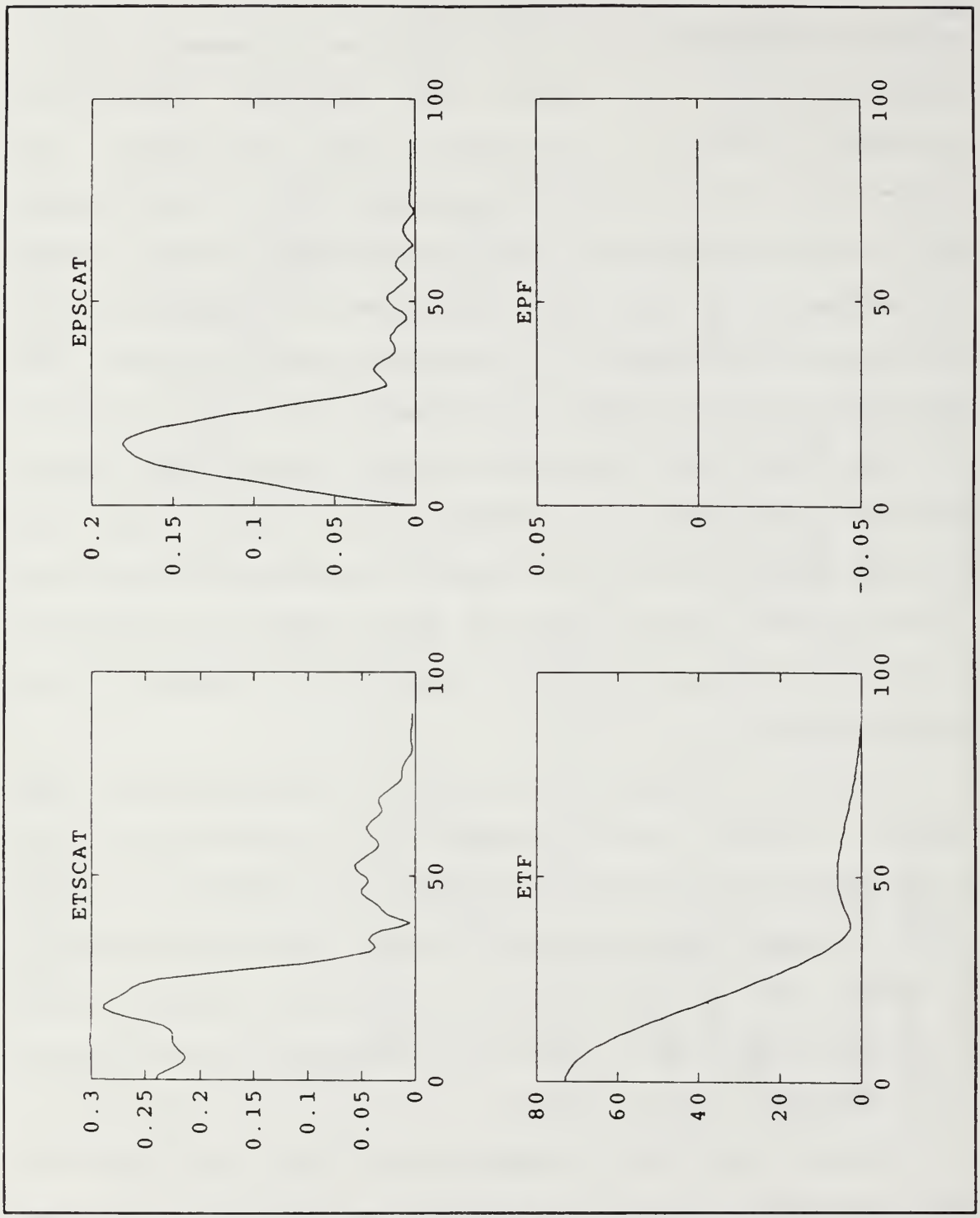

Figure 5.4 Electric Field Components Calculated by LDBORMM.F for Test 1.

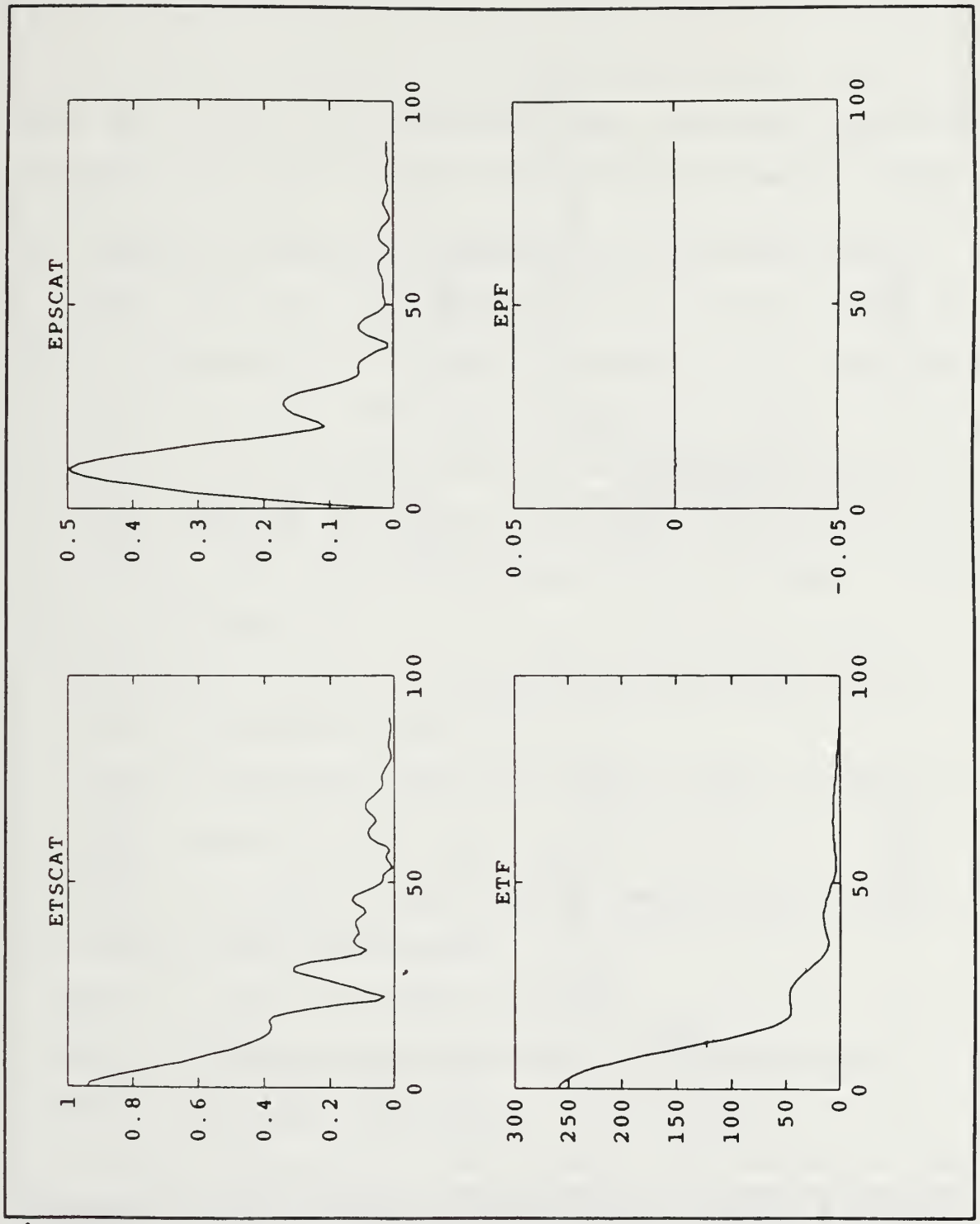

Figure 5.5 Electric Field Components Calculated by LDBORMM.F for Test 2.

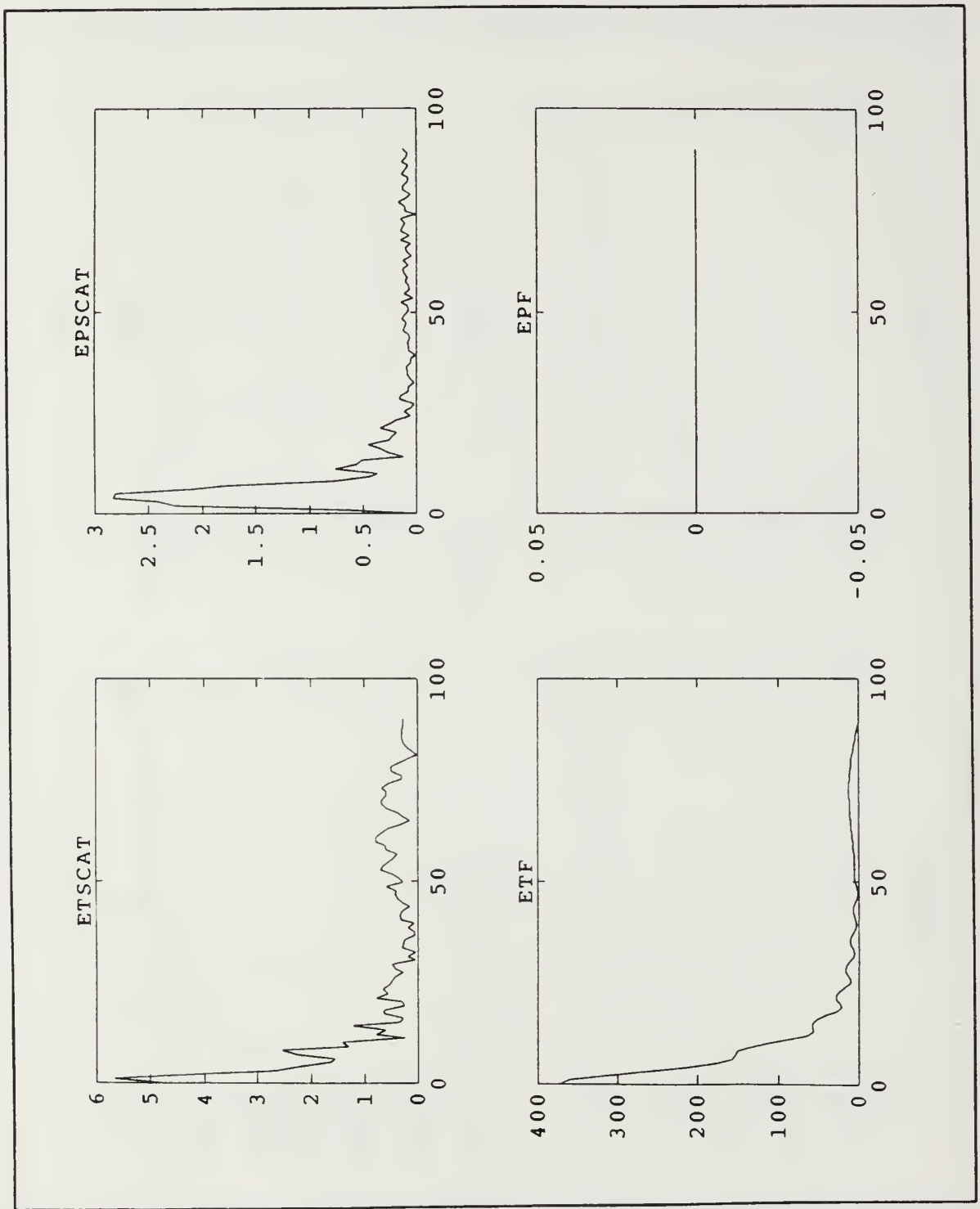

Figure 5.6 Electric Field Components Calculated by LDBORMM.F for Test 3.

When the radome is transparent the calculated radiation pattern becomes the closed form solution of the far field.

B. EFFECTS OF RADOME ON TRANSMISSION OF ELECTRIC FIELD

Test cases were conducted for various radome shapes and surface impedances. In Figures 5.7 through 5.9 the calculated radiation patterns with the radome are compared to the patterns of the isolated antenna. A comparison of the two curves illustrates the effect of the radome on the antenna's performance. The following parameters were constant for the three test cases:

* resistance = 0+j1700 Ω; (reflection coefficient $\Gamma \approx 0.2$.).
* number of azimuthal modes = 2.
* number of integration points;NT=2,NPHI=40,CNRHO=20,CNPHI=40.
* antenna radius $r_o = 2\lambda$.
* radius of the BOR base was 3λ (open base-no body structure).

The radome shapes tested were:

* TEST 1. a sphere of radius, $R=3\lambda$.
* TEST 2. a cone with the half angle = 30°.
* TEST 3. an ogive with a parent circle radius $R = 7.5\lambda$.

The forward direction is the region $\theta < 90°$ while the rear hemisphere is $\theta > 90°$. The plotted data in Figures 5.8 and 5.9 have significant backscatter ($\theta > 90°$) due to the shape of the radome. The electric field magnitude of the sphere (Figure

5.7) for $\theta>90°$ was below a -20 db threshold. This threshold was arbitrarily established for purposes of plotting the data. The backscatter from the sphere is negligible since the radiation from the antenna at each point on the surface is near normal incidence. The cone and the ogive shapes reflect energy towards other parts of the surface. These multiple reflections raise the sidelobes, especially at wide angles from the antenna main beam.

The coupling of the reflected energy to the antenna is assumed to be negligible in this model. This assumption is not valid for geometries or dielectric materials which cause significant backscatter, because the reflections from the radome perturb the antenna excitation. Not only does this effect increase the sidelobes, but also causes an increase in the input VSWR. For a well designed radome, this mutual interaction is a secondary effect.

C. RECOMMENDATIONS FOR FURTHER STUDY

The following suggestions are made for further development and improvement of the program LDBORMM.F :

1. Obtain test data for a real system. Run the program for the data and compare the results of the computer model to the actual measured test data.
2. Develop test data from an experimental model constructed in the ECE Departmental Transient Electromagnetic Scattering Lab.

Compare the measured fields with the predictions of the computer model.

3. Perform a parametric design study to access the impact of radome shape, source location and dielectric profiles on the radiation pattern.

4. Perform an exhaustive study of the convergence properties of the MM solution.

5. To improve the execution time some of the Gaussian integration loops can be replaced with a delta function approximation for the integral.

6. Symmetry between the positive and negative modes can also be exploited to reduce run time.

This thesis has developed flexible, modular code for modeling the electric field radiation pattern for a source enclosed in a dielectric body of revolution. Further work should concentrate on validation and improvements to reduce execution time. After these enhancements are incorporated, the code can be applied to the radome design process.

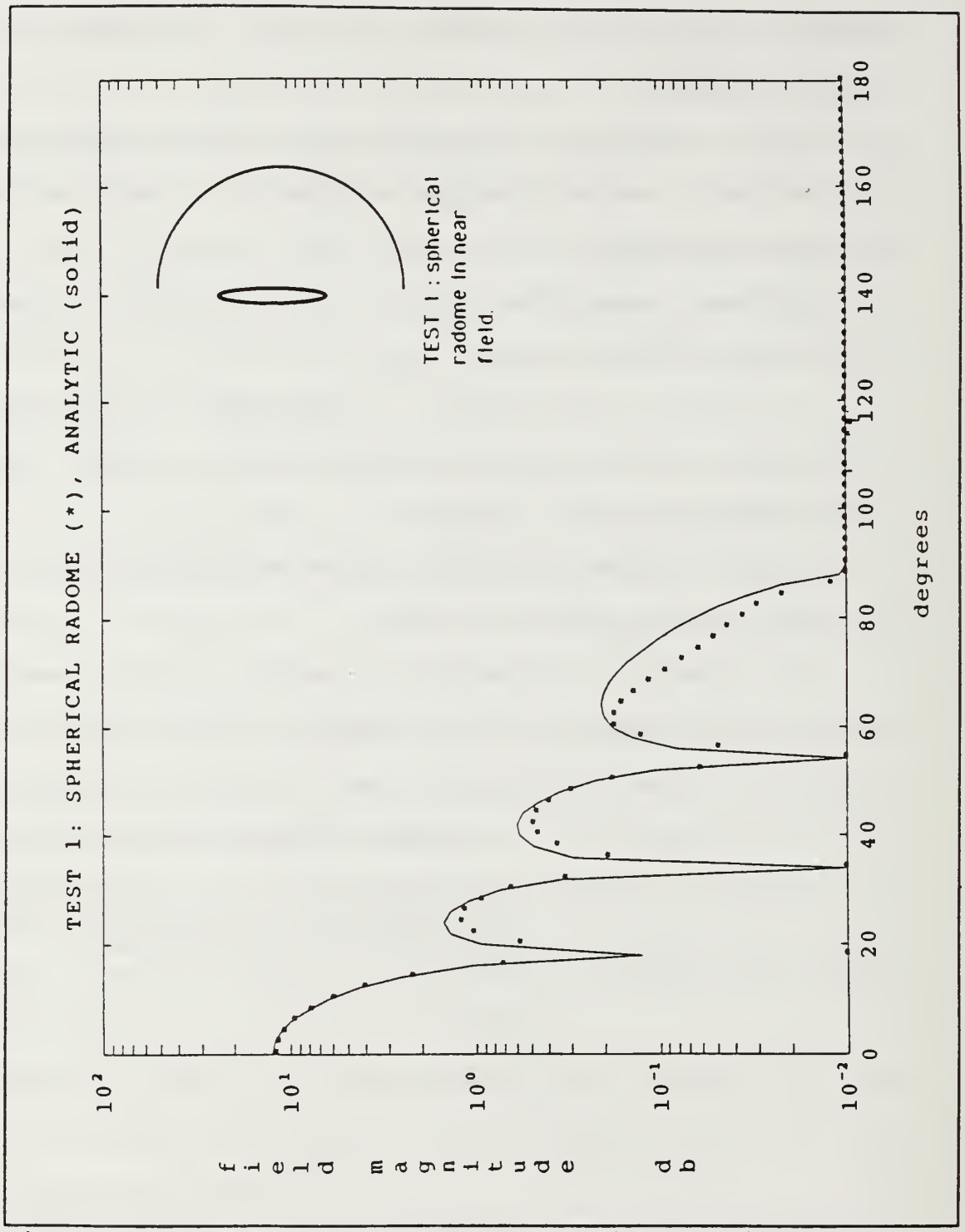

Figure 5.7 Effects of Radome on Far Field Radiation

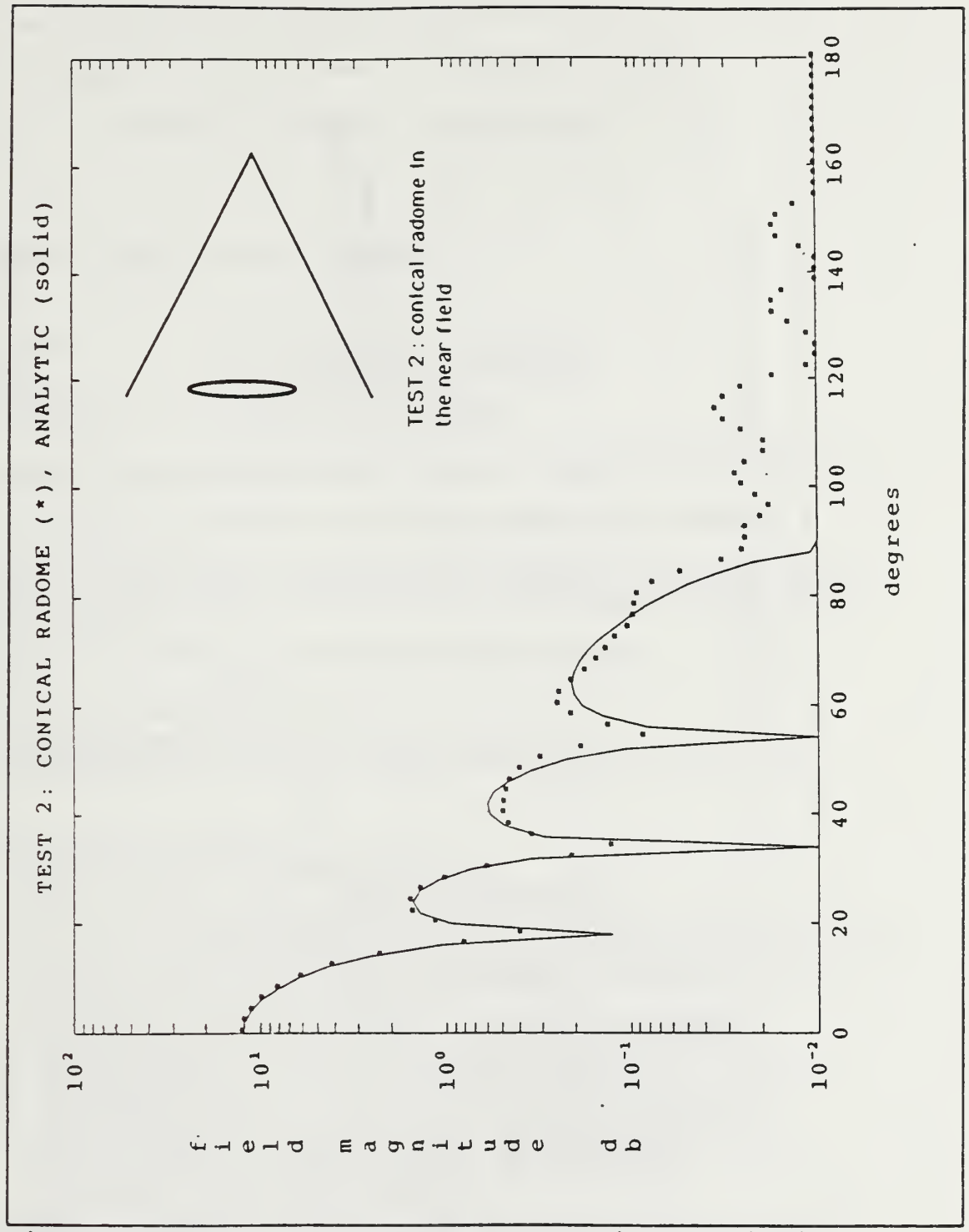

Figure 5.8 Effects of Radome on Far Field Radiation

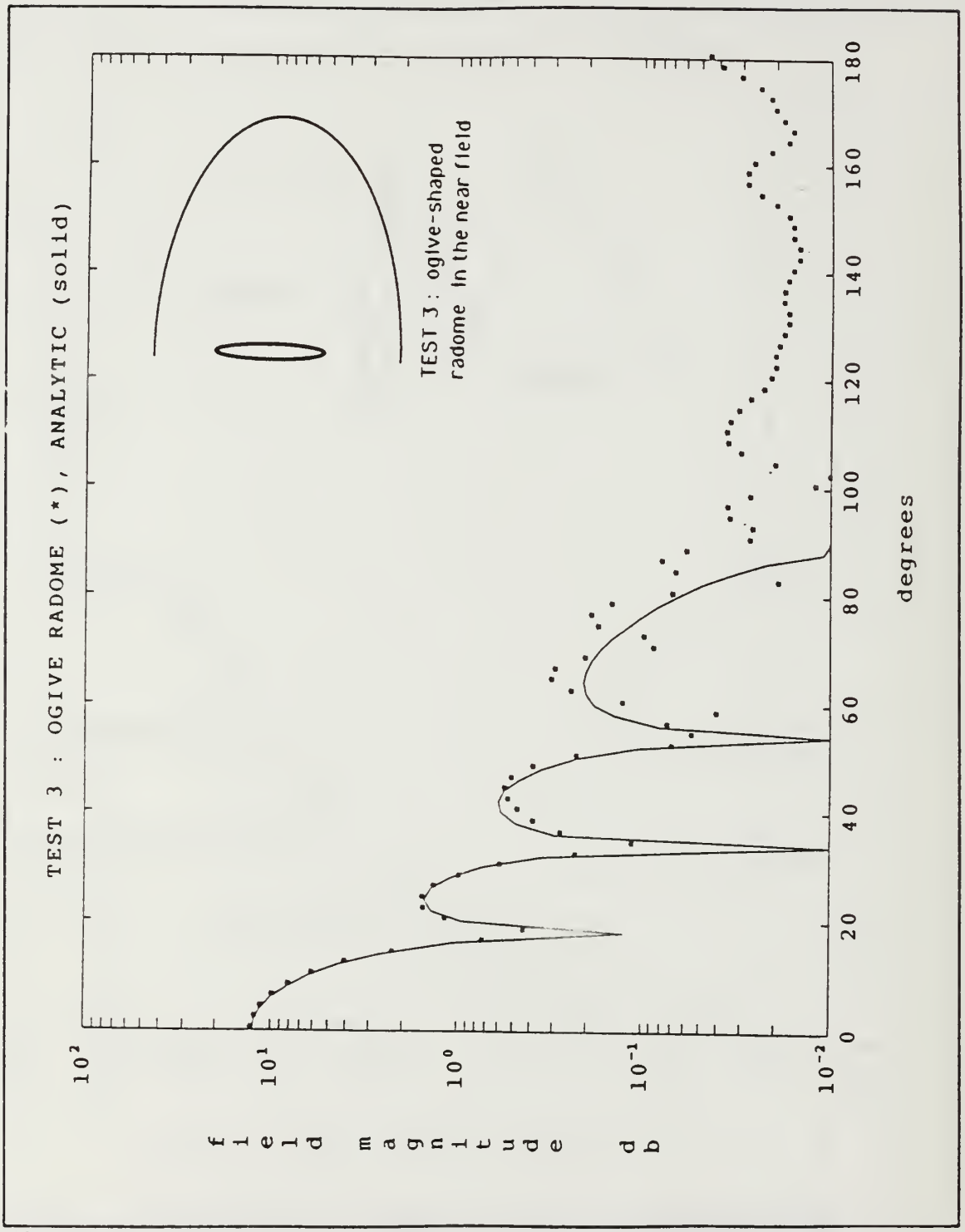

Figure 5.9 Effects of Radome on Far Field Radiation

APPENDIX A. SOURCE CODE AND DATA FILE

A. SOURCE CODE FOR MAIN PROGRAM

```
C  PROGRAM      :  ldbormm.f
C  DATE         :  23 January 1992
C  REVISED      :  21 February 1992
C  PROGRAMMERS : D. JENN, R. FRANCIS
C
C >> SPECIALIZED FOR ARBITRARY CIRCULAR APERTURE EXCITATION <<

C >> EXCITATION IS SPECIFIED IN THE SUBROUTINE GENEX (....) <<
C
c  BASED ON MAUTZ AND HARRINGTON'S COMPUTER PROG FOR BORS.
c  all or part of the surface may be covered with a surface
c  impedance.
C  SOURCE IS AT BOR COORDINATE SYSTEM ORIGIN.
C
c   imp=0 perfect conductor
c   iprint=0 print pattern points to unit 8
c   iseg=0 print the generating curve points to unit 8


C BEGIN MAIN PROGRAM************
      CHARACTER*8 GNT,GNPHI,CGR,CGP
      CHARACTER*14 TPTS,PPTS,PHIPTS,RHOPTS
      COMPLEX EP,ET,Z(100000),R(1600),B(1600),C(800),U,UC
      COMPLEXET1,EP1,ET2,EP2,EC,EX,ZL0(400),ZL(2400),ETF,EPF
      COMPLEX EXP1,EXP2,CONJG,CEXP,CMPLX,CT(3000),IMP,JK
      COMPLEX CIRCTHETA,CIRCPHI
      DIMENSION RH(400),ZH(400),XT(4),AT(4),IPS(800)
      DIMENSION A(100),X(100),EXP(500),ANG(500),ECP(500)
      DIMENSION XP(100),AP(100),XR(50),AR(50)
      DIMENSION ECV(500),EXV(500),PHC(500),PHX(500)
      REAL ETSCAT(500),EPSCAT(500),ETHF(500),EPHF(500)
      INTEGER NT,NPHI,CNRHO,CNPHI,NP,SELECTION
      REAL MODE,BASE,RS,ZP,RHB,ZHB
      DATA PI,START,STOP/3.1415926,0.,90./
      DATA IPRINT/0/
      Rad=PI/180.
      ECX=0.
      BK=2.*PI
      U=(0.,1.)
```

```
      U0=(0.,0.)
      UC=-U/4./PI
      JK=(0.0,6.283185307)
C Select the subroutine to generate BOR.
      WRITE(6,*)'MAKE BOR SELECTION'
      WRITE(6,*)'                                  '
      WRITE(6,*)'Enter number from menu to make selection'
      WRITE(6,*)'                                          '
      WRITE(6,*)'   Selection Number       BOR Geometry'
      WRITE(6,*)'         1                OGIVE'
      WRITE(6,*)'         2                SPHERE'
      READ(5,*)SELECTION
         IF(SELECTION.EQ.1)THEN
           CALL OGIVE(NP,ZH,RH,BASE,RS,ZP)
         ELSEIF(SELECTION.EQ.2)THEN
           CALL TESTSPHERE(NP,ZH,RH,BASE,RS,ZP)
         ENDIF


C*********CALL OGIVE or TESTSPHERE.
      IF (NP.GT.399)THEN
         WRITE(6,*)'MAXIMUM NUMBER OF POINTS(NP) IS 399'
         GOTO 999
      ENDIF
      DT=90.0/FLOAT(NP-1)
      WRITE(6,*)'ENTER THE FILENAMES gaus###'
      WRITE(6,*)'.........................'
      WRITE(6,*)'ENTER THE FILENAME IN T (NT)'
      READ(5,*)GNT
      WRITE(6,*)'ENTER THE FILENAME IN PHI (NPHI)'
      READ(5,*)GNPHI
      WRITE(6,*)'ENTER THE FILENAME IN CNRHO'
      READ(5,*)CGR
      WRITE(6,*)'ENTER THE FILENAME IN CNPHI'
      READ(5,*)CGP
C OPEN THE FILES FOR THE gaus/gaus###
      TPTS='gaus/'//GNT
      PPTS='gaus/'//GNPHI
      RHOPTS='gaus/'//CGR
      PHIPTS='gaus/'//CGP
      OPEN(1,FILE=TPTS,STATUS='
      OPEN(2,FILE=PPTS,STA
      OPEN(3,FILE=RHOPTS,
      OPEN(4,FILE=PHIPTS,STA      OLD')
      READ(1,*)NT
         IF(NT.GT.4)THEN
           WRITE(6,*)'MAXIMUM NUMBER OF POINTS(NT) IS 4'
           GOTO 999
         ENDIF
      READ(2,*)NPHI
         IF(NPHI.GT.200)THEN
```

```
            WRITE(6,*)'MAXIMUM NUMBER OF POINTS(NPHI) IS 200'
            GOTO 999
         ENDIF
      READ(3,*)CNRHO
         IF(CNRHO.GT.50)THEN
            WRITE(6,*)'MAXIMUM NUMBER OF POINTS(CNRHO) IS 50'
            GOTO 999
         ENDIF
      READ(4,*)CNPHI
         IF(CNPHI.GT.100)THEN
            WRITE(6,*)'MAXIMUM NUMBER OF POINTS(CNPHI) IS 100'
            GOTO 999
         ENDIF
C LOAD THE WEIGHTS AND ABSCISSAS IN THE VECTORS.
      DO 1 M=1,NT
         READ(1,*,END=1)XT(M),AT(M)
  1   CONTINUE
      DO 2 M=1,NPHI
          READ(2,*,END=2)X(M),A(M)
  2   CONTINUE
      DO 3 M=1,CNRHO
          READ(3,*,END=3)XR(M),AR(M)
  3   CONTINUE
      DO 4 M=1,CNPHI
          READ(4,*,END=4)XP(M),AP(M)
  4   CONTINUE
      CLOSE(1)
      CLOSE(2)
      CLOSE(3)
      CLOSE(4)
      MP=NP-1
      MT=MP-1
      N=MT+MP
C
      WRITE(6,*)'ENTER MODE (FLOAT)'
      READ(5,*)MODE
      WRITE(6,*)'ENTER PHI (observation) IN DEGREES'
      READ(5,*)P
      PHI=P*RAD
      WRITE(6,*)'ENTER THE SCAN ANGLE IN DEGREES'
      READ(5,*)SA
      SCAN=-SA*RAD
      WRITE(6,*)'ENTER COMPLEX IMPEDANCE'
      READ(5,*)IMP
      WRITE(6,*)'ENTER THE ANTENNA RADIUS (wavelengths)'
      READ(5,*)ARAD
C
C    ENTER THE NUMBER OF AZIMUTHAL MODES
C    (n=-MODES,...,0,...,+MODES)
C
      MODES=MODE
```

```
      NBLOCK=2*MODES+1
      MHI=MODES+1
      OPEN(8,FILE='outldbor')
      WRITE(8,8000) 2.*BASE,NP,RS,ZP
 8000 FORMAT(//,5X,'*** BOR RADIATION PATTERN FOR A CIRCULAR'
     *' DISC RADIATOR USING GENEX ***',
     *//,2X,'BOR DIAMETER (WAVELENGTHS)=',F5.2,/,2X,
     * 'NUMBER OF GENERATING POINTS (NP)=',I4,
     *//,2X,'SURFACE RADIUS',F5.2,2X,'ZPRIME',F5.2)
      WRITE(8,30) NT,NPHI
   30 FORMAT(/,12X,' NT   NPHI',/,10X,I5,2X,I5)
      IF(ISEG.EQ.0) WRITE(8,1300)
1300 FORMAT(/,10X,'INDEX',8X,'Z(I)',10X,'RHO(I)',12X,'SURF
                                                    IMPED')
      DO 52 I=1,NP
      IF(ABS(ZH(I)).LT..001) ZH(I)=0.
      IF(ABS(RH(I)).LT..001) RH(I)=0.
      ZHB=ZH(I)/BK
      RHB=RH(I)/BK
      Zl0(i)=IMP
C
C ASSIGN SURFACE IMPEDANCE AT THIS POINT.  THE SURFACE
C IMPEDANCE OF SEGMENT I IS ZL0(I)
C
      WRITE(8,8004) I,ZHB,RHB,ZL0(I)
52    CONTINUE
8004  FORMAT(11X,I4,4X,F8.3,8X,F8.3,6X,2F8.2)
C
C MODE LOOP TO CALCULATE THE CURRENT COEFFICIENTS. POS AND NEG
C MODES DONE IN THE SAME ITERATION OF THE LOOP


C*************ZLOAD,ZMAT,GENEX,DECOMP,SOLVE
      IF(CABS(IMP).NE.0) CALL ZLOAD(NP,RH,ZH,ZL0,ZL)
      DO 400 M=1,MHI
      NM=M-1
      CALL ZMAT(NM,NM,NP,NPHI,NT,RH,ZH,X,A,XT,AT,Z)
      IF(CABS(IMP).NE.0) CALL ZTOT(MT,MP,ZL,Z)
      CALL GENEX(NM,NP,NT,NPHI,CNRHO,CNPHI,XT,AT,X,A,
     *           XR,AR,XP,AP,SCAN,PHI,ARAD,RH,ZH,B)
      CALL DECOMP(N,IPS,Z)
      CALL SOLVE(N,IPS,Z,B,C)


C************************************
C STORE CURRENT COEFFICIENTS IN ONE LONG COLUMN VECTOR
      NTOP1=MODES-NM
      NTOP2=NBLOCK-(NTOP1+1)
      NS2=NTOP1*N
      NS1=NTOP2*N
C POSITIVE MODE
```

```
      DO 401 L=1,N
401   CT(L+NS1)=C(L)
      IF(NM.NE.0) THEN
C NEGATIVE MODE
      NMN=-NM


C**********************ZMAT,GENEX,DECOMP,SOLVE.
      CALL ZMAT(NMN,NMN,NP,NPHI,NT,RH,ZH,X,A,XT,AT,Z)
      IF(CABS(IMP).NE.0) CALL ZTOT(MT,MP,ZL,Z)
      CALL GENEX(NMN,NP,NT,NPHI,CNRHO,CNPHI,XT,AT,X,A,
     *           XR,AR,XP,AP,SCAN,PHI,ARAD,RH,ZH,B)
      CALL DECOMP(N,IPS,Z)
      CALL SOLVE(N,IPS,Z,B,C)
C**********************************

      DO 402 L=1,N
402   CT(L+NS2)=C(L)
      ENDIF
400   CONTINUE
      IT=NP
      DT=STOP/FLOAT(NP-1.)
C
C BEGIN PATTERN LOOP FROM START TO STOP IN INCREMENTS OF DT
C (ALL IN DEG)
C
      DO 500 I=1,IT
      THETA=FLOAT(I-1)*DT+START
      THX=THETA*RAD
      PHR=PHR0
      RHB=RH(I)/BK
      ZHB=ZH(I)/BK
      IF(THETA.GT.180.) THEN
      PHR=PHR0+PI
      THX=(360.-THETA)*RAD
      ENDIF
      ET1=(0.,0.)
      EP1=(0.,0.)
      ET2=(0.,0.)
      EP2=(0.,0.)
      DO 300 M=1,MHI
      NM=M-1
      EXP1=CEXP(CMPLX(0.,FLOAT(NM)*PHR))
      EXP2=CONJG(EXP1)


C*****************PLANE
      CALL PLANE(NM,NM,NP,NT,RH,ZH,XT,AT,THX,R)
      NTOP1=MODES-NM
      NTOP2=NBLOCK-(NTOP1+1)
      NS2=NTOP1*N
```

```
      NS1=NTOP2*N
      DO 250 L=1,MT
      ET1=ET1+R(L)*CT(L+NS1)*EXP1
      EP1=EP1+R(L+N)*CT(L+NS1)*EXP1
      IF(NM.EQ.0) GO TO 250
      ET1=ET1+R(L)*CT(L+NS2)*EXP2
      EP1=EP1-R(L+N)*CT(L+NS2)*EXP2
250   CONTINUE
      DO 260 L=1,MP
      ET2=ET2+R(L+MT)*CT(L+NS1+MT)*EXP1
      EP2=EP2+R(L+MT+N)*CT(L+NS1+MT)*EXP1
      IF(NM.EQ.0) GO TO 260
      ET2=ET2-R(L+MT)*CT(L+NS2+MT)*EXP2
      EP2=EP2+R(L+MT+N)*CT(L+NS2+MT)*EXP2
260   CONTINUE
300   CONTINUE
C DISK CONTRIBUTION IN THE FAR FIELD IS ETF,EPF
      RRR=SQRT(RHB**2+ZHB**2)

C*************CIRCTHETA,CIRCPHI
      ETF=CIRCTHETA(CNPHI,XP,AP,CNRHO,XR,AR,ARAD,
     *              SCAN,PHI,RHB,ZHB)
      EPF=CIRCPHI(CNPHI,XP,AP,CNRHO,XR,AR,ARAD,
     *            SCAN,PHI,RHB,ZHB)
c i deleted the rrr*cexp(jk*rrr) factor from ETF & EPF.
C************************************

      ETHF(I)=CABS(ETF)
      EPHF(I)=CABS(EPF)
C TOTAL E-THETA AND E-PHI COMPONENTS
      ET=ET1+ET2+ETF
      EP=EP1+EP2+EPF
      ETSCAT(I)=CABS(ET-ETF)
      EPSCAT(I)=CABS(EP-EPF)
      EC=ET
      EX=EP
      ECV(I)=CABS(EC)
      EXV(I)=CABS(EX)
      ECR=REAL(EC)
      ECI=AIMAG(EC)
      EXR=REAL(EX)
      EXI=AIMAG(EX)
      PHC(I)=ATAN2(ECI,ECR+1.e-10)/RAD
      PHX(I)=ATAN2(EXI,EXR+1.e-10)/RAD
      ANG(I)=THETA
      ECX=AMAX1(ECX,ECV(I),EXV(I))
  500 CONTINUE
      WRITE(6,*) 'MAX E VALUE=',ECX
      WRITE(8,103) P,ECX
  103 FORMAT(/,10X,'PHI OF RECEIVER (DEG)=',F8.2,/,10X,
     * 'MAXIMUM FIELD VALUE (V/M)=',E15.5)
```

```
      DO 600 I=1,IT
      ECP(I)=(ECV(I)/ECX)**2
      EXP(I)=(EXV(I)/ECX)**2
      ECP(I)=AMAX1(ECP(I),1.E-10)
      EXP(I)=AMAX1(EXP(I),1.E-10)
      ECP(I)=10.*ALOG10(ECP(I))
      EXP(I)=10.*ALOG10(EXP(I))
  600 CONTINUE
      IF(IPRINT.EQ.0) THEN
      WRITE(8,5015)
 5015 FORMAT(//,7X,'ANGLE',15X,'CO-POL',25X,'X-POL',/,7X,
     1'(DEG)',4X,2('(VOLTS)',4X,'(DEG)',3X,'(DB-REL)',4X))
      DO 9000 L=1,IT
      WRITE(8,5016)ANG(L),ECV(L),PHC(L),ECP(L),EXV(L),PHX(L)
     1,EXP(L)
 5016 FORMAT(5X,F6.2,3X,2(F8.4,3X,F7.2,3X,F7.2,3X))
 9000 CONTINUE
      ENDIF
      OPEN(2,file='bang.m')
      OPEN(3,file='bcpole.m')
      OPEN(4,file='bxpole.m')
      OPEN(7,file='etscat.m')
      OPEN(8,file='epscat.m')
      OPEN(9,file='etf.m')
      OPEN(10,file='epf.m')
      DO 9097 I=1,IT
      WRITE(2,5019) ANG(I)
      WRITE(3,5019) ECV(I)
      WRITE(4,5019) EXV(I)
C change ecv,ecv to ecp & exp to get normalized db  values.
      WRITE(7,5019) ETSCAT(I)
      WRITE(8,5019) EPSCAT(I)
      WRITE(9,5019) ETHF(I)
 9097 WRITE(10,5019) EPHF(I)
 5019 FORMAT(F8.3)
      CLOSE(2)
      CLOSE(3)
      CLOSE(4)
      CLOSE(7)
      CLOSE(8)
      CLOSE(9)
      CLOSE(10)
 999  CONTINUE
      STOP
      END

C**************END OF MAIN PROGRAM.
```

```
C
C**************SUBROUTINE ZMAT.
C REFERENCE: AN IMPROVED E-FIELD SOLUTION FOR CONDUCTING BOR
C             J.R.MAUTZ AND  R.F. HARRINGTON
C             TECHNICAL REPORT TR-80-1
C             ROME AIR DEVELOPMENT CENTER
C             CONTRACT NO. F-30602-79-C-0011
      SUBROUTINE ZMAT(M1,M2,NP,NPHI,NT,RH,ZH,X,A,XT,AT,Z)
C
C COMPUTE THE MM IMPEDANCE MATRIX ELEMENTS.  THIS IS FROM
C MAUTZ AND HARRINGTON (NO CHANGES).
C

COMPLEXZ(100000),U1,U2,U3,U4,U5,U6,U7,U8,U9,UA,UB,G4A(4),G5A
(4)
      COMPLEXG6A(4),G4B(4),G5B(4),G6B(4),H4A,H5A,H6A,H4B,H5B
      COMPLEX H6B,UC,UD,GA(100),GB(100)
      DIMENSION RH(400),ZH(400),X(100),A(100),XT(4),AT(4)
      DIMENSION RS(400),ZS(400),D(400),DR(400),DZ(400)
      DIMENSION DM(400),C2(100),C3(100),R2(4),Z2(4)
     DIMENSION C4(100),C5(100),C6(100),Z7(4),R7(4),Z8(4),R8(4)
      CT=2.
      CP=.1
      DO 10 I=2,NP
      I2=I-1
      RS(I2)=.5*(RH(I)+RH(I2))
      ZS(I2)=.5*(ZH(I)+ZH(I2))
      D1=.5*(RH(I)-RH(I2))
      D2=.5*(ZH(I)-ZH(I2))
      D(I2)=SQRT(D1*D1+D2*D2)
      DR(I2)=D1
      DZ(I2)=D2
      IF(RS(I2).EQ.0.) RS(I2)=1.
      DM(I2)=D(I2)/RS(I2)
   10 CONTINUE
      M3=M2-M1+1
      M4=M1-1
      PI2=1.570796
      DO 11 K=1,NPHI
      PH=PI2*(X(K)+1.)
      C2(K)=PH*PH
      SN=SIN(.5*PH)
      C3(K)=4.*SN*SN
      A1=PI2*A(K)
      D4=.5*A1*C3(K)
      D5=A1*COS(PH)
      D6=A1*SIN(PH)
      M5=K
      DO 29 M=1,M3
      PHM=(M4+M)*PH
      A2=COS(PHM)
```

```
      C4(M5)=D4*A2
      C5(M5)=D5*A2
      C6(M5)=D6*SIN(PHM)
      M5=M5+NPHI
   29 CONTINUE
   11 CONTINUE
      MP=NP-1
      MT=MP-1
      N=MT+MP
      N2N=MT*N
      N2=N*N
      U1=(0.,.5)
      U2=(0.,2.)
      JN=-1-N
      DO 15 JQ=1,MP
      KQ=2
      IF(JQ.EQ.1) KQ=1
      IF(JQ.EQ.MP) KQ=3
      R1=RS(JQ)
      Z1=ZS(JQ)
      D1=D(JQ)
      D2=DR(JQ)
      D3=DZ(JQ)
      D4=D2/R1
      D5=DM(JQ)
      SV=D2/D1
      CV=D3/D1
      T6=CT*D1
      T62=T6+D1
      T62=T62*T62
      R6=CP*R1
      R62=R6*R6
      DO 12 L=1,NT
      R2(L)=R1+D2*XT(L)
      Z2(L)=Z1+D3*XT(L)
   12 CONTINUE
      U3=D2*U1
      U4=D3*U1
      DO 16 IP=1,MP
      R3=RS(IP)
      Z3=ZS(IP)
      R4=R1-R3
      Z4=Z1-Z3
      FM=R4*SV+Z4*CV
      PHM=ABS(FM)
      PH=ABS(R4*CV-Z4*SV)
      D6=PH
      IF(PHM.LE.D1) GO TO 26
      D6=PHM-D1
      D6=SQRT(D6*D6+PH*PH)
   26 IF(IP.EQ.JQ) GO TO 27
```

```
      KP=1
      IF(T6.GT.D6) KP=2
      IF(R6.GT.D6) KP=3
      GO TO 28
   27 KP=4
   28 GO TO (41,42,41,42),KP
   42 DO 40 L=1,NT
      D7=R2(L)-R3
      D8=Z2(L)-Z3
      Z7(L)=D7*D7+D8*D8
      R7(L)=R3*R2(L)
      Z8(L)=.25*Z7(L)
      R8(L)=.25*R7(L)
   40 CONTINUE
      Z4=R4*R4+Z4*Z4
      R4=R3*R1
      R5=.5*R3*SV
      DO 33 K=1,NPHI
      A1=C3(K)
      RR=Z4+R4*A1
      UA=0.
      UB=0.
      IF(RR.LT.T62) GO TO 34
      DO 35 L=1,NT
      R=SQRT(Z7(L)+R7(L)*A1)
      SN=-SIN(R)
      CS=COS(R)
      UC=AT(L)/R*CMPLX(CS,SN)
      UA=UA+UC
      UB=XT(L)*UC+UB
   35 CONTINUE
      GO TO 36
   34 DO 37 L=1,NT
      R=SQRT(Z8(L)+R8(L)*A1)
      SN=-SIN(R)
      CS=COS(R)
      UC=AT(L)/R*SN*CMPLX(-SN,CS)
      UA=UA+UC
      UB=XT(L)*UC+UB
   37 CONTINUE
      A2=FM+R5*A1
      D9=RR-A2*A2
      R=ABS(A2)
      D7=R-D1
      D8=R+D1
      D6=SQRT(D8*D8+D9)
      R=SQRT(D7*D7+D9)
      IF(D7.GE.0.) GO TO 38
      A1=ALOG((D8+D6)*(-D7+R)/D9)/D1
      GO TO 39
   38 A1=ALOG((D8+D6)/(D7+R))/D1
```

```
39 UA=A1+UA
   UB=A2*(4./(D6+R)-A1)/D1+UB
36 GA(K)=UA
   GB(K)=UB
33 CONTINUE
   K1=0
   DO 45 M=1,M3
   H4A=0.
   H5A=0.
   H6A=0.
   H4B=0.
   H5B=0.
   H6B=0.
   DO 46 K=1,NPHI
   K1=K1+1
   D6=C4(K1)
   D7=C5(K1)
   D8=C6(K1)
   UA=GA(K)
   UB=GB(K)
   H4A=D6*UA+H4A
   H5A=D7*UA+H5A
   H6A=D8*UA+H6A
   H4B=D6*UB+H4B
   H5B=D7*UB+H5B
   H6B=D8*UB+H6B
46 CONTINUE
   G4A(M)=H4A
   G5A(M)=H5A
   G6A(M)=H6A
   G4B(M)=H4B
   G5B(M)=H5B
   G6B(M)=H6B
45 CONTINUE
   IF(KP.NE.4) GO TO 47
   A2=D1/(PI2*R1)
   D6=2./D1
   D8=0.
   DO 63 K=1,NPHI
   A1=R4*C2(K)
   R=R4*C3(K)
   IF(R.LT.T62) GO TO 64
   D7=0.
   DO 65 L=1,NT
   D7=D7+AT(L)/SQRT(Z7(L)+A1)
65 CONTINUE
   GO TO 66
64 A1=A2/(X(K)+1.)
   D7=D6*ALOG(A1+SQRT(1.+A1*A1))
66 D8=D8+A(K)*D7
63 CONTINUE
```

```
      A1=.5*A2
      A2=1./A1
      D8=-PI2*D8+2./R1*(BLOG(A2)+A2*BLOG(A1))
      DO 67 M=1,M3
      G5A(M)=D8+G5A(M)
   67 CONTINUE
      GO TO 47
   41 DO 25 M=1,M3
      G4A(M)=0.
      G5A(M)=0.
      G6A(M)=0.
      G4B(M)=0.
      G5B(M)=0.
      G6B(M)=0.
   25 CONTINUE
      DO 13 L=1,NT
      A1=R2(L)
      R4=A1-R3
      Z4=Z2(L)-Z3
      Z4=R4*R4+Z4*Z4
      R4=R3*A1
      DO 17 K=1,NPHI
      R=SQRT(Z4+R4*C3(K))
      SN=-SIN(R)
      CS=COS(R)
      GA(K)=CMPLX(CS,SN)/R
   17 CONTINUE
      D6=0.
      IF(R62.LE.Z4) GO TO 51
      DO 62 K=1,NPHI
      D6=D6+A(K)/SQRT(Z4+R4*C2(K))
   62 CONTINUE
      Z4=3.141593/SQRT(Z4/R4)
      D6=-PI2*D6+ALOG(Z4+SQRT(1.+Z4*Z4))/SQRT(R4)
   51 A1=AT(L)
      A2=XT(L)*A1
      K1=0
      DO 30 M=1,M3
      U5=0.
      U6=0.
      U7=0.
      DO 32 K=1,NPHI
      UA=GA(K)
      K1=K1+1
      U5=C4(K1)*UA+U5
      U6=C5(K1)*UA+U6
      U7=C6(K1)*UA+U7
   32 CONTINUE
      U6=D6+U6
      G4A(M)=A1*U5+G4A(M)
      G5A(M)=A1*U6+G5A(M)
```

```
      G6A(M)=A1*U7+G6A(M)
      G4B(M)=A2*U5+G4B(M)
      G5B(M)=A2*U6+G5B(M)
      G6B(M)=A2*U7+G6B(M)
   30 CONTINUE
   13 CONTINUE
   47 A1=DR(IP)
      UA=A1*U3
      UB=DZ(IP)*U4
      A2=D(IP)
      D6=-A2*D2
      D7=D1*A1
      D8=D1*A2
      JM=JN
      DO 31 M=1,M3
      FM=M4+M
      A1=FM*DM(IP)
      H5A=G5A(M)
      H5B=G5B(M)
      H4A=G4A(M)+H5A
      H4B=G4B(M)+H5B
      H6A=G6A(M)
      H6B=G6B(M)
      U7=UA*H5A+UB*H4A
      U8=UA*H5B+UB*H4B
      U5=U7-U8
      U6=U7+U8
      U7=-U1*H4A
      U8=D6*H6A
      U9=D6*H6B-A1*H4A
      UC=D7*(H6A+D4*H6B)
      UD=FM*D5*H4A
      K1=IP+JM
      K2=K1+1
      K3=K1+N
      K4=K2+N
      K5=K2+MT
      K6=K4+MT
      K7=K3+N2N
      K8=K4+N2N
      GO TO (18,20,19),KQ
   18 Z(K6)=U8+U9
      IF(IP.EQ.1) GO TO 21
      Z(K3)=Z(K3)+U6-U7
      Z(K7)=Z(K7)+UC-UD
      IF(IP.EQ.MP) GO TO 22
   21 Z(K4)=U6+U7
      Z(K8)=UC+UD
      GO TO 22
   19 Z(K5)=Z(K5)+U8-U9
      IF(IP.EQ.1) GO TO 23
```

```
      Z(K1)=Z(K1)+U5+U7
      Z(K7)=Z(K7)+UC-UD
      IF(IP.EQ.MP) GO TO 22
   23 Z(K2)=Z(K2)+U5-U7
      Z(K8)=UC+UD
      GO TO 22
   20 Z(K5)=Z(K5)+U8-U9
      Z(K6)=U8+U9
      IF(IP.EQ.1) GO TO 24
      Z(K1)=Z(K1)+U5+U7
      Z(K3)=Z(K3)+U6-U7
      Z(K7)=Z(K7)+UC-UD
      IF(IP.EQ.MP) GO TO 22
   24 Z(K2)=Z(K2)+U5-U7
      Z(K4)=U6+U7
      Z(K8)=UC+UD
   22 Z(K8+MT)=U2*(D8*(H5A-[illegible]H5B)-A1*UD)
      JM=JM+N2
   31 CONTINUE
   16 CONTINUE
      JN=JN+N
   15 CONTINUE
      RETURN
      END


C***************SUBROUTINE SOLVE.
C REFERENCE : TECHNICAL REPORT TR-80-1
      SUBROUTINE SOLVE(N,IPS,UL,B,X)
C
C SEE MAUTZ & HARRINGTON FOR DETAILS
C
      COMPLEX UL(100000),B(800),X(800),SUM
      DIMENSION IPS(800)
      NP=N+1
      IP=IPS(1)
      X(1)=B(IP)
      DO 2 I=2,N
      IP=IPS(I)
      IPB=IP
      IM1=I-1
      SUM=(0.,0.)
      DO 1 J=1,IM1
      SUM=SUM+UL(IP)*X(J)
    1 IP=IP+N
    2 X(I)=B(IPB)-SUM
      K2=N*(N-1)
      IP=IPS(N)+K2
      X(N)=X(N)/UL(IP)
      DO 4 IBACK=2,N
      I=NP-IBACK
```

```
      K2=K2-N
      IPI=IPS(I)+K2
      IP1=I+1
      SUM=(0.,0.)
      IP=IPI
      DO 3 J=IP1,N
      IP=IP+N
    3 SUM=SUM+UL(IP)*X(J)
    4 X(I)=(X(I)-SUM)/UL(IPI)
      RETURN
      END


C******SUBROUTINE DECOMP
C REFERENCE: TECHNICAL REPORT TR-80-1
      SUBROUTINE DECOMP(N,IPS,UL)
C
C SEE MAUTZ & HARRINGTON FOR DETAILS
C

      COMPLEX UL(100000),PIVOT,EM
      DIMENSION SCL(800),IPS(800)
      DO 5 I=1,N
      IPS(I)=I
      RN=0.
      J1=I
      DO 2 J=1,N
      ULM=ABS(REAL(UL(J1)))+ABS(AIMAG(UL(J1)))
      J1=J1+N
      IF(RN-ULM) 1,2,2
    1 RN=ULM
    2 CONTINUE
      SCL(I)=1./RN
    5 CONTINUE
      NM1=N-1
      K2=0
      DO 17 K=1,NM1
      BIG=0.
      DO 11 I=K,N
      IP=IPS(I)
      IPK=IP+K2
      SIZE=(ABS(REAL(UL(IPK)))+ABS(AIMAG(UL(IPK))))*SCL(IP)
      IF(SIZE-BIG) 11,11,10
   10 BIG=SIZE
      IPV=I
   11 CONTINUE
      IF(IPV-K) 14,15,14
   14 J=IPS(K)
      IPS(K)=IPS(IPV)
      IPS(IPV)=J
   15 KPP=IPS(K)+K2
```

```
      PIVOT=UL(KPP)
      KP1=K+1
      DO 16 I=KP1,N
      KP=KPP
      IP=IPS(I)+K2
      EM=-UL(IP)/PIVOT
   18 UL(IP)=-EM
      DO 16 J=KP1,N
      IP=IP+N
      KP=KP+N
      UL(IP)=UL(IP)+EM*UL(KP)
   16 CONTINUE
      K2=K2+N
   17 CONTINUE
      RETURN
      END


C************FUNCTION BLOG
C REFERENCE: TECHNICAL REPORT TR-80-1 ;(page 56)
      FUNCTION BLOG(X)
      IF(X.GT..1) GO TO 1
      X2=X*X
      BLOG=((.075*X2-.1666667)*X2+1.)*X
      RETURN
    1 BLOG=ALOG(X+SQRT(1.+X*X))
      RETURN
      END


C******************SUBROUTINE PLANE
C REFERENCE: TECHNICAL REPORT TR-80-1 ;(pages 57-64)
      SUBROUTINE PLANE(M1,M2,NP,NT,RH,ZH,XT,AT,THR,R)
C
C PLANE WAVE EXCITATION VECTOR. FROM MAUTZ AND HARRINGTON.
C MODIFIED TO DO ONLY ONE ANGLE AND FREQUENCY PER CALL.
C
      COMPLEX R(1600),U,U1,UA,UB,FA(5),FB(5),F2A,F2B,F1A,F1B
      COMPLEX U2,U3,U4,U5
      DIMENSION RH(400),ZH(400),XT(4),AT(4),R2(4)
      DIMENSION Z2(4),BJ(2000)
      MP=NP-1
      MT=MP-1
      N=MT+MP
      N2=2*N
      CC=COS(THR)
      SS=SIN(THR)
      U=(0.,1.)
      U1=3.141593*U**M1
      M3=M1+1
      M4=M2+3
```

```
      IF(M1.EQ.0) M3=2
      M5=M1+2
      M6=M2+2
      DO 12 IP=1,MP
      K2=IP
      I=IP+1
      DR=.5*(RH(I)-RH(IP))
      DZ=.5*(ZH(I)-ZH(IP))
      D1=SQRT(DR*DR+DZ*DZ)
      R1=.25*(RH(I)+RH(IP))
      IF(R1.EQ.0.) R1=1.
      Z1=.5*(ZH(I)+ZH(IP))
      DR=.5*DR
      D2=DR/R1
      DO 13 L=1,NT
      R2(L)=R1+DR*XT(L)
      Z2(L)=Z1+DZ*XT(L)
   13 CONTINUE
      D3=DR*CC
      D4=-DZ*SS
      D5=D1*CC
      DO 23 M=M3,M4
      FA(M)=0.
      FB(M)=0.
   23 CONTINUE
      DO 15 L=1,NT
      X=SS*R2(L)
      IF(X.GT..5E-7) GO TO 19
      DO 20 M=M3,M4
      BJ(M)=0.
   20 CONTINUE
      BJ(2)=1.
      S=1.
      GO TO 18
   19 M=2.8*X+14.-2./X
      IF(X.LT..5) M=11.8+ALOG10(X)
      IF(M.LT.M4) M=M4
      BJ(M)=0.
      JM=M-1
      BJ(JM)=1.
      DO 16 J=4,M
      J2=JM
      JM=JM-1
      J1=JM-1
      BJ(JM)=J1/X*BJ(J2)-BJ(JM+2)
   16 CONTINUE
      S=0.
      IF(M.LE.4) GO TO 24
      DO 17 J=4,M,2
      S=S+BJ(J)
   17 CONTINUE
```

```
   24 S=BJ(2)+2.*S
   18 ARG=Z2(L)*CC
      UA=AT(L)/S*CMPLX(COS(ARG),SIN(ARG))
      UB=XT(L)*UA
      DO 25 M=M3,M4
      FA(M)=BJ(M)*UA+FA(M)
      FB(M)=BJ(M)*UB+FB(M)
   25 CONTINUE
   15 CONTINUE
      IF(M1.NE.0) GO TO 26
      FA(1)=FA(3)
      FB(1)=FB(3)
   26 UA=U1
      DO 27 M=M5,M6
      M7=M-1
      M8=M+1
      F2A=UA*(FA(M8)+FA(M7))
      F2B=UA*(FB(M8)+FB(M7))
      UB=U*UA
      F1A=UB*(FA(M8)-FA(M7))
      F1B=UB*(FB(M8)-FB(M7))
      U4=D4*UA
      U2=D3*F1A+U4*FA(M)
      U3=D3*F1B+U4*FB(M)
      U4=DR*F2A
      U5=DR*F2B
      K1=K2-1
      K4=K1+N
      K5=K2+N
      R(K2+MT)=-D5*(F2A+D2*F2B)
      R(K5+MT)=D1*(F1A+D2*F1B)
      IF(IP.EQ.1) GO TO 21
      R(K1)=R(K1)+U2-U3
      R(K4)=R(K4)+U4-U5
      IF(IP.EQ.MP) GO TO 22
   21 R(K2)=U2+U3
      R(K5)=U4+U5
   22 K2=K2+N2
      UA=UB
   27 CONTINUE
   12 CONTINUE
      RETURN
      END

C*************SUBROUTINE ZLOAD.
C REFERENCE: COMPUTATION OF RADIATION AND SCATTERING FOR
C            LOADED BODIES OF REVOLUTION
C            HARRINGTON AND MAUTZ
C            REPORT AFCRL-70-0046
C            AIRFORCE CAMBRIDGE RESEARCH LABS
C            CONTRACT NO. F-19628-68-C-0180
```

```
      SUBROUTINE ZLOAD(NP,RH,ZH,Z0,Z)

C
C COMPUTES IMPEDANCE MATRIX ELEMENTS FOR LOADED BODIES OF REV
C Z0(I) IS THE SURF IMPEDANCE OF THE ITH SEGMENT (NP-1
C SEGMENTS) Z(.) ARE THE IMPEDANCE MATRIX TERMS (TRIDIAGONAL
C FOR T-T SUBMATRIX; DIAGONAL FOR P-P SUBMATRIX). STORED IN
C COL VECTOR.
C

      COMPLEXC1,C2,Z0(400),Z(2400),X1,X2,X3,Y1,Y2,Y3,FN(400)
      COMPLEX U1,U2,U3,XI,YI
      DIMENSION RH(400),ZH(400),RS(400),D(400),SV(400)
      PI=3.14159
      MT=NP-2
      MP=NP-1
      N=MT+MP
      DO 10 IP=2,NP
      II=IP-1
      DR=RH(IP)-RH(II)
      DZ=ZH(IP)-ZH(II)
      D(II)=SQRT(DR*DR+DZ*DZ)
      SV(II)=DR/D(II)
      RS(II)=.5*(RH(IP)+RH(II))
      DS=D(II)*SV(II)/2.
      Q1=RS(II)+DS
      Q2=RS(II)-DS
      FN(II)=1.
      IF((ABS(Q2).GT.1.E-6).AND.(ABS(Q1).GT.1.E-6))
     * FN(II)=ALOG(Q1/Q2)
   10 CONTINUE
      L0=MT*3-2
      DO 20 I=1,MP
      C1=PI*Z0(I)
      IF(I.EQ.MP) GO TO 80
      KI=2
      IF(I.EQ.1) KI=1
      IF(I.EQ.MT) KI=3
      II=I+1
      C2=PI*Z0(II)
      A=SV(I)
      IF(ABS(A).LT.1.E-6) GO TO 41
      X1=C1*FN(I)/2./A
      X2=C1*2./A*(1.-RS(I)*FN(I)/D(I)/A)
      X3=-X2*RS(I)/D(I)/A
      GO TO 42
   41 CONTINUE
      X1=C1/2./RS(I)*D(I)
      X2=(0.,0.)
      X3=C1*D(I)/6./RS(I)
   42 CONTINUE
```

```
      A=SV(II)
      IF(ABS(A).LT.1.E-6) GO TO 45
      Y1=C2*FN(II)/2./A
      Y2=C2*2./A*(1.-RS(II)*FN(II)/D(II)/A)
      Y3=-Y2*RS(II)/D(II)/A
      GO TO 40
   45 CONTINUE
      Y1=C2/2./RS(II)*D(II)
      Y2=(0.,0.)
      Y3=C2*D(II)/6./RS(II)
   40 CONTINUE
C
C DEFINE TRIDIAGONAL ELEMENTS FOR T-T SUBMATRIX (STORED IN
C COLS) (U1- DIAG; U2- LOWER; U3- UPPER)
C
      XI=X1+X2+X3
      YI=Y1-Y2+Y3
      IF(KI.EQ.1) XI=C1/SV(I)
C     IF(KI.EQ.3) YI=C2/SV(II)
      U1=XI+YI
      U2=X1-X3
      U3=Y1-Y3
      L=2+(I-2)*3
      IF(KI.EQ.1) L=0
      L1=L+1
      L2=L+2
      L3=L+3
      go to (50,60,70),ki
   50 Z(L1)=U1
      Z(L2)=U2
      GO TO 80
   60 Z(L1)=U3
      Z(L2)=U1
      Z(L3)=U2
      GO TO 80
   70 Z(L1)=U3
      Z(L2)=U1
   80 Z(L0+I)=2.*C1*D(I)/RS(I)
   20 CONTINUE
      RETURN
      END
      SUBROUTINE ZTOT(MT,MP,ZL,Z)
C
C ADDS THE SURF IMPEDANCE TERMS TO THE TRIDIAGONAL ELEMENTS OF
C THE BOR IMPEDANCE MATRIX Z.
C
      COMPLEX ZL(2400),Z(100000)
      N=MT+MP
      M0=MT*3-2
      DO 100 I=1,MP
      L0=MT*N+(I-1)*N+MT
```

```
      IF(I.EQ.MP) GO TO 80
      KI=2
      IF(I.EQ.1) KI=1
      IF(I.EQ.MT) KI=3
      L2=(I-1)*N+I
      L1=L2-1
      L3=L2+1
      M=2+3*(I-2)
      IF(KI.EQ.1) M=0
      M1=M+1
      M2=M+2
      M3=M+3
      go to (50,60,70),ki
   50 Z(L2)=Z(L2)+ZL(M1)
      Z(L3)=Z(L3)+ZL(M2)
      GO TO 80
   60 Z(L1)=Z(L1)+ZL(M1)
      Z(L2)=Z(L2)+ZL(M2)
      Z(L3)=Z(L3)+ZL(M3)
      GO TO 80
   70 Z(L1)=Z(L1)+ZL(M1)
      Z(L2)=Z(L2)+ZL(M2)
   80 Z(L0+I)=Z(L0+I)+ZL(M0+I)
  100 CONTINUE
      RETURN
      END


C*********SUBROUTINE OGIVE
C SUBROUTINE  : OGIVE
C DATE        : 4 SEPTEMBER 1991
C PROGRAMMER  : R.M. FRANCIS
C REVISED     : 26 JANUARY 1992
C COMMENTS    :
C THIS SUBROUTINE WILL GENERATE DATA FOR A BODY OF REVOLUTION
C (BOR) IN THE FORM OF AN OGIVE.
C DIMENSIONS ARE NORMALIZED TO WAVELENGTH.
C ZH = Z CO-ORDINATE * 2*PI
C RH = RADIUS *2*PI

      SUBROUTINE  OGIVE(NP,ZH,RH,BASE)

C NP = NUMBER OF POINTS ON THE OGIVE SURFACE, MAXIMUM = 1000
C ZP   = ZPRIME, THE POSITION ON Z WHERE THE RADIUS OF
C CURVATURE STARTS
C BASE = BASE RADIUS
C RS   = RADIUS OF CURVATURE IN THE RZ,Z PLANE OF THE OGIVE

      INTEGER I,NP
      REAL  RH(400),ZH(400),ZP,BASE,RS,ZCOORD,RADIUS,AL
      PI=3.1415926
```

```
C INPUT THE VARIABLES FOR THE OGIVE,ZP,B,RS,NP

 WRITE(6,*) 'ENTER SURFACE CURVATURE (wavelengths)'
 READ(5,*) RS
 WRITE(6,*) 'ENTER ZPRIME,WHERE CURVATURE STARTS(wavelengths)'
 READ(5,*) ZP
 WRITE(6,*) 'ENTER BASE RADIUS (wavelengths)'
 READ(5,*) BASE

C PERFORM CALCULATIONS
          AL=SQRT(2.*BASE*RS-BASE**2)
         ZMAX= AL + ZP
          ANG=ASIN(AL/RS)
            L=ANINT((RS*ANG+ZP)*5)
          NP=2*L+1
         WRITE(6,*)'NUMBER OF POINTS IS: ',NP
         DZ= ZMAX/FLOAT(NP-1)
      DO 10  I=1,NP
         ZCOORD= (I-1)*DZ
         ZH(I)=2*PI*ZCOORD
           IF (ZCOORD.LE.ZP) THEN
               RADIUS=BASE
           ELSE
              RADIUS=SQRT(RS**2-(ZCOORD-ZP)**2)+(BASE-RS)
           ENDIF
         RH(I)=2*PI*RADIUS
   10 CONTINUE
      RETURN
      END


C*********SUBROUTINE GENEX.
C SUBROUTINE  : GENEX
C DATE        : 14 JANUARY 1992
C REVISED     : 17 February 1992
C PROGRAMMER  : R.M. FRANCIS

      SUBROUTINE GENEX(NM,NP,NT,NPHI,CNRHO,CNPHI,XT,AT,X,A,
     *                 XR,AR,XP,AP,SCAN,PHI,ARAD,RH,ZH,R)

C SOURCE ON Z AXIS AT Z=0.
C THE EXCITATION VECTOR IS COMPUTED FOR THE GIVEN R,THETA AND
C PHI COMPONENTS SPECIFIED IN FUNCTION SUBROUTINES
C CIRCTHETA,CIRCRHO,CIRCPHI.

COMPLEX R(1600),CEXP,PSI,ST1,ST2,ST3,ST4,SP,S1,S2,S3,S4,S5
      COMPLEX CIRCTHETA,CIRCRHO,CIRCPHI
      DIMENSION RH(400),ZH(400),XT(4),AT(4),X(100),A(100)
      REAL XP(100),AP(100),XR(50),AR(50),SCAN,PHI,ARAD,RHB,ZHB
      INTEGER NM,NP,NT,NPHI,CNRHO,CNPHI,I,N,MP,MT
      PI=3.141592654
```

```
      BK=2.*PI
      MP=NP-1
      MT=MP-1
      N=MT+MP
C LIMITS ON PHI INTEGRATION
      P1=(2.*PI-0.)/2.
      P2=(2.*PI+0.)/2.
      DO 30 IP=1,MP
C QUANTITIES FOR THE FIRST SEGMENT (POSITIVE SLOPE)
      I=IP+1
      II=IP
      DR=RH(I)-RH(II)
      DZ=ZH(I)-ZH(II)
      D1=SQRT(DR*DR+DZ*DZ)
      R1=.5*(RH(I)+RH(II))
      Z1=.5*(ZH(I)+ZH(II))
      SVP1=DR/D1
      CVP1=DZ/D1
      V1=ATAN2(DR,DZ+1.E-5)
C QUANTITIES FOR THE SECOND SEGMENT (NEGATIVE SLOPE)
C (SKIP IF LAST SEGMENT)
      I=IP+2
      II=IP+1
      DR=RH(I)-RH(II)
      DZ=ZH(I)-ZH(II)
      D2=SQRT(DR*DR+DZ*DZ)
      R2=.5*(RH(I)+RH(II))
      Z2=.5*(ZH(I)+ZH(II))
      SVP2=DR/D2
      CVP2=DZ/D2
      V2=ATAN2(DR,DZ+1.E-5)
C BEGIN PHI INTEGRATION: R TERMS IN S1 AND S2; THETA TERM IN
C S3 AND S4; PHI TERM IN S5.
      ST1=(0.,0.)
      ST2=(0.,0.)
      ST3=(0.,0.)
      ST4=(0.,0.)
      SP=(0.,0.)
      DO 20 J=1,NPHI
      PH=P1*X(J)+P2
      PSI=CEXP(CMPLX(0.,-MODE*PH))
      S1=(0.,0.)
      S2=(0.,0.)
      S3=(0.,0.)
      S4=(0.,0.)
      S5=(0.,0.)
      IF(IP.LE.MT) THEN
C t-CURRENT INTEGRATION FOR THE POSITIVE SLOPE
      DO 13 L=1,NT
      TP=D1*XT(L)/2.
      RHB=(R1+TP*SVP1)/BK
```

```
      ZHB=(Z1+TP*CVP1)/BK
      TH=ATAN2(RHB,ZHB+1.E-5)
      CC=COS(V1-TH)
      SS=SIN(V1-TH)
      RR=SQRT(RHB**2+ZHB**2)

S1=S1+AT(L)*(.5+TP/D1)*CC*CIRCRHO(CNPHI,XP,AP,CNRHO,XR,AR,
     *   ARAD,SCAN,PHI,RHB,ZHB)

S2=S2+AT(L)*(.5+TP/D1)*SS*CIRCTHETA(CNPHI,XP,AP,CNRHO,XR,AR,
     *   ARAD,SCAN,PHI,RHB,ZHB)
13    CONTINUE
      S1=S1*D1/2.
      S2=S2*D1/2.
C t-CURRENT INTEGRATION FOR THE NEGATIVE SLOPE
      DO 14 L=1,NT
      TP=D2*XT(L)/2.
      RHB=(R2+TP*SVP2)/BK
      ZHB=(Z2+TP*CVP2)/BK
      TH=ATAN2(RHB,ZHB+1.E-5)
      SS=SIN(V2-TH)
      CC=COS(V2-TH)
      RR=SQRT(RHB**2+ZHB**2)

S3=S3+AT(L)*(.5-TP/D2)*CC*CIRCRHO(CNPHI,XP,AP,CNRHO,XR,AR,
     *   ARAD,SCAN,PHI,RHB,ZHB)

S4=S4+AT(L)*(.5-TP/D2)*SS*CIRCTHETA(CNPHI,XP,AP,CNRHO,XR,AR,
     *   ARAD,SCAN,PHI,RHB,ZHB)
14    CONTINUE
      S3=S3*D2/2.
      S4=S4*D2/2.
      ENDIF
C phi-CURRENT INTEGRATION
      DO 15 L=1,NT
      TP=D1*XT(L)/2.
      RHB=(R1+TP*SVP1)/BK
      ZHB=(Z1+TP*CVP1)/BK
      TH=ATAN2(RHB,ZHB+1.E-5)
      RR=SQRT(RHB**2+ZHB**2)
      S5=S5+AT(L)*CIRCPHI(CNPHI,XP,AP,CNRHO,XR,AR,
     *   ARAD,SCAN,PHI,RHB,ZHB)/R1*(RHB*BK)
15    CONTINUE
      S5=S5*D1/2.
      SP=SP+A(J)*PSI*S5
      IF(IP.LE.MT) THEN
      ST1=ST1+A(J)*PSI*S1
      ST2=ST2+A(J)*PSI*S2
      ST3=ST3+A(J)*PSI*S3
      ST4=ST4+A(J)*PSI*S4
      ENDIF
```

```
20    CONTINUE
C COMPONENTS ARE STORED IN A COLUMN VECTOR: VT(1,MT),
C VP(MT+1,N)
      IF(IP.LE.MT) THEN
      R(IP)=(ST1+ST2+ST3+ST4)*P1
      ENDIF
      R(IP+MT)=SP*P1
30    CONTINUE
      RETURN
      END


C*******FUNCTION CIRCTHETA.
C FUNCTION     :        CIRCTHETA
C DATE         :        1 OCTOBER 1991
C REVISED      :        17 February 1992
C PROGRAMMER   :        R.M. FRANCIS

C COMMENTS :  THIS FUNCTION WILL RIGOROUSLY CALCULATE THE
C ELECTRIC FIELD FOR A CIRCULAR APERTURE. THE FIELD IS
C CALCULATED AT THE BOUNDARY DEFINED BY AN OGIVE. THE APERTURE
C IS LOCATED AT Z = 0, AND IS BORE SIGHTED ON THE Z AXIS. THE
C SUBROUTINE OGIVE IS THE SOURCE OF THE GEOMETRIC DATA
C REQUIRED BY CIRC TO PERFORM COMPUTATIONS.
C ALL PHYSICAL DIMENSIONS ARE NORMALIZED TO WAVELENGTH.


COMPLEX FUNCTION CIRCTHETA(CNPHI,XP,AP,CNRHO,XR,AR,ARAD,SCAN,
     *                              PHI,RHB,ZHB)
      INTEGER CNPHI,CNRHO,M,N
      REAL XP(100),AP(100),XR(50),AR(50),
     *     ARAD,SCAN,PHI,RHB,ZHB
C LOCAL VARIABLES
      REAL Z,RZ,PHIPRIME,PI,S,C,
     *     R,RP,X2,Y1,Y2,K
      COMPLEX J,JK,G1,G2,X1,CON,CC,
     *        sumx,sumy,sumz,CIRCTHETA
      RR1=(ARAD+0.)/2.
      RR2=(ARAD-0.)/2.
      PI=3.141592654
       K=6.283185307
      J = (0.0,1.0)
      JK= (0.0,6.283185307)
      CON=(0.0,-15.0)
      CC= CON*RR1
C OUTER  LOOP: INTEGRATE OVER PHI...-PI<PHI<PI.
C INNER  LOOP: INTEGRATE OVER RHO... 0 <RHO<ANT
      RZ=RHB
      Z=ZHB
        S=RZ/SQRT(RZ**2+Z**2)
        C=Z/SQRT(RZ**2+Z**2)
```

```
        sumx=(0.0,0.0)
        sumy=(0.0,0.0)
        sumz=(0.0,0.0)
          DO 50 M=1,CNPHI
             PHIPRIME=PI*XP(M)
            DO 60 N=1,CNRHO
      RP=RR1*XR(N)+RR2

R=SQRT(((RZ-RP)**2+Z**2)+(4*RZ*RP*SIN((PHI-PHIPRIME)/2)**2))
      G1=(((K*R)**2)-1-(JK*R))/R**3
      G2=(3+(3*JK*R)-(K*R)**2)/R**5
      X1=JK*((RP*COS(PHIPRIME)*SIN(SCAN))-R)
      Y1=(RZ*COS(PHI))-(RP*COS(PHIPRIME))
      X2=Y1**2
      Y2=(RZ*SIN(PHI))-(RP*SIN(PHIPRIME))
         sumx=sumx+(CC*AP(M)*AR(N)*(G1+(X2*G2))*CEXP(X1)*RP)
         sumy=sumy+(CC*AP(M)*AR(N)*Y1*Y2*G2*CEXP(X1)*RP)
         sumz=sumz+(CC*AP(M)*AR(N)*Y1*Z*G2*CEXP(X1)*RP)
   60    CONTINUE
   50    CONTINUE
      CIRCTHETA=(C*COS(PHI)*sumx)+(C*SIN(PHI)*sumy)-(S*sumz)
      RETURN
      END


C***********FUNCTION CIRCRHO.
C FUNCTION     :        CIRCRHO
C DATE         :        1 OCTOBER 1991
C REVISED      :        17 February 1992
C PROGRAMMER   :        R.M. FRANCIS


      COMPLEX FUNCTION CIRC          ,XP,AP,CNRHO,XR,AR,ARAD,
     *                               ,PHI,RHB,ZHB)
      INTEGER CNPHI,CNRH
      REAL XP(100),AP(10          ),AR(50),
     *     ARAD,SCAN,PHI,RHB,ZHB
C LOCAL VARIABLES
      REAL Z,RZ,PHIPRIME,PI,S,C,
     *     R,RP,X2,Y1,Y2,K
      COMPLEX J,JK,G1,G2,X1,CON,CC,
     *        sumx,sumy,sumz,CIRCRHO
      RR1=(ARAD-0.)/2.
      RR2=(ARAD+0.)/2.
      PI=3.141592654
       K=6.283185307
      J = (0.0,1.0)
      JK= (0.0,6.283185307)
      CON=(0.0,-15.0)
      CC=CON*RR1
C OUTER  LOOP: INTEGRATE OVER PHI...-PI<PHI<PI.
```

```
C INNER  LOOP: INTEGRATE OVER RHO... 0 <RHO<ANT
       RZ=RHB
       Z=ZHB
         S=RZ/SQRT(RZ**2+Z**2)
         C=Z/SQRT(RZ**2+Z**2)
        sumx=(0.0,0.0)
        sumy=(0.0,0.0)
        sumz=(0.0,0.0)
          DO 50 M=1,CNPHI
             PHIPRIME=PI*XP(M)
            DO 60 N=1,CNRHO
      RP=RR1*XR(N)+RR2

R=SQRT(((RZ-RP)**2+Z**2)+(4*RZ*RP*SIN((PHI-PHIPRIME)/2)**2))
      G1=(((K*R)**2)-1-(JK*R))/R**3
      G2=(3+(3*JK*R)-(K*R)**2)/R**5
      X1=JK*((RP*COS(PHIPRIME)*SIN(SCAN))-R)
      Y1=(RZ*COS(PHI))-(RP*COS(PHIPRIME))
      X2=Y1**2
      Y2=(RZ*SIN(PHI))-(RP*SIN(PHIPRIME))
         sumx=sumx+(CC*AP(M)*AR(N)*(G1+(X2*G2))*CEXP(X1)*RP)
         sumy=sumy+(CC*AP(M)*AR(N)*Y1*Y2*G2*CEXP(X1)*RP)
         sumz=sumz+(CC*AP(M)*AR(N)*Y1*Z*G2*CEXP(X1)*RP)
   60    CONTINUE
   50    CONTINUE
      CIRCRHO=(S*COS(PHI)*sumx)+(S*SIN(PHI)*sumy)+(C*sumz)
      RETURN
      END


C*******FUNCTION CIRCPHI.
C FUNCTION     :        CIRCPHI
C DATE         :        1 OCTOBER 1991
C REVISED      :        17 Feb 1992
C PROGRAMMER   :        R.M. FRANCIS
      COMPLEX FUNCTION CIRCPHI(CNPHI,XP,AP,CNRHO,XR,AR,ARAD,
     *                         SCAN,PHI,RHB,ZHB)
      INTEGER CNPHI,CNRHO,M,N
      REAL XP(100),AP(100),XR(50),AR(50),
     *     ARAD,SCAN,PHI,RHB,ZHB
C LOCAL VARIABLES
      REAL Z,RZ,PHIPRIME,PI,S,C,
     *     R,RP,X2,Y1,Y2,K,RR1,RR2
      COMPLEX J,JK,G1,G2,X1,CON,CC,
     *        sumx,sumy,sumz
      PI=3.141592654
       K=6.283185307
      RR1=(ARAD-0.)/2.
      RR2=(ARAD+0.)/2.
      J = (0.0,1.0)
      JK= (0.0,6.283185307)
```

```
      CON=(0.0,-15.0)
      CC=CON*RR1
C OUTER  LOOP: INTEGRATE OVER PHI...-PI<PHI<PI.
C INNER  LOOP: INTEGRATE OVER RHO... 0 <RHO<ANT
       RZ=RHB
       Z=ZHB
         S=RZ/SQRT(RZ**2+Z**2)
         C=Z/SQRT(RZ**2+Z**2)
        sumx=(0.0,0.0)
        sumy=(0.0,0.0)
        sumz=(0.0,0.0)
          DO 50 M=1,CNPHI
             PHIPRIME=PI*XP(M)
           DO 60 N=1,CNRHO
      RP=RR1*XR(N)+RR2

R=SQRT(((RZ-RP)**2+Z**2)+(4*RZ*RP*SIN((PHI-PHIPRIME)/2)**2))
      G1=(((K*R)**2)-1-(JK*R))/R**3
      G2=(3+(3*JK*R)-(K*R)**2)/R**5
      X1=JK*((RP*COS(PHIPRIME)*SIN(SCAN))-R)
      Y1=(RZ*COS(PHI))-(RP*COS(PHIPRIME))
      X2=Y1**2
      Y2=(RZ*SIN(PHI))-(RP*SIN(PHIPRIME))
         sumx=sumx+(CC*AP(M)*AR(N)*(G1+(X2*G2))*CEXP(X1)*RP)
         sumy=sumy+(CC*AP(M)*AR(N)*Y1*Y2*G2*CEXP(X1)*RP)
         sumz=sumz+(CC*AP(M)*AR(N)*Y1*Z*G2*CEXP(X1)*RP)
   60    CONTINUE
   50    CONTINUE
       CIRCPHI=(-SIN(PHI)*sumx)+(COS(PHI)*sumy)
      RETURN
      END


C*********SUBROUTINE TESTSPHERE
C SUBROUTINE     :   TESTSPHERE
C DATE           :   21 FEBRUARY 1992
C PROGRAMMER     :   R. M. FRANCIS
C COMMENTS       :   GENERATES A SPHERE, WITH PLOTTED POINTS
C                    AT EQUAL INTERVALS IN THETA.


      SUBROUTINE TESTSPHERE(NP,ZH,RH,BASE,RS,ZP)
      INTEGER NP,I
      REAL ZH(400),RH(400),BASE,RS,ZP,SPRAD
      PI=3.1415926
      BK=2.*PI
      ZP=0.0
      WRITE(6,*)'ENTER AN EVEN NUMBER OF POINTS (NP):'
      READ(5,*)NP
      WRITE(6,*)'ENTER SPHERE RADIUS'
      READ(5,*)SPRAD
```

```
      BASE=SPRAD
        RS=SPRAD
      DO 1241 I=1,NP
         ANGLE=PI*FLOAT(I-1)/(2.*FLOAT(NP-1))
         ZH(I)=BK*SPRAD*COS(ANGLE)
         RH(I)=BK*SPRAD*SIN(ANGLE)
1241  CONTINUE
      RETURN
      END
```

B. SAMPLE DATA FILE OUTLDBOR

*** BOR RADIATION PATTERN FOR A CIRCULAR DISC RADIATOR USING GENEX ***

BOR DIAMETER (WAVELENGTHS)=*****
NUMBER OF GENERATING POINTS (NP)= 70

SURFACE RADIUS50.00 ZPRIME 0.00

NT	NPHI
4	60

INDEX	Z(I)	RHO(I)	SURF IMPED	
1	50.000	0.000	10000.00	0.00
2	49.987	1.138	10000.00	0.00
3	49.948	2.276	10000.00	0.00
4	49.883	3.412	10000.00	0.00
5	49.793	4.547	10000.00	0.00
6	49.676	5.679	10000.00	0.00
7	49.534	6.808	10000.00	0.00
8	49.366	7.934	10000.00	0.00
9	49.173	9.056	10000.00	0.00
10	48.954	10.173	10000.00	0.00
11	48.710	11.285	10000.00	0.00
12	48.440	12.390	10000.00	0.00
13	48.146	13.490	10000.00	0.00
14	47.826	14.582	10000.00	0.00
15	47.482	15.667	10000.00	0.00
16	47.113	16.744	10000.00	0.00
17	46.720	17.812	10000.00	0.00
18	46.302	18.871	10000.00	0.00
19	45.861	19.920	10000.00	0.00
20	45.395	20.959	10000.00	0.00
21	44.906	21.987	10000.00	0.00
22	44.394	23.003	10000.00	0.00
23	43.859	24.008	10000.00	0.00
24	43.301	25.000	10000.00	0.00
25	42.721	25.979	10000.00	0.00
26	42.119	26.945	10000.00	0.00
27	41.494	27.897	10000.00	0.00

28	40.848	28.834	10000.00	0.00
29	40.182	29.756	10000.00	0.00
30	39.494	30.663	10000.00	0.00
31	38.786	31.554	10000.00	0.00
32	38.057	32.429	10000.00	0.00
33	37.309	33.287	10000.00	0.00
34	36.542	34.128	10000.00	0.00
35	35.755	34.951	10000.00	0.00
36	34.951	35.755	10000.00	0.00
37	34.128	36.542	10000.00	0.00
38	33.287	37.309	10000.00	0.00
39	32.429	38.057	10000.00	0.00
40	31.554	38.786	10000.00	0.00
41	30.663	39.494	10000.00	0.00
42	29.756	40.182	10000.00	0.00
43	28.834	40.848	10000.00	0.00
44	27.897	41.494	10000.00	0.00
45	26.945	42.119	10000.00	0.00
46	25.979	42.721	10000.00	0.00
47	25.000	43.301	10000.00	0.00
48	24.008	43.859	10000.00	0.00
49	23.003	44.394	10000.00	0.00
50	21.987	44.906	10000.00	0.00
51	20.959	45.395	10000.00	0.00
52	19.920	45.861	10000.00	0.00
53	18.871	46.302	10000.00	0.00
54	17.812	46.720	10000.00	0.00
55	16.744	47.113	10000.00	0.00
56	15.667	47.482	10000.00	0.00
57	14.582	47.826	10000.00	0.00
58	13.490	48.146	10000.00	0.00
59	12.390	48.440	10000.00	0.00
60	11.285	48.710	10000.00	0.00
61	10.173	48.954	10000.00	0.00
62	9.056	49.173	10000.00	0.00
63	7.934	49.366	10000.00	0.00
64	6.808	49.534	10000.00	0.00
65	5.679	49.676	10000.00	0.00
66	4.547	49.793	10000.00	0.00
67	3.412	49.883	10000.00	0.00
68	2.276	49.948	10000.00	0.00
69	1.138	49.987	10000.00	0.00
70	0.000	50.000	10000.00	0.00

PHI OF RECEIVER (DEG)= 0.00
MAXIMUM FIELD VALUE (V/M)= 0.16659E+03

ANGLE	CO-POL			X-POL		
(DEG)	(VOLTS)	(DEG)	(DB-REL)	(VOLTS)	(DEG)	(DB-REL)
0.00	6.9271	-104.51	-27.62	0.0000	-92.95	-100.00
1.30	3.6864	-106.76	-33.10	1.1253	131.93	-43.41
2.61	2.6516	-50.40	-35.96	0.7957	163.87	-46.42
3.91	4.8350	-14.07	-30.74	0.5577	-172.05	-49.50
5.22	6.0401	-5.71	-28.81	0.2076	-139.66	-58.09
6.52	4.7465	-2.93	-30.91	0.2741	5.44	-55.68
7.83	1.3824	-4.09	-41.62	0.5842	30.18	-49.10
9.13	2.8075	-174.09	-35.47	0.7556	57.97	-46.87
10.43	5.8878	-174.09	-29.03	0.9056	82.84	-45.29
11.74	6.3663	-172.38	-28.36	0.9042	101.87	-45.31
13.04	3.9668	-170.31	-32.46	0.6473	118.37	-48.21
14.35	0.9093	7.83	-45.26	0.2436	-130.52	-56.70
15.65	6.0107	6.17	-28.85	1.0247	-96.02	-44.22
16.96	8.2390	4.51	-26.12	1.2154	-95.19	-42.74
18.26	6.7229	7.30	-27.88	0.9426	-80.30	-44.95
19.57	2.3749	15.98	-36.92	0.4040	-54.39	-52.31
20.87	3.7384	-170.33	-32.98	0.5796	72.59	-49.17
22.17	9.6622	-170.82	-24.73	1.3618	88.39	-41.75
23.48	10.7713	-175.50	-23.79	1.5721	81.57	-40.50
24.78	6.6302	-160.18	-28.00	0.6277	115.25	-48.48
26.09	3.5922	-149.07	-33.33	0.8164	137.53	-46.20
27.39	7.2792	27.16	-27.19	0.9508	-75.15	-44.87
28.70	13.9956	3.03	-21.51	2.1212	-107.94	-37.90
30.00	12.6783	26.06	-22.37	1.1997	-71.27	-42.85
31.30	14.4138	12.62	-21.26	2.0480	-86.02	-38.21
32.61	1.4466	93.02	-41.23	0.5246	44.99	-50.04
33.91	5.0101	-168.15	-30.44	0.7135	42.79	-47.37
35.22	18.2410	-161.85	-19.21	2.3460	82.73	-37.03
36.52	22.8067	-158.28	-17.27	2.5909	93.03	-36.16
37.83	17.8045	-160.35	-19.42	2.0096	80.80	-38.37
39.13	18.0824	-146.48	-19.29	2.4138	124.03	-36.78
40.43	9.1689	3.14	-25.19	1.7552	-103.63	-39.55
41.74	13.8129	38.91	-21.63	0.9059	-103.47	-45.29
43.04	30.3979	9.45	-14.78	4.3773	-120.67	-31.61
44.35	47.4641	29.97	-10.91	5.2557	-84.81	-30.02
45.65	36.1417	33.25	-13.27	3.3511	-87.55	-33.93
46.96	31.6252	32.13	-14.43	3.2704	-81.37	-34.14
48.26	14.5891	62.48	-21.15	2.0676	-25.23	-38.12
49.57	18.9270	-170.31	-18.89	2.8516	41.68	-35.33
50.87	45.8795	-157.68	-11.20	5.2496	54.10	-30.03
52.17	78.0162	-154.23	-6.59	8.1824	59.69	-26.18
53.48	106.099	-152.60	-3.92	10.9266	61.19	-23.66
54.78	136.447	-152.71	-1.73	13.7615	65.23	-21.66
56.09	160.822	-147.27	-0.31	14.3460	71.03	-21.30
57.39	161.358	-145.24	-0.28	13.9190	68.77	-21.56
58.70	166.587	-146.15	0.00	14.2015	67.31	-21.39
60.00	162.565	-144.37	-0.21	13.4435	67.27	-21.86
61.30	153.157	-144.83	-0.73	12.5463	66.68	-22.46
62.61	143.692	-144.21	-1.28	11.3471	67.74	-23.34

```
65.22 108.369 -140.84     -3.73     7.6142     65.73    -26.80
66.52 85.0397 -139.06     -5.84     5.6224     60.07    -29.43
67.83 67.7272 -140.66     -7.82     4.2600     58.69    -31.84
69.13 59.7937 -143.81     -8.90     3.8263     67.63    -32.78
70.43 47.3499 -145.20    -10.93     3.1370     62.89    -34.50
71.74 30.9244 -145.07    -14.63     2.1385     43.54    -37.83
73.04 19.4698 -143.32    -18.65     1.2247     37.25    -42.67
74.35 12.7001 -149.46    -22.36     0.8089     32.28    -46.28
75.65  5.2649 -153.77    -30.01     0.8572    -15.23    -45.77
76.96  8.7952 -119.58    -25.55     0.7979   -159.71    -46.39
78.26 12.4865  173.28     -22.50     1.4228     77.84    -41.37
79.57 11.0782   91.40     -23.54     1.4678    -11.88    -41.10
80.87  3.7571   -1.39     -32.94     1.0531   -129.37    -43.98
82.17  6.6444  103.97     -27.98     1.0604     30.52    -43.92
83.48  6.3822   -4.11     -28.33     1.0668   -128.96    -43.87
84.78  3.0249 -158.22     -34.82     0.2984    104.94    -54.94
86.09  1.8402   75.64     -39.14     0.2566     -5.90    -56.25
87.39  3.9405 -150.16     -32.52     0.8277    166.07    -46.08
88.70  7.3638  110.06     -27.09     1.1926     21.33    -42.90
90.00  7.6190   -5.04     -26.79     1.2270   -108.00    -42.66
```

C. SOURCE CODE FOR GENPLT.M

```
%PROGRAM   :   genplt.m
%DATE      :   15 February 1992
%PROGRAMMER:   R.M. FRANCIS
%Comments  : This program is a plotting routine for the data
% points generated by the main program LDBORMM.F and the
% program TEST.M. Enter parameters iaw the runs of test.m and
% LDBORMM.F.


 load bang.m
 load bxpole.m
 load bcpole.m
 load ctest
 for i=1:np
   if bcpole(i)<=0.0
      bcpole(i)=eps;
   end
   if bxpole(i)<=0.0
      bxpole(i)=eps;
   end
   el(i)=10*log(bcpole(i));
   ep(i)=10*log(bxpole(i));
   zl(i)=10*log(z(i));
   if zl(i)<-50
      zl(i)=-50;
   end
```

```
   if el(i)<-50
      el(i)=-50;
   end
   if ep(i)<-50
      ep(i)=-50;
   end
 end
 subplot(221),plot(deg,z,bang,bcpole,'.')
 title('TEST OF LDBORMM.F'),xlabel('degrees')
 ylabel('magnitude')
 subplot(222),plot(deg,zl,bang,el,'.')
 title('LOG PLOT (db)'),xlabel('degrees')
 ylabel('magnitude')
 text(.1,.4,'analytical (solid), LDBORMM.F(.)','sc')
 text(.1,.3,'PARAMETERS:','sc')
 text(.1,.25,'number of points = 90','sc')
 text(.5,.25,'scan angle = 60 deg.','sc')
 text(.5,.15,'CNRHO = 20','sc')
 text(.5,.2,'CNPHI = 60','sc')
 text(.1,.2,'NPHI = 100','sc')
 text(.1,.15,'NT = 10','sc')
 text(.1,.1,'distance = 50','sc')
 text(.5,.1,'aperture radius = 5','sc')
 text(.1,.05,'complex impedance = (10000.0, 0.0)','sc')
pause
%print
clg
 load etscat.m
 load epscat.m
 load etf.m
 load epf.m
 subplot(221),plot(bang,etscat)
 title('ETSCAT')
 subplot(222),plot(bang,epscat)
 title('EPSCAT')
 subplot(223),plot(bang,etf)
 title('ETF')
 subplot(224),plot(bang,epf)
 title('EPF')
%print
```

APPENDIX B

TABLE B.1. VARIABLES IN SUBROUTINE GENEXX

VARIABLE	TYPE	DESCRIPTION	RANGE
NM	integer	Number of modes in ϕ	$1< NM < \infty$
NP	integer	Even number of points on surface of the BOR	$2< NP <400$
NT	integer	Even number of points of integration in T on BOR	$2< NT <4$
NPHI	integer	Even number of points of integration in ϕ on BOR	$2<NPHI<100$
CNRHO	integer	Even number of points of integration in ρ'(source)	$2<CNRHO<50$
CNPHI	integer	Even number of points of integration in ϕ'(source)	$2<CNPHI<100$
XT,X,XR, XP	real	Abscissa of the function (χ_n) in T,ϕ,ρ' and ϕ'	$-1<\chi_n<1$
AT,A,AR, AP	real	Weights of the series terms(for χ_n) approximating the integral	$0<\omega_n<1$
SCAN	real	angular displacement (in degrees) of source boresight and Z axis	$-90<\theta_s<90$
PHI	real	orientation in ϕ of receiver	$0<\phi<180$
ARAD	real	dimensionless radius of source antenna (a/λ)	$0<\rho'< \infty$
RH(i)	real	the product of the wave number (k) and the radius of the BOR, units in radians	$0< r < \infty$ $3< i < 399$
ZH(i)	real	the product of the wave number (k) and the distance z on the BOR axis, units in radians	$0< z < \infty$ $3< i < 399$
R(i)	complex	the excitation vector $i_{max}=2NP-3$	$-\infty< R(i)<\infty$ $4< i < 1600$

APPENDIX C

A. PROGRAM TO GENERATE DATA FILES FOR GAUSS QUADRATURE INTEGRATION

```
C PROGRAM      :  GAUS.F
C DATE         :  12 SEPTEMBER 1991
C PROGRAMMER   :  R. FRANCIS, D. JENN
C PROGRAM TO COMPUTE WEIGHTS AND ABSCISSAS FOR GAUSSIAN INT.
      CHARACTER*7 FNAME
      DIMENSION X(500),A(500)
      WRITE(6,*) 'ENTER FILE NAME (gaus---)'
      READ(5,*)FNAME
      WRITE(6,*) 'ENTER AN EVEN NUMBER (max pts is 500)'
      READ(5,*) N
      OPEN(2,FILE=FNAME)
      WRITE(2,*) N
      CALL GAUSLEG(-1.,1.,X,A,N)
      DO 10 I=1,N
10    WRITE(2,*) X(I),A(I)
      STOP
      END
      SUBROUTINE GAUSLEG(X1,X2,X,W,N)
      IMPLICIT REAL*8 (A-H,O-Z)
      REAL*4 X1,X2,X(N),W(N)
      PARAMETER (EPS=3.D-14)
      M=(N+1)/2.
      XM=.5D0*(X2+X1)
      XL=.5D0*(X2-X1)
      DO 12 I=1,M
       Z=COS(3.1415926535D0*(I-.25D0)/(N+.5D0))
1      CONTINUE
         P1=1.D0
         P2=0.D0
         DO 11 J=1,N
          P3=P2
          P2=P1
          P1=((2.D0*J-1.D0)*Z*P2-(J-1.D0)*P3)/J
11       CONTINUE
         PP=N*(Z*P1-P2)/(Z*Z-1.D0)
         Z1=Z
         Z=Z1-P1/PP
       IF(ABS(Z-Z1).GT.EPS) GO TO 1
       X(I)=XM-XL*Z
       X(N+1-I)=XM+XL*Z
       W(I)=2.D0*XL/((1.D0-Z*Z)*PP*PP)
       W(N+1-I)=W(I)
12    CONTINUE
```

```
      RETURN
      END
```

B. SAMPLE DATA FILE GENERATED BY GAUS.F

The following is an example of the external sequential data file generated by the program GAUS.F. The first row is an even integer (N). The data in rows two through N are the abscissa and weights for the series approximation of the integral calculation.

Sample data file: gaus20

```
  20
  -0.993129       1.76140E-02
  -0.963972       4.06014E-02
  -0.912234       6.26720E-02
  -0.839117       8.32767E-02
  -0.746332       1.01930E-01
  -0.636054       0.118195
  -0.510867       0.131689
  -0.373706       0.142096
  -0.227786       0.149173
  -7.65265E-02    0.152753
   7.65265E-02    0.152753
   0.227786       0.149173
   0.373706       0.142096
   0.510867       0.131689
   0.636054       0.118195
   0.746332       1.01930E-01
   0.839117       8.32767E-02
   0.912234       6.26720E-02
   0.963972       4.06014E-02
   0.993129       1.76140E-02
```

APPENDIX D

A. ARGUMENTS: CIRCTHETA, CIRCRHO AND CIRCPHI

TABLE D.1. VARIABLE LIST FOR FUNCTION SUBPROGRAMS.

VARIABLE	TYPE	DESCRIPTION	RANGE
CNPHI	integer	see Table B.1.	same
CNRHO	integer	see Table B.1	same
XP,XR	real	see Table B.1	same
AP,AR	real	see Table B.1	same
ARAD	real	see Table B.1	same
SCAN	real	see Table B.1	same
PHI	real	see Table B.1	same
RHB	real	same as RH(i) of Table B.1	same
ZHB	real	same as ZH(i) of Table B.1	same
circtheta circrho circphi	complex	E_θ, E_ρ and E_ϕ calculated at the point on the BOR surface defined by RHB,ZHB and PHI	all complex numbers

B. TEST PROGRAM: CIRCSUB.F

The following program was used to test for convergence the numerical methods used to calculate the electric field components for a uniformly illuminated circular aperture. Before executing the main program LDBORMM.F, it is desirable to determine the minimum number of terms required (CNPHI and CNRHO) for the series approximation of the source field to converge to the analytical solution of Equation (3.26). The

following programs are provided to test for the number of terms required for convergence.

The programs CIRCSUB.F, TEST.M and SCANPLT.M are executed in the same directory. To minimize the number of files in the main directory, maintain these programs in a subdirectory named "circtest". CIRCSUB.F creates the external sequential data files ang.m, etheta.m, erho.m and ephi.m. These data files are vectors of length NP, containing the angle (θ) and the magnitude of E_θ, E_ρ and E_ϕ. The matlab program TEST.M calculates the analytic solution for E_θ in accordance Equation (3.26) and writes the data to a file CTEST.MAT. The matlab program SCANPLT.M loads the data files and plots the results.

1. Source Code for CIRCSUB.F

```
C TESTPROGRAM  :        CIRCSUB.F
C DATE         :        1 OCTOBER 1991
C REVISED      :        12 JANUARY 1992
C PROGRAMMER   :        R.M. FRANCIS
C COMMENTS :  THIS SUBROUTINE CALCULATES THE ELECTRIC FIELD
C FOR A CIRCULAR APERTURE. THE FIELD IS CALCULATED AT THE
C BOUNDARY DEFINED BY AN OGIVE. THE APERTURE IS LOCATED AT Z
C = 0, AND IS BORE SIGHTED ON THE Z AXIS. THE SUBROUTINE
C OGIVE IS THE SOURCE OF THE GEOMETRIC DATA REQUIRED BY CIRC
C TO PERFORM COMPUTATIONS.
C ALL PHYSICAL DIMENSIONS ARE NORMALIZED TO WAVELENGTH.


C********* PROGRAM CIRC
C DECLARE VARIABLES INTEGER NP,NPHI,NRHO,I,M,N
C THE CHARACTER STRING PHIPTS/RHOPTS WILL ACCESS THE
C APPROPIATE FILE WITH THE X'S AND COEEFFICIENTS, TO PERFORM
C INTEGRATION BY GAUSSIAN QUADRATURE. EG. GAUS10 YEILDS, 10
C POINTS;GAUS20, 20PTS, ETC.

      CHARACTER*15 PHIPTS,RHOPTS,GP,GR
      REAL XP(400),AP(400),XR(100),AR(100),S,C,P,PI,SPRAD,
     *     SCAN,Z,RZ,PHI,PHIPRIME,DEG,SA,K,ET,ER,EP,
```

```
     *     R,RP,X2,Y1,Y2,ARAD,RH(400),ZH(400),angle(400)
      COMPLEX J,JK,G1,G2,X1,CON,CC,
     *        sumx,sumy,sumz,
     *        ETHETA(400),ERHO(400),EPHI(400)
      PI=3.141592654
      J = (0.0,1.0)
      JK= (0.0,6.283185307)
       K=6.283185307
      CON=(0.0,-15.0)
 WRITE(6,*)'ENTER THE RADIUS OF THE ANTENNA,(in wavelengths)'
      READ(5,*) ARAD
      ANT=ARAD/2.
      WRITE(6,*)'ENTER PHI,(OBSERVATION) IN DEGREES'
      READ(5,*)P
      PHI=P*PI/180.
      WRITE(6,*)'ENTER SCAN ANGLE IN DEGREES'
      READ(5,*)SA
      SCAN=-SA*PI/180.
      WRITE(6,*)'ENTER PHIPTS STRING: "gaus### ",(max 400)'
      READ(5,*)GP
      PHIPTS='gaus/'//GP
      WRITE(6,*)'ENTER RHOPTS STRING: "gaus### ",(max 100)'
      READ(5,*)GR
      RHOPTS='gaus/'//GR
C     CALL OGIVE(NP,ZH,RH)
C make loop to enter test sphere.
      write(6,*)'enter the sphere radius'
       read(5,*)SPRAD
      write(6,*)'enter the number of points'
      read(5,*)NP
       do 888 I=1,NP
         angle(I)=PI*(I-1)/(2*(NP-1))
         RH(I)=SPRAD*SIN(angle(I))*K
         ZH(I)=SPRAD*COS(angle(I))*K
         write(6,*)angle(I),RH(I),ZH(I)
 888    continue
      OPEN(2,FILE=PHIPTS)
      OPEN(3,FILE=RHOPTS)
      OPEN(4,FILE='etheta.m')
      OPEN(8,FILE='erho.m')
      OPEN(9,FILE='ephi.m')
      OPEN(10,FILE='ang.m')
      READ(2,*)NPHI
      READ(3,*) NRHO
      DO 20 M=1,NPHI
      READ(2,*,END=20)XP(M),AP(M)
  20  CONTINUE
      DO 30 N=1,NRHO
      READ(3,*,END=30)XR(N),AR(N)
  30  CONTINUE
C OUTER LOOP : SOLVES FOR THE SPHERICAL COMPONENTS OF E AT
```

```
C EACH POINT ON THE SURFACE OF THE OGIVE.
C MIDDLE LOOP: INTEGRATE OVER PHI...-PI<PHI<PI.
C INNER  LOOP: INTEGRATE OVER RHO... 0 <RHO<ANT
      DO 40 I=1,NP
            Z=ZH(I)/K
           RZ=RH(I)/K
            S=RZ/SQRT(RZ**2+Z**2)
            C= Z/SQRT(RZ**2+Z**2)
          DEG=angle(I)*180/PI
        sumx=(0.0,0.0)
        sumy=(0.0,0.0)
        sumz=(0.0,0.0)
          DO 50 M=1,NPHI
             PHIPRIME=PI*XP(M)
            DO 60 N=1,NRHO
      RP=(ANT*XR(N))+ANT

R=SQRT((RZ-RP)**2+(Z**2)+(4*RZ*RP*SIN((PHI-PHIPRIME)/2)**2))
      G1=(((K*R)**2)-1-(JK*R))/R**3
      G2=(3+(3*JK*R)-(K*R)**2)/R**5
      X1=JK*((RP*COS(PHIPRIME)*SIN(SCAN))-R)
      Y1=(RZ*COS(PHI))-(RP*COS(PHIPRIME))
      X2=Y1**2
      Y2=(RZ*SIN(PHI))-(RP*SIN(PHIPRIME))
      CC=CON*ANT
         sumx=sumx+(CC*AP(M)*AR(N)*(G1+(X2*G2))*CEXP(X1)*RP)
         sumy=sumy+(CC*AP(M)*AR(N)*Y1*Y2*G2*CEXP(X1)*RP)
         sumz=sumz+(CC*AP(M)*AR(N)*Y1*Z*G2*CEXP(X1)*RP)
   60    CONTINUE
   50    CONTINUE
C CALCULATE THE SPHERICAL COMPONENTS AT THE SURFACE.

ETHETA(I)=((C*COS(PHI)*sumx)+(C*SIN(PHI)*sumy)-(S*sumz))
      ERHO(I)  =((S*COS(PHI)*sumx)+(S*SIN(PHI)*sumy)+(C*sumz))
       EPHI(I)  =((-SIN(PHI)*sumx)+(COS(PHI)*sumy))
         ET=CABS(ETHETA(I))
         ER=CABS(ERHO(I))
         EP=CABS(EPHI(I))
             WRITE(4,*)ET
             WRITE(8,*)ER
             WRITE(9,*)EP
             WRITE(10,*)DEG
   40 CONTINUE
      STOP
      END
```

```
C SUBROUTINE  : OGIVE
C DATE        : 4 SEPTEMBER 1991
C PROGRAMMER  : R.M. FRANCIS
C REVISED     : 13 JANUARY 1992
C COMMENTS    :
C THIS SUBROUTINE WILL GENERATE DATA FOR A BODY OF REVOLUTION
C (BOR) IN THE FORM OF AN OGIVE.
C DIMENSIONS ARE NORMALIZED TO WAVELENGTH.
C ZH = Z CO-ORDINATE * 2*PI
C RH = RADIUS *2*PI

C*****************

      SUBROUTINE  OGIVE(NP,ZH,RH)

C NP = NUMBER OF POINTS ON THE OGIVE SURFACE, MAXIMUM = 1000
C ZP = ZPRIME, THE POSITION ON Z WHERE THE RADIUS OF CURVATURE
C STARTS
C B    = BASE RADIUS
C RS   = RADIUS OF CURVATURE IN THE RZ,Z PLANE OF THE OGIVE
      INTEGER I,NP
      REAL  RH(400),ZH(400),ZP,BASE,RS,ZCOORD,RADIUS,PI
      PI= 3.141592654
C INPUT THE VARIABLES FOR THE OGIVE,ZP,B,RS,NP
      WRITE(6,*)'ENTER AN EVEN NUMBER OF POINTS, MAX IS 400'
      READ(5,*)NP
      WRITE(6,*) 'ENTER SURFACE CURVATURE (wavelengths)'
      READ(5,*) RS
WRITE(6,*) 'ENTER ZPRIME,WHERE CURVATURE STARTS (wavelengths)'
      READ(5,*) ZP
      WRITE(6,*) 'ENTER BASE RADIUS (wavelengths)'
      READ(5,*) BASE
C PERFORM CALCULATIONS
         ZMAX= SQRT((2*BASE*RS)-BASE**2) + ZP
         DZ= ZMAX/(float(NP)-1.)
      DO 10  I=1,NP
         ZCOORD= (float(I)-1.)*DZ
         ZH(I)=2.*PI*ZCOORD
           IF (ZCOORD.LE.ZP) THEN
               RADIUS=BASE
           ELSE
              RADIUS=SQRT(RS**2-(ZCOORD-ZP)**2)+(BASE-RS)
           ENDIF
         RH(I)=2.*PI*RADIUS
   10 CONTINUE
      RETURN
      END
```

2. Source Code for TEST.M

```
% PROGRAM   :  TEST.M
% DATE      :  3 OCTOBER 1992
% REVISED   :  15 FEBRUARY 1992
%Program TEST.M-- generate analytic soln. for circular
% aperture.
%saves the data to "mat file", ctest.
npts=input('enter the number of points:')
R=input('enter the distance (R):')
r=input('enter the radius (in wavelengths): ')
scan=input('enter the scan angle(degrees)')
sa=scan*pi/180;
eta= 120*pi;
k=2*pi;
j=sqrt(-1);
nmax=2*(npts-1);
c1=j*k*eta*r^2*exp(-j*k*R)/R;
% calculate the solution from 0 to 90 degrees.*******
for i=0:npts-1
ang(i+1)=pi*i/nmax;
deg(i+1)=90*i/(npts-1);
fac=0.5*cos(ang(i+1));
if sin(ang(i+1))-sin(sa)== 0.0
        a(i+1)=eps;
   else
        a(i+1)=2*pi*r*(sin(ang(i+1))-sin(sa));
end
        z(i+1)=fac*abs(c1*bessel(1,a(i+1))/a(i+1));
end
np=npts;
save ctest deg z np
```

3. Data file CTEST.MAT

```
   0.0000000e+00   5.9217626e+01   20
   4.7368421e+00   5.7051528e+01
   9.4736842e+00   5.0941450e+01
   1.4210526e+01   4.1944793e+01
   1.8947368e+01   3.1506384e+01
   2.3684211e+01   2.1103366e+01
   2.8421053e+01   1.1933350e+01
   3.3157895e+01   4.7301405e+00
   3.7894737e+01   2.6730656e-01
   4.2631579e+01   3.2224083e+00
   4.7368421e+01   4.5450714e+00
   5.2105263e+01   4.7331488e+00
   5.6842105e+01   4.2520406e+00
   6.1578947e+01   3.4672834e+00
   6.6315789e+01   2.6244918e+00
   7.1052632e+01   1.8607876e+00
   7.5789474e+01   1.2307921e+00
```

```
   8.0526316e+01   7.3451071e-01
   8.5263158e+01   3.4018017e-01
   9.0000000e+01   2.4512433e-16
```

4. Source code for SCANPLT.M

```
%PROGRAM   :   scanplt.m
%DATE      :   15 February 1992
%Comments  : This program is a plotting routine for the data
% points generated by the test program CIRCSUB.F and the
% program TEST.M. Enter parameters iaw the runs of
% TEST.M and CIRCSUB.F.
 load ang.m
 load etheta.m
 load ctest
 subplot(211),plot(deg,z,ang,etheta,'.')
 title('TEST OF SUBROUTINE CIRCTHETA'),xlabel('degrees')
 ylabel('magnitude')
 text(.1,.4,'analytical (solid), CIRCTHETA (.)','sc')
 text(.1,.3,'PARAMETERS:','sc')
 text(.1,.25,'number of points = 90','sc')
 text(.5,.25,'scan angle = 60 deg.','sc')
 text(.1,.2,'CNRHO = 20','sc')
 text(.5,.2,'CNPHI = 60','sc')
 text(.1,.15,'distance = 2500','sc')
 text(.5,.15,'aperture radius = 5','sc')
```

APPENDIX E. MATH NOTES

A. PLOTS GENERATED BY SUBROUTINE OGIVE

Plots generated by the subroutine OGIVE do not have equal spacing in the angle θ. As the angle increases the points are spaced more closely. Equation 2.1 defines r(z). It follows that

$$\theta = \tan^{-1}\left(\frac{r(z)}{z}\right) \qquad \text{(E.1)}$$

as z approaches zero, θ approaches 90 degrees. The rate at which θ approaches 90 degrees decreases as z decreases since

$$\frac{d\theta}{dz} = \frac{z^2}{z^2 + r(z)^2} \qquad \text{(E.2)}$$

clearly demonstrates in the limit

$$\lim_{z \to 0} \frac{d\theta}{dz} = 0 \qquad \text{(E.3)}$$

Where the subroutine OGIVE generates the points RH and ZH, the density of plotted values increases with angle θ.

B. PLOTS GENERATED BY SUBROUTINE TESTSPHERE

In the subroutine TESTSPHERE, the variables RH and ZH are defined in terms of a sphere radius (SPRAD) and the angle θ . The following pseudocode applies

$$\begin{aligned} \theta\ (i) &= \theta_{start} + \Delta\ \theta \\ RH(i) &= SPRAD * \sin(\theta(i)) \\ ZH(i) &= SPRAD * \cos(\theta(i)) \end{aligned} \qquad \text{(E.4)}$$

where $\Delta\theta$ is a constant given by

and NP is the number of points on the BOR.

$$\Delta\ \theta = \frac{\theta_{stop} - \theta_{start}}{NP - 1} \qquad \text{(E.5)}$$

C. NEAR FIELD EQUATIONS FOR A CIRCULAR APERTURE

The Equations 3.13 to 3.22 were adapted from Equations (6-108a) to (6-108c) on page 283 of reference 5. To implement the near field integrals for a circular aperture bounded by a BOR the cartesian representation of the equations in reference ?? were converted to polar coordinates as follows

$$\begin{aligned} x' &= \rho' \cos \phi' \\ y' &= \rho' \sin \phi' \\ ds' &= dx'\, dy' = \rho'\, d\rho'\, d\phi' \end{aligned} \qquad \text{(E.6)}$$

Where the primed notation denotes a source coordinate. Straight forward substitution of Equation (E.6) into the equations of reference 5 yeild Equations 3.13 to 3.22.

The cartesian components of the electric field E(x,y,z) are transformed to spherical components by

$$\begin{bmatrix} E_\theta \\ E_\rho \\ E_\phi \end{bmatrix} = \begin{bmatrix} \cos(\theta)\cos(\phi) & \cos(\theta)\sin(\phi) & -\sin(\theta) \\ \sin(\theta)\cos(\phi) & \sin(\theta)\sin(\phi) & \cos(\theta) \\ -\sin(\phi) & \cos(\phi) & 0 \end{bmatrix} \begin{bmatrix} E_x \\ E_y \\ E_z \end{bmatrix} \qquad \text{(E.7)}$$

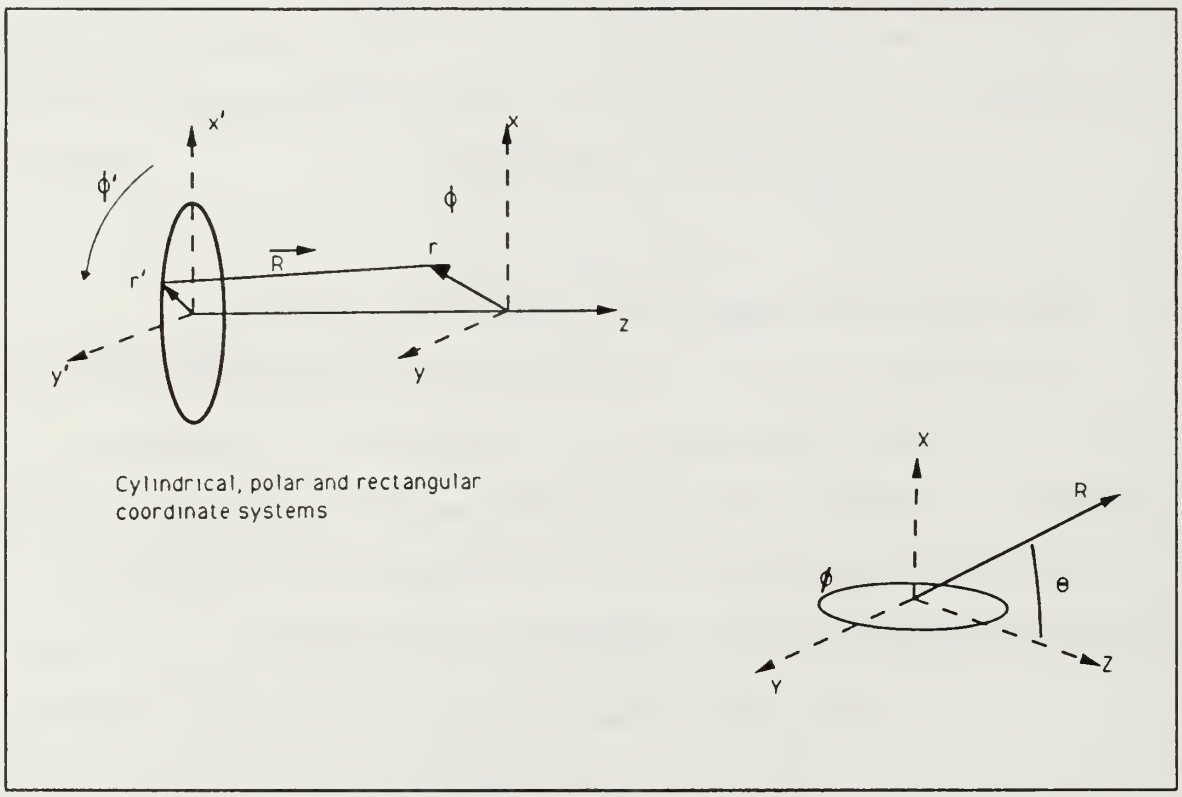

Figure E.1. Polar Geometry for Conversion of E(x,y,z) to Spherical Components,E(R,θ,ϕ).

Figure E.1. illustrates the geometry.

LIST OF REFERENCES

1. Vince, Robert Johnston, " An Electromagnetic Radome Model using an Interactive Micro-Computer Finite Element Algorithm", Master's thesis, Naval Postgraduate School, Monterey, California, December 1989.

2. Cheng, David K., Field and Wave Electromagnetics, second edition, pp. 341-343, Addison-Wesley, Reading, Massachusetts, 1989.

3. Long, William H. and Harringer, Keith A., Medium PRF for the AN/APG-66 Radar", pp. 301-311, Proceedings IEEE, Volume 73, No. 2, February 1985.

4. Skolnik, Merrill I., Introduction to Radar Systems, pp. 264-268, McGraw-Hill, New York, 1980.

5. Balanis, Constantine A., Advanced Engineering Electromagnetics, pp. 282-284, 670-706, John Wiley & Sons, New York, 1989.

6. Mautz, Joseph R. and Harrington, Roger F., "H-Field, E-Field and Combined Field Solutions for Bodies of Revolution," Technical Report No. TR-77-2, Syracuse University, Syracuse, New York, February 1977.

7. Mautz, Joseph R. and Harrington, Roger F., "An Improved E-Field Solution for a Conducting Body of Revolution," Technical Report No. TR-80-1, Syracuse University, Syracuse, New York, January 1980.

8. Borse, G. J., Fortran 77 and Numerical Methods for Engineers, pp. 522-536,PWS-KENT, Boston, Massachusetts, 1985.

9. Balanis, Constantine A., Antenna Theory: Analysis and Design, pp. 478-487, John Wiley & Sons, New York, 1982.

10. Banerjee, Partha P. and Poon, Ting-Chung, Principles of Applied Optics, pp. 95-96, Aksen Associates, Boston, Massachusetts, 1991.

11. Harrington, Roger F. and Maultz, Joseph R, "An Impedance Sheet Approximation for Thin Dielectric Shell", IEEE Transactions on Antennas and Propagation, pp. 531,532, July 1975.

INITIAL DISTRIBUTION LIST

		No. Copies
1.	Defense Technical Information Center Cameron Station Alexandria, VA 22304-6145	2
2.	Library, Code 52 Naval Postgraduate School Monterey, CA 93943-5002	2
3.	Chairman, Code EC Department of Electrical and Computer Engineering Naval Postgraduate School Monterey, CA 93943-5000	1
4.	Professor D.C. Jenn, Code EC/Jn Department of Electrical and Computer Engineering Naval Postgraduate School Monterey, CA 93943-5000	2
5.	Professor Michael A. Morgan, Code EC/Mm Department of Electrical and Computer Engineering Naval Postgraduate School Monterey, CA 93943-5000	1
6.	Lieutenant S.E. Engle 2860 Hayloft Way Morgan Hill, CA 95037	1
7.	Lieutenant R.M. Francis c/o Commanding Officer Charleston Naval Shipyard Prouction Department / Code 330 BLDG 1119 Charleston, S.C. 29408-6100	4